

Ministry of Higher Education and Scientific Research

وزارة التعليم العالي والبحث العلمي

Badji Mokhtar Annaba University
Université Badji Mokhtar – Annaba
Faculty of Technology



جامعة باجي مختار – عنابة

كلية التكنولوجيا

Civil Engineering Department

قسم الهندسة المدنية

Thesis

Presented to obtain the degree of

Doctorate Third Cycle (LMD)

Field: Civil Engineering

Specialty: Structural Analysis

By:

LAGAGUINE Maroua

Theme:

Nonlinear dynamic analysis of soil-foundation-structure interaction

PhD thesis defended on 11/23/2023 in front of the jury composed of:

N°	Full name	Grade	Establishment	Quality
01	MERZOUUD Mouloud	Prof.	University of Badji Mokhtar Annaba	President
02	SBARTAI Badreddine	Prof.	University of Badji Mokhtar Annaba	Reporter
03	MESSAST Salah	Prof.	University of 20 aout, Skikda	Examiner
05	TAHAR BERRABAH Amina	Prof.	University of B.B. Ain Témouchent	Examiner
06	HAMMOUDA Aziz	MCA	University of Badji Mokhtar Annaba	Examiner

DEDICATION

I dedicate this work

- ❖ *To my parents (**Dad and Mom**), who remembered me in their prayers for ultimate success. I consider myself nothing without them. They have given me enough moral support, encouragement and motivation to achieve my personal goals. My two lifelines (parents) have always provided me with their encouragement, love and understanding, their unwavering support and motivation throughout this Ph.D. project was incredible.*
- ❖ *To my sister, **Lati**, and her husband, **Boubaker Bouaoud**, for always encouraging me and pulling me up when I was down and out. Words cannot express my gratitude and appreciation to you. You have been my source of inspiration, support and guidance.*
- ❖ *To my brothers, **Djallel eddine** and **Zine eddine** for your unwavering support. You have taught me to be unique, to be determined, to believe in myself, and to always persevere. I am truly grateful and honored to have you as my brothers.*
- ❖ *To all of you who have been there for me: Thank you for your support and encouragement.*

*This work is for you **Maroua**, for you **Baba** and **Mama**, my dear **Lati** and **Boub**, **Djallel** and **Zino**, I love you.*

Maroua Sagaguine

ACKNOWLEDGEMENTS

*I would like to thank my advisor, **Prof. Badreddine Sbartai**, Badji Mokhtar University of Annaba, for his invaluable advice, continuous support and motivation throughout my Ph.D. studies. His immense knowledge and wealth of experience have been an encouragement to me throughout my academic research.*

*I am also extremely grateful to my laboratory director, **Prof. Kamel Djeghaba**, Badji Mokhtar University of Annaba, for his invaluable supervision, support, feedback, advice and guidance during the course of my Ph.D. studies.*

I would like to thank the remaining members of my dissertation defense committee for graciously taking the time to review this dissertation and help make it a reality.

*I would also like to remember my lab mates and colleagues: **Sami Houhamdi, Ismahen Zaid, Mohamed Said Djebbar, Mohammed Amin Benbouras, Dounia Derdour, Hanane Amara, Kamel Akroum, Mohammed Benzerara, Djihad Charmati, Samira Bouteraa, Ouahab Rahim and Ouafa Boulhouchate**, for the good times we spent together. I've been lucky to know you. You were my second family.*

*I would like to thank my friends, **Amina, Zahia Bouroubi, Fateh Boudjdja, Abdelhak kaid, Souhaila Beguirat, Saad Rihani, Rania Djeddar, Malek Bentayb and Amel Segueni**, for their constant support and encouragement.*

*Finally, a big thank you to my parents, my sister **Lati** and her husband **Boubaker Bouaoud**, my two brothers **Djallel eddine** and **Zine eddine** for always encouraging me, but also sometimes listening to my complaints and trusting me. It's mainly thanks to you that I have come this far. I thank you from the bottom of my heart. I love you all.*

Thank you all for your help.

« تحليل ديناميكي غير خطي لتفاعل التربة-الاساس-الهيكل »

المخلص:

في ظل السلوك الخطي المكافئ للتربة الناتج عن زلزال قوي، يمكن أن تتأثر خصائص التربة كالصلابة و التخامد بها وكذا الاستجابة الديناميكية. بناء على ذلك، يهدف هذا العمل إلى دراسة تأثير سلوك التربة الخطي المكافئ للتربة على الاستجابة الزلزالية للمنظومة المكونة من التربة والهيكل الانشائي، وذلك وفق منهجيات حديثة تعتمد على برنامج CALDYNASOIL المطور من قبل Filali و Sbartai (2012). حيث تم تحليل سلوك التربة غير الخطي لمستويات مختلفة من التشوه (منخفضة ومتوسطة وعالية) بالاستناد إلى الطريقة الخطية المكافئة و باستخدام نموذج القطع المكافئ لمasing (1926)، تم تحليل السلوك غير الخطي للتربة لمستويات مختلفة من التشوه (منخفض، متوسط، مرتفع). باستخدام طريقة البنية السفلية للمنشأ، تم الحصول على الاستجابة الزلزالية للهيكل المختار لسلوك التربة غير الخطي ولشككين من دوال المقاومة. تم إجراء نوعين من التحليلات: الأول، من خلال صيغة تحليلية تستند إلى معادلات التوازن الديناميكي لمنظومة (التربة-المنشأ) حيث تم عمل نموذج تمثيلي من ثلاث درجات من الحرية، والآخر عن طريق التحليل الرقمي المبني على طريقة العناصر المحدودة ثنائية الأبعاد باستخدام برنامج ABAQUS. وتمت مقارنة نتائج هذا الأخير بالنتائج التحليلية. أخيراً وليس أخراً، اقترحنا علاقات تحليلية جديدة غير خطية تربط بين إزاحة الهيكل، مستوى التسارع الزلزالي، وترددات الإثارة. مع أخذ السلوك الخطي المكافئ للتربة بعين الاعتبار.

يُظهر التغير في سلوك التربة بسبب الحركة الزلزالية المستخدمة في هذا العمل تأثيراً كبيراً على استجابة الهيكل وإزاحته. هذا التأثير يتميز بالتقدير الزائد لإزاحة الهيكل والاعتماد القوي على نوع دالة المقاومة وخصائص التربة. تم الحصول على اتفاق ممتاز بين تحليل العناصر المحدودة والنتائج التحليلية بفضل التمثيل المعقول للنموذج.

كلمات مفتاحية: تفاعل المتبادل بين التربة والمنشأ؛ نموذج اللزوجة؛ نموذج التربة الخطية المكافئة؛ Caldynasoil؛ سلوك التربة غير الخطية؛ وظيفة المعاوقة؛ الاستجابة الزلزالية.

« Analyse dynamique non-linéaire de l'interaction sol-fondation-structure »

Résumé :

En présence d'un comportement linéaire équivalent du sol induit par un fort séisme, les caractéristiques de rigidité et d'amortissement du sol ainsi que la réponse dynamique de la structure peuvent être affectées. Par conséquent, ce travail vise à étudier l'influence du comportement linéaire équivalent du sol sur la réponse sismique du système sol-structure avec une nouvelle approche utilisant le code de calcul CALDYNASOIL de Sbartai et Filali (2012). Basé sur la méthode linéaire équivalente avec le modèle hyperbolique de Masing (1926), le comportement non linéaire du sol a été analysé pour différents niveaux de déformation (faible, moyen et élevé). En utilisant la méthode de la sous-structure, la réponse sismique de la structure sélectionnée a été obtenue pour un comportement non linéaire du sol et pour deux formes de fonctions d'impédance. Deux types d'analyses ont été effectués : d'abord, par une formulation analytique basée sur l'équilibre dynamique du système sol-structure modélisé par un modèle analogique à trois degrés de liberté, puis par une analyse numérique réalisée avec une modélisation par éléments finis en 2D à l'aide du logiciel ABAQUS. Les résultats de ce dernier type d'analyse ont été comparés à ceux de la solution analytique. Enfin, nous proposons de nouvelles relations analytiques non linéaires entre les déplacements de la structure, le niveau d'accélération sismique et les fréquences d'excitation, en tenant compte du comportement linéaire équivalent du sol.

Le changement de comportement du sol dû au mouvement sismique imposé dans ce travail montre un effet significatif sur la réponse et le déplacement de la structure. Cet effet est caractérisé par une surestimation du déplacement de la structure et une forte dépendance au type de fonction d'impédance et aux propriétés du sol. Un excellent accord entre l'analyse par éléments finis et les résultats analytiques a été obtenu grâce à la représentation raisonnable du modèle.

Mots clés : Interaction sol-structure (ISS) ; modèle viscoélastique ; modèle de sol linéaire équivalent ; CALDYNASOIL ; comportement non linéaire du sol ; fonction d'impédance ; réponse sismique.

« **Nonlinear dynamic analysis of soil-foundation-structure interaction** »

Abstract:

In the event of equivalent linear soil behavior caused by a strong earthquake, the soil's stiffness, damping characteristics, and the dynamic response of the structure can be impacted. Thus, this study employs the CALDYNASOIL computational code developed by Sbartai and Filali (2012) to investigate how such equivalent linear soil behavior influences the seismic response of the soil-structure system utilizing a novel approach. Based on the Masing's hyperbolic model (1926), the equivalent linear method was used to examine the nonlinear soil behavior at various levels of deformation (low, medium, and high). The substructure method was then applied to determine the seismic response of the structure under nonlinear soil conditions and two forms of impedance functions. Two types of analyses were conducted: first, through an analytical formulation based on the dynamic equilibrium of the soil-structure system modeled by an analog model with three degrees of freedom, and then through a numerical analysis performed with 2D finite element modeling using ABAQUS software. The findings of the latter analysis were compared to those of the analytic solution. Finally, we propose new analytical, nonlinear relationships between the structure's displacements, seismic acceleration levels, and excitation frequencies while considering the equivalent linear soil behavior.

The seismic motion induced change in soil behavior significantly affects structure response and displacement. This effect leads to a higher displacement of the structure along with increased dependence on the impedance function type and soil properties. Our finite element analysis and analytical results display excellent correlation, which we attribute to our model's reasonable representation.

Key words: Soil-structure interaction (SSI); Viscoelastic model; Equivalent linear soil model; CALDYNASOIL; Nonlinear soil behavior; impedance function; seismic response.

TABLE OF CONTENTS

LIST OF FIGURES	VI
LIST OF TABLES	IX
GENERAL INTRODUCTION	8
CHAPTER I: SOIL-STRUCTURE INTERACTION (SSI) - EFFECTS AND METHODS OF ANALYSIS	8
I.1. INTRODUCTION.....	9
I.2. THE SOIL-STRUCTURE INTERACTION PHENOMENON.....	10
I.3. THE COMPONENTS OF THE SOIL-STRUCTURE INTERACTION.....	15
I.3.1. Kinematic interaction.....	15
I.3.2. Inertial interaction.....	16
I.4. METHODS OF ANALYSIS OF DYNAMIC SOIL STRUCTURE INTERACTION PHENOMENON.....	18
I.4.1. The direct method.....	18
I.4.2. The substructure method.....	20
I.4.3. The hybrid method.....	23
I.5. IMPEDANCE FUNCTIONS.....	24
I.6. SOIL-STRUCTURE INTERACTION IN SEISMIC CODES:.....	28
I.7. CONCLUSION.....	29
CHAPTER II: DYNAMIC PROPERTIES OF SOILS	31
II.1. INTRODUCTION.....	32
II.2. LINEAR SOIL BEHAVIOR.....	34
II.3. NON-LINEAR SOIL MODEL.....	35
II.3.1. Nonlinear soil models under cyclic loading.....	36
II.4. METHODS FOR ANALYZING THE SEISMIC RESPONSE OF SOILS.....	39
II.4.1. Equivalent Linear Analysis.....	39
II.5. CONCLUSION.....	44
CHAPTER III: ANALYTICAL ANALYSIS WITH VISCOELASTIC SOIL BEHAVIOR ..	45
III.1. INTRODUCTION.....	46
III.2. SYSTEM AND METHOD OF ANALYSIS.....	46
III.2.1. Dynamic soil-foundation-structure model.....	46
III.2.2. Case of Frequency Independent Expressions:.....	51
III.2.3. Case of Frequency-Dependent Expressions:.....	52
III.3. PARAMETRIC ANALYSIS AND RESULTS.....	53
III.3.1. Natural frequency and damping of the soil-structure system.....	54
III.3.2. Relative and absolute displacement of the structure.....	60
III.4. NEW ANALYTICAL NONLINEAR RELATIONSHIPS.....	64
III.5. CONCLUSION.....	72
CHAPTER IV: ANALYTICAL ANALYSIS WITH EQUIVALENT LINEAR SOIL BEHAVIOR	74

IV.1. INTRODUCTION.....	75
IV.2. SYSTEM AND METHOD OF ANALYSIS.....	76
IV.2.1. Methodology for calculating nonlinear soil behavior parameters	76
IV.2.2. Presentation of the calculation program	78
IV.2.3. Dynamic properties of nonlinear soil behavior	83
IV.3. PARAMETRIC ANALYSIS AND RESULTS.....	87
IV.3.1. Natural frequency and damping of the soil-structure system	88
IV.3.2. Relative and absolute displacement of the structure	91
IV.3.3. Superposition of the different studied cases	95
IV.4. NEW ANALYTICAL NONLINEAR RELATIONSHIPS	99
IV.5. CONCLUSION	106
CHAPTER V: NUMERICAL ANALYSIS	109
V.1. INTRODUCTION	110
V.2. ABAQUS	111
V.2.1. Element Types in ABAQUS.....	112
V.3. REPRESENTATION OF THE STUDIED MODEL:	113
V.3.1. Calculation assumptions, model geometry and material properties	113
V.4. COMPARISON BETWEEN THE ANALYTICAL AND NUMERICAL RESULTS	115
V.4.1. Part I: Viscoelastic soil behavior	117
V.4.2. Part II: Equivalent linear soil behavior	120
V.5. CONCLUSION.....	124
GENERAL CONCLUSION	125
REFERENCES	129

LIST OF FIGURES

Fig. I.1. Illustration of the SSI. (Pecker, 2007)	12
Fig. I.2. A spectral reading that shows the effect of taking the SSI into account. (Mylonakis & Gazetas, 2000)	15
Fig. I.3. (a)The SSI phenomenon; (b)Decomposition into kinematic and inertial interaction; (c)Two-step analysis of the inertial interaction. (Mylonakis & Voyagaki, 2006).....	17
Fig. I.4. The direct method model.....	19
Fig. I.5. The direct method solution scheme. (Tahar Berrabah, 2012).....	20
Fig. I.6. The substructure method model	22
Fig. I.7. The most important steps of the substructure approach	23
Fig. I.8. The soil-structure system considered in hybrid methods.....	24
Fig. I.9. Vertical impedance of a simple oscillator	26
Fig. I.10. Impedance functions of rigid circular foundations on homogeneous half-space. (G. Gazetas, 1983)	28
Fig. II.1. Illustration of Linear Behavior. (Davidovici, 1985)	34
Fig. II.2. Variations in shear modulus and damping as a function of shear strain. (Davidovici, 1985).....	35
Fig. II.3. Shear modulus and damping fraction of the hyperbolic model. (Ishihara, 1996).....	37
Fig. II.4. Relationship between shear modulus and damping fraction (Ishihara, 1996)	38
Fig. II.5. Hyperbolic stress-strain relationship (Hardin and Drnevich, 1972b)	39
Fig. II.6. Number of Soil Layers vs. Calculation Accuracy.....	40
Fig. III.1. simplified soil-structure interaction model (for a single-degree-of-freedom structure) ..	47
Fig.III.2. Schematic representation of a rigid cylindrical foundation embedded in a layer of soil over half the space	50
Fig. III.3. Properties of the equivalent one degree of freedom system ($\bar{m}=3$, $\nu=0.33$, $\xi=0.025$, $\xi_g=0.05$), varying slenderness ratio \bar{h}	55
Fig. III.4. Properties of the equivalent one degree of freedom system ($\bar{h}=1$, $\nu=0.33$, $\xi=0.025$, $\xi_g=0.05$), varying slenderness ratio \bar{m}	56
Fig. III.5. Properties of the equivalent one degree of freedom system ($\bar{m}=3$, $\bar{h}=1$, $\nu=0.33$, $\xi=0.025$, $\xi_g=0.05$, $D=0$), varying the dimensionless circular frequency α_0	58
Fig. III.6. Properties of the equivalent one degree of freedom system ($\bar{m}=3$, $\bar{h}=1$, $\nu=0.33$, $\xi=0.025$, $\xi_g=0.05$, $\alpha_0=1$), varying the embedment ratio D	59
Fig. III.7. Influence of soil-structure interaction as a function of excitation frequency ($\bar{m}=3$, $\bar{h}=1$, $\nu=0.33$, $\xi=0.025$, $\xi_g=0.05$, $D=0$) (a), (b).	61
Fig. III.8. Influence of soil-structure interaction as a function of excitation frequency ($\bar{m}=3$, $\bar{h}=1$, $\nu=0.33$, $\xi=0.025$, $\xi_g=0.05$, $D=0$), varying α_0	63
Fig. III.9. Influence of soil-structure interaction as a function of excitation frequency ($\bar{m}=3$, $\bar{h}=1$, $\nu=0.33$, $\xi=0.025$, $\xi_g=0.05$, $\alpha_0=1$), varying D	64
Fig. III.10. Max Displacement- the foundation embedment ratio D ($\bar{m}=3$, $\bar{h}=1$, $\nu=0.33$, $\xi=0.025$, $\xi_g=0.05$, $\alpha_0=3$).....	65
Fig. III.11. Max Structural distortion versus the foundation embedment ratio D ($\bar{h}=1$, $\bar{m}=3$, $\nu=0.33$, $\xi=0.025$, $\xi_g=0.05$, α_0 (= 1, 2, 4, 5, and 6)).....	67
Fig. III.12. Max absolute displacement versus the foundation embedment ratio D ($\bar{h}=1$, $\bar{m}=3$, $\nu=0.33$, $\xi=0.025$, $\xi_g=0.05$, α_0 (= 1, 2, 4, 5, and 6)).....	69

Fig. III.13. Variation of the coefficients b_0 and b_1 with a_0	70
Fig. III.14. Variation of the coefficients b_2 , b_3 , b_4 and b_5 with a_0	70
Fig. IV.1. Lumped Mass Model. (Filali and Sbartai 2017).....	76
Fig. IV.2. Main interface of the Caldynasoil software. (Kamel Filali 2018)	79
Fig. IV.3. Analysis method selection.	80
Fig. IV.4. Calculation precision (ERS)	80
Fig. IV.5. Selecting the Seismic Acceleration.	81
Fig. IV.6. Start Calculation Step	81
Fig. IV.7. Results window.....	82
Fig. IV.8. Dynamic soil property values after analysis	82
Fig. IV.9. Soil characteristics.	83
Fig. IV.10. Seismic accelerations used in this study.	84
Fig. IV.11. Variation of shear modulus (G/G_{max}) and damping coefficient (ξ/ξ_{max}) as a function of shear strain (γ/γ_r) due to acceleration of "Diamond HTs" , 1989 (0.1g).....	85
Fig. IV.12. Variation of shear modulus (G/G_{max}) and damping coefficient (ξ/ξ_{max}) as a function of shear strain (γ/γ_r) due to acceleration of of Nahanni, 1985 (0.2g).....	85
Fig. IV.13. Variation of shear modulus (G/G_{max}) and damping coefficient (ξ/ξ_{max}) as a function of shear strain (γ/γ_r) due to acceleration of the El-Centro, 1940 (0.3g)... ..	86
Fig. IV.14. Variation of shear modulus (G/G_{max}) and damping coefficient (ξ/ξ_{max}) as a function of shear strain (γ/γ_r) due to acceleration of the Loma Preita,1989 (0.4g).. ..	86
Fig. IV.15. Variation of shear modulus (G/G_{max}) and damping coefficient (ξ/ξ_{max}) as a function of shear strain (γ/γ_r) due to acceleration of the Northridge ,1994 (0.50g).	87
Fig. IV.16. Properties of the equivalent one degree of freedom system for the frequency-independent impedance function expressions with equivalent linear soil behavior ($\bar{m}=3$, $\bar{h}=1$, $\nu=0.33$, $\xi=0.025$, $\xi_g=0.05$).	89
Fig. IV.17. Properties of the equivalent one degree of freedom system for the frequency-dependent impedance function expressions with equivalent linear soil behavior ($\bar{h}=1$, $\bar{m}=3$, $\nu=0.33$, $\xi=0.025$, $\xi_g=0.05$, $\alpha_0=3$).	90
Fig. IV.18. Influence of soil-structure interaction as a function of excitation frequency (case for the frequency-independent impedance function expressions with equivalent linear soil behavior) ($\bar{m}=3$, $\bar{h}=1$, $\nu=0.33$, $\xi=0.025$, $\xi_g=0.05$).	93
Fig. IV.19. Influence of soil-structure interaction as a function of excitation frequency (case for the frequency-dependent impedance function expressions with equivalent linear soil behavior) ($\bar{m}=3$, $\bar{h}=1$, $\nu=0.33$, $\xi=0.025$, $\xi_g=0.05$, $\alpha_0=1$).	94
Fig. IV.20. Influence of soil-structure interaction as a function of excitation frequency (case for the frequency-dependent impedance function expressions with equivalent linear soil behavior) ($\bar{m}=3$, $\bar{h}=1$, $\nu=0.33$, $\xi=0.025$, $\xi_g=0.05$, $\alpha_0=3$).	95
Fig. IV.21. Comparison of the four analysis cases with the fixed base case ($\bar{m}=3$, $\bar{h}=1$, $\nu=0.33$, $\xi=0.025$, $\xi_g=0.05$, $\alpha_0=3$).	97
Fig. IV.22. Max Displacement-Seismic acceleration curves of the soil-structure system ($\bar{m}=3$, $\bar{h}=1$, $\nu=0.33$, $\xi=0.025$, $\xi_g=0.05$, $\alpha_0=3$).	100
Fig. IV.23. Max Structural distortion versus seismic acceleration levels of the soil-structure system: $\bar{h}=1$, $\bar{m}=3$, $\nu=0.33$, $\xi=0.025$, $\xi_g=0.05$, α_0 (= 1, 2, 4, 5, and 6).	102
Fig. IV.24. Max absolute displacement versus seismic acceleration levels of the soil-structure system: $\bar{h}=1$, $\bar{m}=3$, $\nu=0.33$, $\xi=0.025$, $\xi_g=0.05$, α_0 (= 1, 2, 4, 5, and 6).	103
Fig. IV.25. Variation of the coefficients b_0 and b_1 with a_0	104
Fig. IV.26. Variation of the coefficients b_2 , b_3 , b_4 and b_5 with a_0	105

Fig. V.1. The main window of the Abaqus CAE 2021 software.	112
Fig. V.2. Some of the most commonly used elements (Abaqus document).	113
Fig. V.3. Representation of the Abaqus model in the initial states (a) fixed base (b) flexible base.	114
Fig. V.4. Harmonic input motion (Abaqus, 2021).	115
Fig. V.5. Representation of the Abaqus model in deformed state (a) fixed base (b) flexible base.	115
Fig. V.6. Absolute displacement of the fixed base structure (Abaqus, 2021).	116
Fig. V.7. Different displacements of the flexible base structure: total or relative displacement ($\mathbf{u} + \mathbf{u}_0 + \mathbf{h}\phi$; red line); displacement of the base ($\mathbf{u}_0 + \mathbf{h}\phi$; blue line); horizontal displacement of the base (\mathbf{u}_0 ; purple line) (Abaqus, 2021).	117
Fig. V.8. Numerical results of the properties of the equivalent one-degree-of-freedom system for the viscoelastic soil behavior ($\bar{m}=3, \bar{h}=1, \nu=0.33, \xi=0.025, \xi_g=0.05$): (a), (b).	118
Fig. V.9. Numerical results of the relative and absolute displacements of the structure for the viscoelastic soil behavior: (a), (b).	119
Fig. V.10. Numerical results of the properties of the equivalent one-degree-of-freedom system for the various cases studied ($\bar{m}=3, \bar{h}=1, \nu=0.33, \xi=0.025, \xi_g=0.05$): (a), (b).	121
Fig. V.11. Numerical results of the relative and absolute displacements of the structure: (a), (b).	122
Fig. V.12. Comparative study between the analytical and numerical analysis: (a), (b).	123

LIST OF TABLES

Table II.1. Soil Behavior Model and Analysis Method as a Function of Cyclic Deformation Amplitude According to Davidovici (1985).	33
Table III.1. The fitting functions of the b0 and b1 coefficients.	71
Table III.2. The fitting functions of the b2, b3, b4 and b5 coefficients.	71
Table IV.1. Variations of the nonlinear dynamic properties of the soil vs the acceleration level of the earthquakes	87
Table IV.2. Difference margin of pics of displacements and their frequencies for an SSI system and equivalent linear soil behavior. (Iagaguine and Sbartai 2023)	98
Table IV.3. The fitting functions of the b0 and b1 coefficients.	105
Table IV.4. The fitting functions of the b2, b3, b4 and b5 coefficients.	105

GENERAL INTRODUCTION

GENERAL INTRODUCTION

The dynamic (seismic) response of an engineered structure depends on many structural characteristics, seismic input, structural typology, and material properties, among others. A significant contributor to the dynamic response is the influence of soil-structure interaction (SSI) (Farghaly and Ahmed 2013; Harichane, Guellil, and Gadouri 2018; Park, Choo, and Cho 2013; Sbartai and Boumekik 2008; Sobhi and Far 2021), the consideration of which mostly modifies the seismic response of structures by increasing or decreasing the displacement values and their natural frequency. However, many building codes (EC8-2004) ignore its effects under the assumption that its inclusion generally leads to a conservative design and that it is only considered in the case of massive structures on soft ground (Abdel Raheem, Ahmed, and Alazrak 2015). Regardless of the type of analytical or numerical analysis used, Soil-Structure Interaction (SSI) has been subjected to numerous studies over the past few decades (Awchat and Monde 2021; Çakır and Coşkun 2021; Thejaswini, Govindaraju, and Devaraj 2021), their conclusions on the beneficial or detrimental effects of the phenomenon have been controversial (Mylonakis and Gazetas 2000; Renzi, Madaï, and Vannucchi 2013; Abate and Massimino 2017), pointing to the importance of considering its effects to ensure the safety and economic efficiency of structures during earthquakes. This problem is particularly severe for structures located in relatively soft soils. In seismically active regions, the shear wave velocity of the supporting soil is less than 100 m/s. (Boliseti 2015; Çelebi, Göktepe, and Karahan 2012; Karabork, Deneme, and Bilgehan 2014)

Most seismic analyses and risk assessments are now performed under fixed base conditions. Although several studies have shown the importance of soil effects on buildings, relating these effects to nonlinear soil behavior remains a complex problem due to its difficulty and lack of data. This is despite the fact that soils subjected to seismic loading generally exhibit nonlinear soil physical behavior. It is recommended to use the same soil behavior model for the site response analysis and the SSI analysis to obtain more accurate and fair results. Usually, the SSI is considered in the dynamic analysis by assuming linear viscoelastic soil behavior. This is due to the ease of use of this model. However, the dynamic interactions between the soil and the structure can be affected by the deformations due to strong seismic accelerations, which can cause soil strains outside the elastic behavior of the soil. These effects lead to a reduction of stiffness at the base of the structure on the one hand, and an increase of energy dissipation in the soil on the other hand. Therefore, it is very important to develop methods that account for the nonlinear soil behavior in the soil-structure

interaction, as this nonlinear behavior cannot be captured by an elastic or viscoelastic model.(Andrzej Truty 2018; Martakis et al. 2021)

Several studies have been conducted on the subject of soil-structure interaction with nonlinear soil behavior, such as the study by Petridis and Pitilakis (2020), which investigated how soil-structure interaction (SSI) and nonlinear soil behavior affect the seismic fragility of reinforced concrete (RC) buildings with shallow foundations. They used nonlinear dynamic models to derive fragility curves for a wide range of building typologies and soil profiles. They found that site amplification and SSI effects together resulted in greater fragility. This highlights the differences that result from nonlinear soil dynamics and SSI. In addition, Petridis and Pitilakis (2021) investigated the effectiveness of a wide range of fragility modifiers (FM) to account for nonlinear soil behavior and/or SSI effects in large-scale seismic risk assessment procedures, and applied their strategy to an existing block of mostly residential structures in Thessaloniki, Greece. The usefulness of the proposed FM for large-scale risk assessment and the importance of considering soil-related effects were demonstrated by comparing the results in terms of fragility and vulnerability. Meanwhile, Massimino et al. (2019) compared two different strategies to account for soil nonlinearity in 2D numerical analyses of a fully coupled soil-structure system, using seven accelerograms scaled to the same PGA, regarding the estimated seismicity of Catania. The results of the fully coupled system studies were compared with those of the free field (FF) site response in the time and frequency domains. The obtained ground gain ratios and the response spectra have also been compared with those specified in the Italian technical standards (NTC 2008). Their comparative study showed that, when comparing the alignment under the structure with the alignment in free field conditions, the presence of the structure generated a strong gain at the ground surface for certain accelerograms that were subjected to a much lower gain in free field conditions, and that the presence of the structure has clearly altered the frequency content of the ground. This finding emphasizes the importance of considering the soil-structure interaction when evaluating the seismic safety of buildings. The work of Garevski and Ansal (2010) presents the results of the incremental dynamic analysis (IDA) of a basic structural system with nonlinear soil-structure interaction.

For the soil-foundation system, a nonlinear dynamic macroelement is used to simplify the analysis. The results are compared to studies without SSI (fixed-base structure) and with linear SSI to illustrate the differences in structure behavior when SSI is accounted for either with a linear or non-linear assumption, they also emphasize the importance of foundation non-

linearities in decreasing the superstructure's ductility demand. While, Bahuguna and Firoj (2021) performed static, cyclic, and dynamic analysis using the IDA method on an NPP of FEM model resting on layered soil. they found that ignoring SSI and the raft's embedment impact can result in an inaccurate estimate of NPP's seismic response and uneconomical design. They also found that accounting for superstructure nonlinearity using CDP and soil nonlinearity with the Drucker–Prager model increases the response of NPP structure by a significant amount. As a result, they insisted that these issues should be reviewed for crucial and vital facilities such as NPP structures, as erroneous and inaccurate seismic response evaluation might result in serious structural damage and health effects.

The dynamic impedance functions (i.e., stiffness and damping) of a soil-foundation system are among the most important subtasks in soil-structure interaction analysis. Many studies have focused on identifying and investigating the effect of the latter. For the sake of simplicity, most of their research has been based on the use of frequency-independent impedances or on simple rheological models, due to the convincing and very interesting results obtained with this type of analysis. Therefore, the effect of frequency-dependent dynamic impedance functions is neglected (Çelebi, Firat, and Çankaya 2006; Guellil et al. 2017; Lesgidis, Sextos, and Kwon 2017), although it is well known that the nature of the soil-structure interaction mainly depends on the excitation frequency. So, to what extent can impedance function form influence the response of the structure to address the SSI problem?

According to EC8-2004, if the ground acceleration is equal to or greater than 0.1g, the shear modulus must be multiplied by the average reduction factor. Therefore, the fact that higher ground motion intensity leads to nonlinear soil response at certain depths, more complex dynamic behavior of the soil field, and possibly more significant differences in the corresponding impedance functions, which is reflected in the difference between frequency-dependent and frequency-independent models, cannot be ignored. So how can the response of the structure to an SSI problem be affected by the type of impedance function and the nonlinear behavior of the soil due to a seismic event?

In order to answer the above questions, the present work presents an illustrative example of the influence of the change of the soil behavior under seismic excitation on the seismic response of a building (frequency, damping ratio, shear modulus, displacement...). The inspiration behind this work stems from Sbartai's studies (Badreddine and Fillali 2012; Filali and Sbartai 2017) on how a semi-infinite soil profile responds to seismic activity, using

an equivalent linear model of soil behavior. The seismic response of the chosen structure in this thesis, under nonlinear soil behavior, was obtained using two types of analysis. Firstly, an analytical formulation based on the dynamic equilibrium of the soil-structure system was modeled through an analog model with three degrees of freedom. Secondly, a numerical analysis was generated using ABAQUS software with 2D finite element modeling. The results of the numerical analysis were compared to those of the analytical solution. In this study, the superstructure in each SSI model is represented as a linear SDOF system. The research aims to examine differences in the dynamic response of the soil-structure system for both linear and nonlinear soil behavior due to the effects of impedance functions. Springs and dashpots with two frequency cases, independent and dependent frequencies (static impedance function, dynamic impedance function), are used. Finally, based on the comparable linear soil behavior, we suggest a fresh analytical nonlinear connection among the building's displacements, the seismic acceleration rate, and the stimulation frequencies.

The change in soil behavior caused by seismic activity has a significant impact on the structure's response and can lead to an overestimation of displacement. This effect is characterized by an overestimation of the displacement of the structure. It is also strongly dependent on the type of impedance function and the soil properties. Excellent agreement has been achieved between finite element analysis and analytical results due to the simple model representation.

The novelties of the present work are as follows

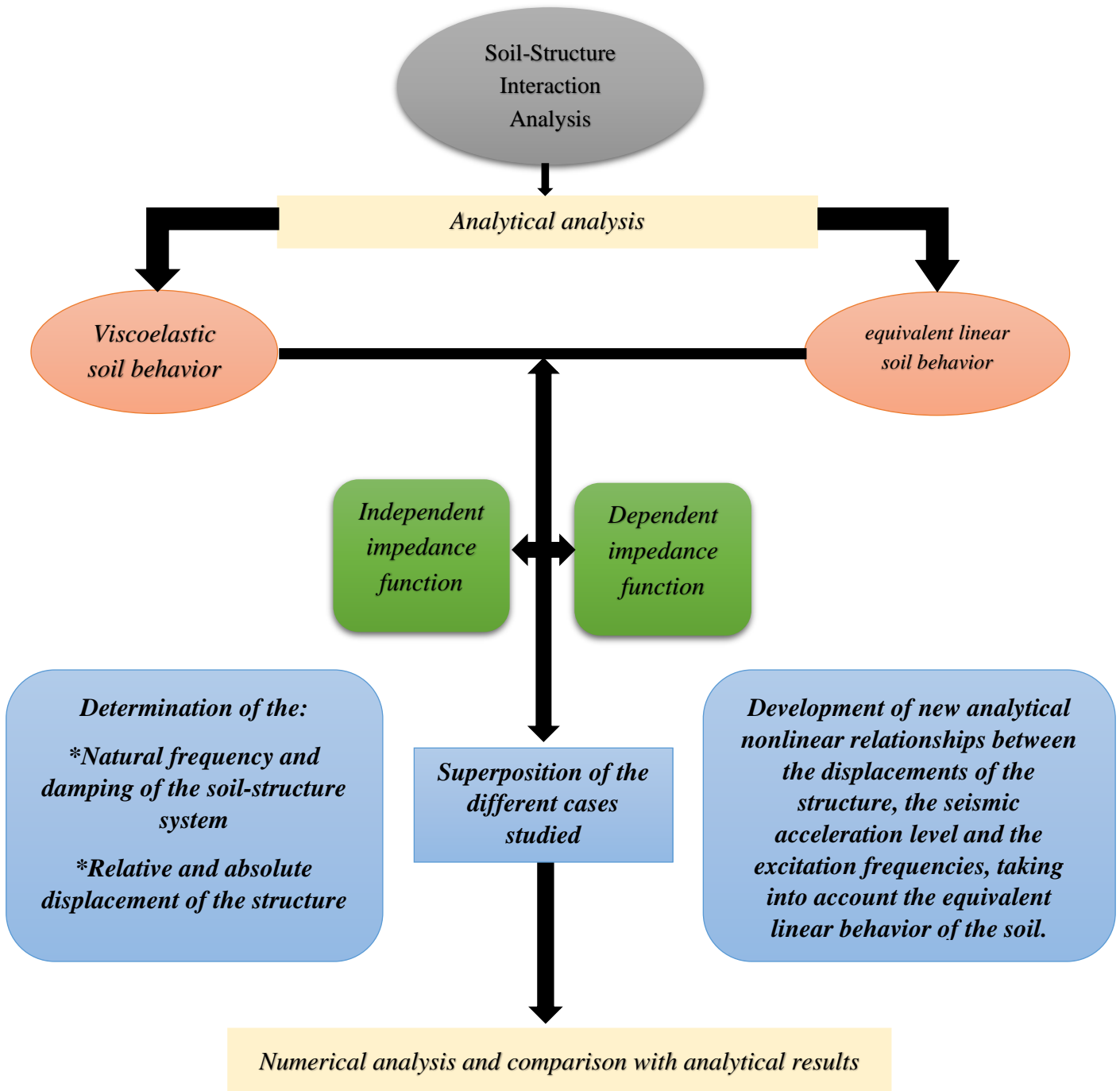
- To emphasize the importance of the shape of the impedance function on the dynamic behavior of the soil-structure system;
- Evaluation of the dynamic nonlinear soil parameters (G , ξ_g) using an equivalent linear model by the CALDYNASOIL computational code of Sbartai and Filali (2012);
- Evaluation of the influence of nonlinear soil behavior on the seismic response of structures resting on shallow foundations;
- To propose new analytic nonlinear relations between the displacements of the structure, the seismic acceleration level, and the excitation frequencies, taking into account the equivalent linear behavior of the soil;

- Considering the equivalent linear behavior of the soil, to propose new analytical nonlinear relationships between the displacements of the structure, the seismic acceleration level and the excitation frequencies;

This thesis is divided into three main parts, as follows:

- Analytical analysis of the soil structure system with viscoelastic soil behavior.
- Analytical analysis of the soil structure system with equivalent linear soil behavior.
- Numerical analysis and comparison with analytical results.

The organization chart below represents the structure of the work reported in this thesis manuscript.



***CHAPTER I: SOIL-STRUCTURE INTERACTION (SSI)
- EFFECTS AND METHODS OF ANALYSIS***

I.1. INTRODUCTION

The 19th and early 20th centuries were a period of rapid innovation and development in structural design and analysis. Today, structures are becoming taller and larger, and several factors can affect their seismic response. Many of these things are still ignored by engineers and building codes, even though several studies have demonstrated their importance and impact. Soil-Structure Interaction (SSI) is one of these factors that can cause many complex effects. The structure, the foundation, and the underlying and surrounding soil all influence the response of the structure during an earthquake. However, it is still common for the influence of SSI to be completely ignored when designing a structure, assuming that the integration of SSI results in a conservative design (Abdel Raheem et al., 2015). Despite its effect, which can be beneficial or detrimental (Abate & Massimino, 2017; Mylonakis & Gazetas, 2000), it is still a controversial topic (Renzi et al., 2013). However, in both cases, it should be taken into account because it could lead to a significant overestimation of the design response spectra for buildings (Guellil et al., 2020), as a result uneconomic designs, it is imperative to encourage the studies of coupled soil-structure systems, because without them, a risk of rough and inaccurate assessment of the seismic response of the structure. (Massimino et al., 2019)

Many analytical, numerical, and experimental studies have been conducted on this topic, especially on soil-structure interaction, highlighting its important role in the analysis of structures. Among these studies, the influence of soil-structure interaction on the behavior and dynamic response of structures, such as the work of Worku (2014), which shows the importance of SSI in increasing the total lateral deformation of buildings and its beneficial effect in reducing the design spectral values or base shear in most building structures. Gao et al., (2020), using the Response Spectrum Method (RSM), investigated the effect of seismic SSI on a structure with a shallow foundation. Other studies that investigate the effect of SSI on the dynamic properties/response of the base-isolated structure, Abdeddaim et al., (2022); Karabork et al., (2014); Spyarakos et al., (2009), analyzed the dynamic behavior of multistory structures with an isolated base under the influence of three different types of earthquakes with and without SSI using the SAP2000 computer program. The results showed that SSI is an important factor to be considered when selecting the appropriate isolator for isolated base structures in soft soils. Other studies have focused on the influence of SSI on the fragility

curves and seismic vulnerability assessment of structures. (Karapetrou et al., 2015; Rajeev & Tesfamariam, 2012)

It has been well demonstrated that the nature of the SSI is essentially frequency dependent (Saitoh, 2007; Wolf & Preisig, 2003), and thus the dynamic impedance functions are affected by the frequency content of the seismic motion input. However, due to various difficulties in the numerical analysis, the simplified hypotheses have been adopted. The frequency-independent representation of the soil-structure interaction in a structure can, under certain circumstances, lead to a structural behavior that is very different from the actual behavior and, therefore, can cause misdirection in the design engineer's decision. For example, Lesgidis et al., (2017) investigated the effect of the frequency dependence of the soil-structure interaction on the fragility of RC bridges by comparing the predicted fragility of a reference bridge using both a conventional, frequency-independent Kelvin-Voigt model and the lumped parameter formulation developed by the same authors. Several studies have shown that the simplified, frequency-independent approach can both underestimate and overestimate the actual fragility curves of a bridge, resulting in a structural behavior that is significantly different from the actual one. According to Betti et al., (1993), the outcome of the response of the structure to seismic excitation depends on the characteristics of the ground motion and the dynamic properties of the structure and the underlying soil, and these influencing factors should be sufficiently considered to correctly estimate the behavior of the structure under seismic loading.

This thesis deals with the dynamic soil-structure interaction (SSI), which is often ignored in the dynamic analysis of reinforced concrete structures. This first chapter illustrates the complexity of the SSI phenomenon by focusing on the kinematic and inertial interaction. It presents the different analysis methods used to model this phenomenon and the dynamic impedance of the foundation, which is an essential parameter to represent the SSI and obtain the response of the soil-foundation-structure system.

I.2. THE SOIL-STRUCTURE INTERACTION PHENOMENON

Consider two identical structures, one embedded in rock and the other resting on a softer soil mass. Under seismic loading, we can imagine that the two structures will behave very differently. The structure embedded in rock has no effect on the behavior of the soil in the free field. The stiffness of the rock is infinite. Therefore, embedding the structure in the

rock does not change the stiffness of the soil-structure system. Similarly, the inertial forces generated by the mass of the structure have no effect on the very stiff rock. In the case of a structure resting on a soft soil mass, whose stiffness and natural frequencies are less important than those of a structure embedded in rock, it is possible that more amplified displacements will occur. This indicates that the soil properties have a significant effect on the dynamic behavior of the structure. Conversely, the behavior of the soil can be modified by the presence of the structure. In fact, the behavior of the soil in the free field can be significantly different from that in the presence of the structure. The term free field is used to describe the motion that occurs unaffected by vibrating structures. If structures are present, the motion in the vicinity of the foundations may be different from the free field motion.

Thus, soil-structure interaction refers to the way in which the soil and a structure built on it interact with each other; it evaluates the collective response of the structure, the foundation, and the soil underlying and surrounding the foundation to a given ground motion. The behavior of the soil and the structure can influence each other, and understanding this interaction is important for designing safe and efficient buildings, bridges, and other structures. This interaction is, of course, more or less important depending on the nature of the soil, the characteristics of the structure, and the type of foundation. The soil-structure interaction can have a significant effect on the behavior of the structure during loading events, such as earthquakes. Therefore, SSI analysis is an essential part of the design process for structures that must withstand extreme loading events.

Fig. I.1, illustrates the SSI problem. This figure shows the general case of a raft-type foundation embedded in the ground and supported by piles crossing several layers of soil resting on a rigid or rocky layer. However, the SSI problem is the same for all types of foundations. The soil layer surrounding a structure is subject to different types of seismic waves, such as shear waves (S waves), compressional waves (P waves), and surface waves (R or L waves). (Pecker, 2007)

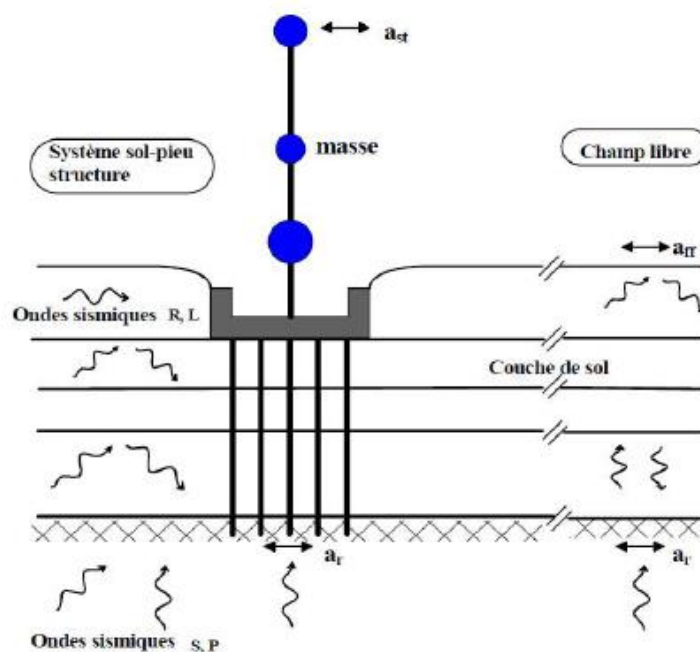


Fig. I.1. Illustration of the SSI. (Pecker, 2007)

There are several factors that can affect soil-structure interaction, such as the characteristics of the soil, the geometry and stiffness of the structure, and the type and magnitude of loads applied to the system. Some of these key factors are:

- **Soil type and properties:** Different soil types have different properties, such as stiffness, strength, and permeability, that can affect the way they interact with structures. For example, loose, sandy soils are generally less stiff than dense, clay soils, which can affect the deformation and stability of structures founded on these soils.
- **Geometry and stiffness of the structure:** The geometry and stiffness of the structure can affect the way it interacts with the soil. For example, tall, slender structures are more susceptible to wind loads and may sway more than shorter, more squat structures.
- **Loads applied to the structure:** The type and magnitude of loads applied to the structure can also affect the soil-structure interaction. For example, seismic loads can cause the soil to liquefy, which can affect the stability and deformation of the structure.

To perform a comprehensive analysis of soil-structure interaction, several factors must be considered, including the variation of soil properties with depth, the nonlinear behavior of the soil, the three-dimensional nature of the problem, the complex pattern of wave propagation that generates motion, and the interaction with adjacent structures. Observations

and post-seismic analyses have shown that the interaction between the soil and the structure plays an important role in the seismic damage. (Sbartai, 2016, 2018)

Studies of coupled soil-structure systems should be strongly encouraged, because without them there is a risk of misinterpreting the seismic response of a structure (Abate & Massimino, 2017; Massimino et al., 2019; Mylonakis & Gazetas, 2000). Thus, there are several important reasons to consider soil-structure interaction in the design and construction of structures (Guéguen et al., 2000):

- To include deformation modes and movements at the base of the structure in the analysis by considering a coupled soil-structure system.
- To obtain a better knowledge of the vibration frequency of the coupled system, which will be extended with implications for its dimensioning or for its evaluation.
- To fully evaluate the behavior of critical structures.

In contrast to the commonly assumed fixed base model, the soil-structure system is certainly more flexible. Therefore, SSI effects (Crouse & McGuire, 2001; Pitilakis et al., 2005) have been reported in the literature as natural period elongation and additional composite damping. In general (V. Davidovici, 1999), soil deformability leads to:

- A lengthening of the period of vibration of the first mode in particular, which can cause a plus or minus variation of the acceleration value depending on the zone. (Awchat & Monde, 2021)
- A non-negligible damping (radiation damping + material damping). Not taking it into account leads to an overestimation of the response.
- A rotation of the foundation, which can significantly change the calculation of the modal deformation and thus the distribution of the accelerations over the height of the building.
- The ground motion at the base of the building is assumed to be identical to that of the free field, and in most cases this approximation is considered acceptable.

The SSI effect is most significant for stiff and/or heavy structures supported on relatively soft soils. However, for soft and/or light structures supported on stiff soils, the SSI effect is generally small.

Dynamic SSI can have several complex effects, and the beneficial or detrimental effect of seismic SSI is still a controversial issue, and neglect of SSI in the analysis can lead to unconservative design (Abdel Raheem et al., 2015). For structures for which the consideration of SSI is not required by Eurocode 8 or Eurocode 5, the effects of SSI tend to be beneficial, since they generally allow a reduction of the loads by dissipation at the ground level and by a more favorable spectral value. In fact, we can see in **Fig. I.2** that the consideration of SSI allows to increase the natural period of the structure, which in most cases reduces the value of the seismic response. Furthermore, on the same figure, we can see that the higher the damping, the lower the response. Other observations show that soil-structure interaction can have a detrimental effect on the structural response and that simplification of the SSI effect in seismic codes can lead to poor structural design. Shakib & Fuladgar, (2004) showed that soil-foundation-structure interaction reduces lateral displacement and torsion of asymmetric buildings. Numerical simulations by Jeremic et al., (2004) showed that the interaction between the soil and the structure can have a beneficial or detrimental effect on the behavior of the structures, depending on the characteristics of the soil and those of the seismic loading. Mylonakis & Gazetas, (2000) have shown that an increase in the fundamental period of the structure does not always lead to a decrease in the amplitude of the seismic response. Consequently, the Soil-Structure Interaction (SSI) can have a detrimental effect on the structural response and simplifying the SSI effect in seismic codes can lead to poor design of structures.

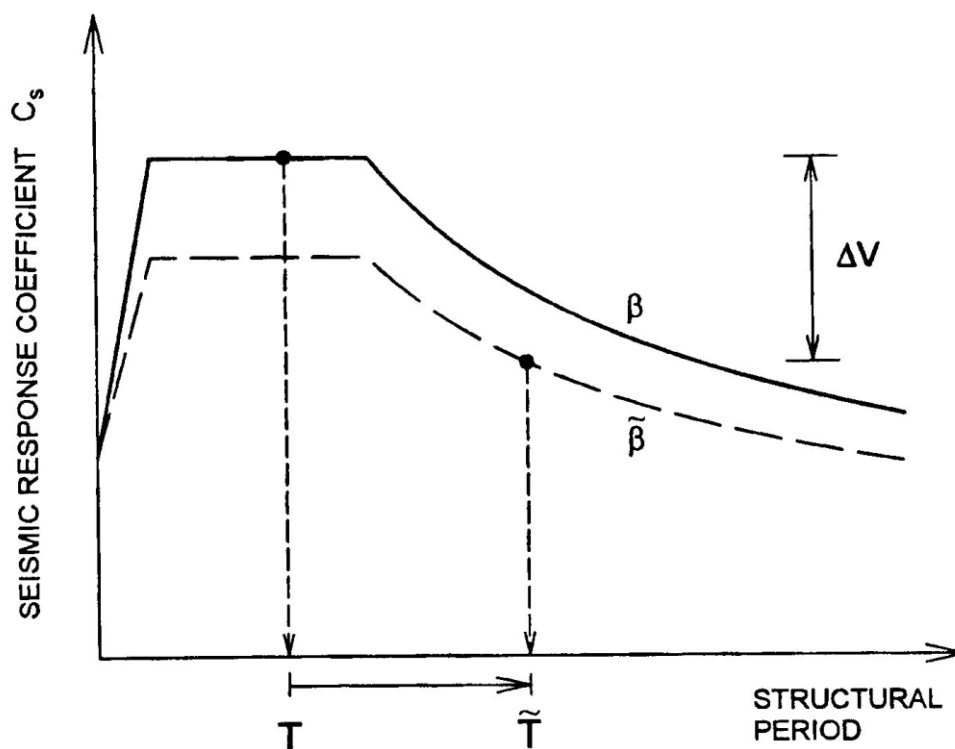


Fig. I.2. A spectral reading that shows the effect of taking the SSI into account.

(Mylonakis & Gazetas, 2000)

I.3. THE COMPONENTS OF THE SOIL-STRUCTURE INTERACTION

Since the ground is very rigid, the addition of a structure does not change its behavior. The mass of the structure does not change either, since the inertial forces generated by the structure on the rigid rock do not affect it. On the other hand, for the structure resting on the flexible soil, two phenomena of interaction occur simultaneously between the structure, the foundation and the soil: Kinematic interaction and inertial interaction.

I.3.1. Kinematic interaction

It is due to the difference between the movement of the foundation and the movement of the free ground. The excavation and insertion of a rigid foundation on or in the ground will change the characteristics and subsequently modify the free field movement (ground without foundation and superstructure). In fact, under seismic loads, the deformation of the ground will force the foundations to move and consequently drag the supported structure. Even without the superstructure, the total ground motion in the near field of the foundation and the motion of the foundation will be different from that of the ground in the free field because of

the difference in stiffness between the ground and the foundation. Incident waves are also reflected and scattered by the foundation, which in turn develops bending moments (**Fig. I.3**). Since the soil is flexible, there must also be additional deformations at the foundation (horizontal displacement and rocking) that are different from the case of a foundation embedded in a rigid soil (Mahsuli & Ghannad, 2009; Mylonakis & Voyagaki, 2006). Thus, this interaction between the rigid foundation and the soil (kinematic interaction) modifies the seismic motion acting on the base and consequently leads to accelerations (inertial forces) along the height of the structure that are different from those developed in the structure embedded in the rock mass (embedded base). The kinematic interaction can be interpreted as the response of the soil-foundation-structure system when the foundation-structure system is considered massless and rigid interface connections are introduced at the soil-foundation interface. The main effect of the introduction of the rigid foundation with negligible mass in the soil is the modification of the input motion in the foundation from the free field ground motion. The kinematic interaction analyses predict frequency-dependent transfer function amplitudes between foundation and free-field motion (Jiachun, 2005). The kinematic interaction effect is particularly important for massive deep foundations such as caissons (Beltrami et al., 2006). In most cases, the kinematic interaction leads to a response \ddot{u} that is smaller than the free field response but contains a rotational component. (Mylonakis & Voyagaki, 2006)

I.3.2. Inertial interaction

The second and more important form of SSI is known as inertial interaction. It is caused by the presence of structural masses (**Fig. I.3**). The motion induced in the foundation generates vibrations in the superstructure, resulting in inertial forces that are transmitted back to the foundation in the form of forces and moments, creating a wave field that propagates from the structure back into the ground. As the soil is flexible, these forces generate displacements and rotations at the soil-foundation interface which contribute significantly to the flexibility of the whole structure and increase the period of the structure (NEHRP 2012). This in turn changes the movement at the base of the structure again. (J-I, 2008; Murono & Nishimura, 2000; Stewart et al., 2003; Tileylioglu et al., 2011; Uildings et al., 1999) The energy generated by the motion of the structure is dissipated in two ways: a hysteretic (material) damping due to the nonlinearities present in the soil and in the foundation, and a radiative damping due to the radiation of the waves in the soil, where the foundation manifests itself as a wave source. In the general case of surface foundations without a large

rigid foundation slab, the effects of the inertial interactions are more important than the effects of the kinematic interactions for the foundation.

The generic term that encompasses both of these phenomena is called Soil-Structure Interaction (SSI). However, most engineers use this term to refer to inertial loading and ignore the portion due to kinematic load. This is because:

- In some cases, the kinematic interaction is negligible.
- Most seismic codes, except some including Eurocode 8, do not mention it.
- The effects of kinematic interaction are more difficult to evaluate rigorously than the inertial effects.

This is also consistent with the results of most researchers who find that the kinematic interaction is significantly less important than the inertial interaction. (Avilés & Pérez-Rocha, 2005a, 2005b). The importance of these two phenomena depends on the characteristics of the structure, the foundation, the soil and the nature of the seismic waves.

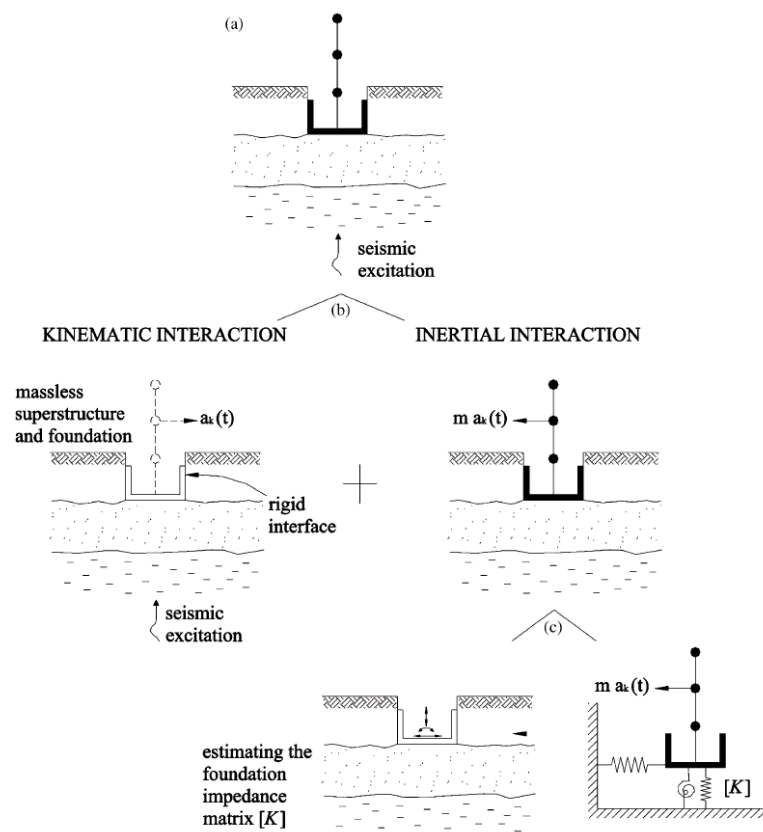


Fig. I.3. (a)The SSI phenomenon; (b)Decomposition into kinematic and inertial interaction; (c)Two-step analysis of the inertial interaction. (Mylonakis & Voyagaki, 2006)

I.4. METHODS OF ANALYSIS OF DYNAMIC SOIL STRUCTURE INTERACTION PHENOMENON

In general, the most commonly used methods for soil-structure interaction analysis can be classified into three categories, each corresponding to a schematization of the soil-structure model: the direct (global) method, which consists of modeling the soil and structure in a single model, the substructure method, which decomposes the problem into simpler sub problems and is applicable only in the linear domain and for weakly nonlinear systems (MYLONAKIS et al., 1997), where the superposition principle can be justified (Jeremić et al., 2009; Pecker, 2007). and the hybrid method that was developed by Gupta et al in 1980. The methods are described and detailed in numerous works. (Mohammadioun & Pecker, 1984; Wolf, 1989). They are briefly presented in the following section:

I.4.1. The direct method

The first class of existing methods for SSI analysis, as mentioned before, is the direct method. This method deals with the problem of soil-structure interaction in its entirety so as to obtain the response of the soil and the structure simultaneously, it consists in directly solving the equation of motion in the whole of the soil-structure system. The calculation is performed in single step (Burman et al., 2012; Seghir & Torres-Martínez, 2011). As can be seen in **Fig. I.4**, the calculation is performed in one step by directly solving the equation of motion (**Eq. (I.1)**) in the whole soil-structure system:

$$M\ddot{u} + C\dot{u} + Ku = F \quad (\text{I.1})$$

Where M , C and K are the mass, damping, and stiffness matrices of the system, respectively, u is the displacement vector of the system, and F is the load vector applied to the outer boundary of the system. To solve this system of equations, numerical methods (Finite Element Methods) are widely used, because their direct solution is very complex. **Fig. I.5** shows the solution scheme of the global method. One of the main advantages of global (direct) methods is their ability to integrate into the numerical model the material heterogeneities of the soil and the structure, the geometrical singularities of the problem, and the behavioral laws well adapted to take into account the nonlinearities in the soil or at the soil-foundation interface of the system, under strong ground motions; thus, the soil and structure foundation elements are considered with their behavior and contact condition in the same analysis (G. Gazetas et al., 2008; Jingbo & Yandong, 1998; Maharjan & Bahadur, 2021;

Mohammadioun & Pecker, 1984). It is also possible to treat with this type of method the condition of radiation and energy dissipation (radiative damping) in the infinite part of the unbounded soil. The main techniques used to treat this condition are the use of absorbing boundaries, finite element-boundary element coupling and finite element-infinite element coupling, as well as other techniques (B. Galy, 2013). Direct methods are expensive, especially for three-dimensional problems. It requires mastery of specialized computational software programs and a good knowledge of the laws of material behavior and the boundaries between different parts of the system. Despite its complexity, this method remains realistic. However, it is essential to formulate simpler and easier methods.

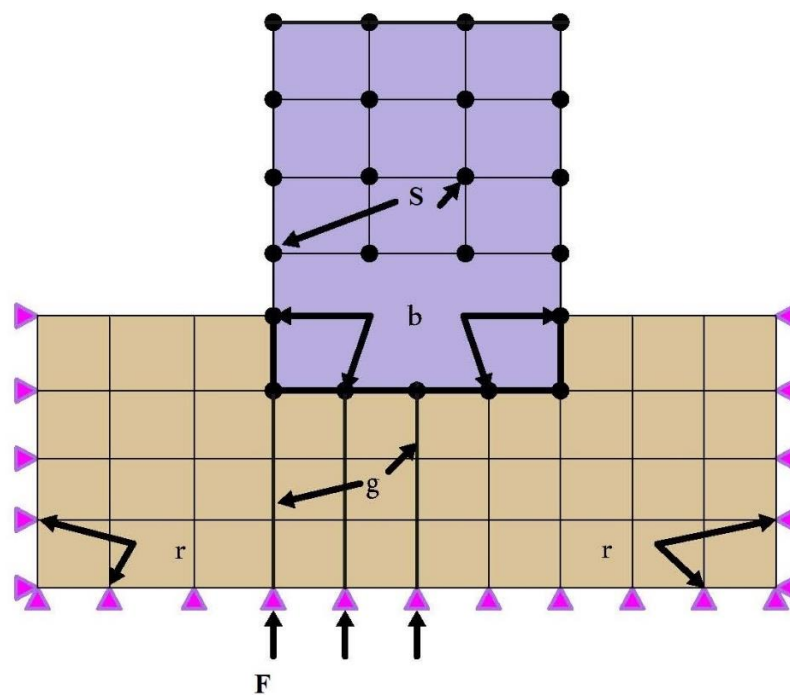


Fig. I.4. The direct method model.

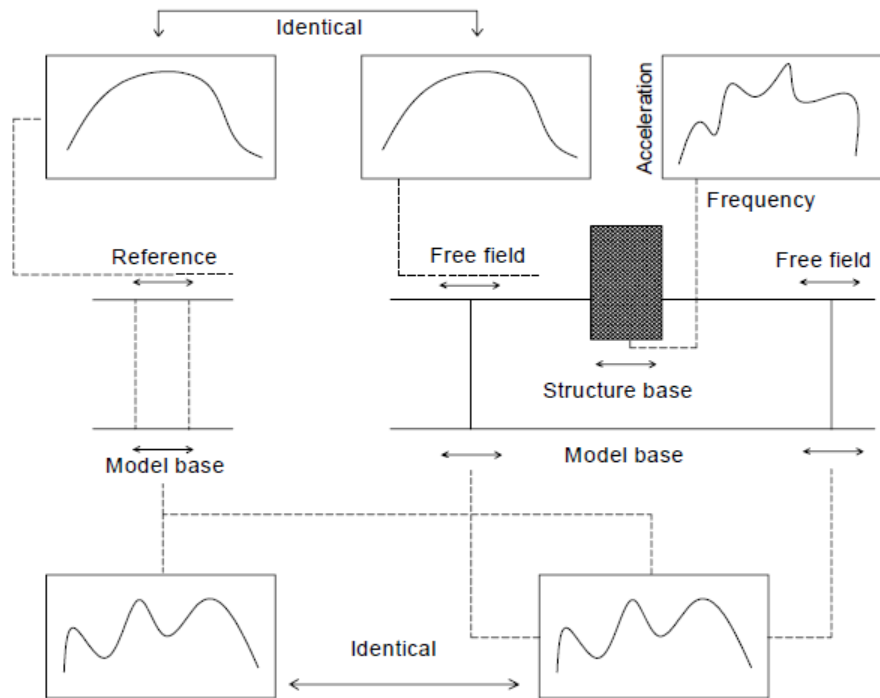


Fig. I.5. The direct method solution scheme. (Tahar Berrabah, 2012)

I.4.2. The substructure method

The substructure model (Wolf 1994) (**Fig. I.6**) has been widely used in SSI seismic analysis of surface structures. In contrast to direct methods, the model consists of analyzing the SSI problem in several successive steps, each of which is considered easier to solve from a modeling or processing perspective than the global problem (direct method). This approach generally decouples the kinematic and inertial analyses and uses the principle of superposition developed by Kausel et al., (1978). Like any superposition problem, these methods are quite limited in that they are only applicable to linear problems. However, a lot of work has shown that this technique can give very good results (Pitilakis et al., 2008). The most important key step in this method is the determination of a coupling element between the structure and the soil-foundation system. In the linear elastic domain, this coupling element corresponds to impedance functions that are applied to the foundation of the structure to determine its response (Çelebi et al., 2006). The sequential steps of this approach, shown in **Fig. I.7**, are as follows (Zhang and Wolf, 1998):

- First, the substructure consisting of the geotechnical profile and the foundation without mass is considered. The soil-foundation interface is assumed to be infinitely rigid. A

motion is applied to the base of the geotechnical profile to calculate the response \ddot{u} of the system at the rigid soil-foundation interface. The presence of the rigid foundation modifies the motion that would be obtained in the free field. This modification is known as the kinematic interaction. This step can be neglected if there is a shallow foundation and the structure is subjected to a wave that propagates only vertically (i.e., the kinematic interaction is considered to be zero). (G. Gazetas et al., 2008; Pecker, 2007; Stewart et al., 1999)

- The second step concerns the determination of the dynamic impedance of the foundations, it consists in replacing the soil-foundation system by spring-damper elements (Boumekik, 1985). The calculation of the dynamic impedances is the first step in the analysis of the inertial interaction and the analysis of the kinematic interaction. In most studies, the impedances are estimated by analytical, semi-analytical and numerical methods (the boundary element method, the finite element method and the boundary element method coupled with the finite element method) or by approximate expressions (G. Gazetas, 1983; G. Gazetas & Stokoe, 1991; Kausel et al., 1975; Sbartai & Boumekik, 2008; Stewart et al., 2003; Wong & Luco, 1985). The impedance functions have a real and an imaginary part depending on the frequency. The real part of the impedance corresponds to the stiffness of the soil-foundation system, while the imaginary part represents the radiation damping. This impedance is a characterization of the dynamic forces acting on a foundation of negligible mass when subjected to a harmonic load of unit amplitude. For each of the six degrees of freedom (three translations and three rotations) of the foundation, complex impedance functions are calculated that depend on the frequency of the applied load. *The definition of impedance functions is presented in Section I.5.*
- In the third step, we determine the dynamic response of the structure connected to the mass of the ground through the impedance springs calculated in the second step and subjected to the seismic loading obtained in the first step. The solution of this problem remains classical and often uses the finite element method.

The substructure method reduces the computation time compared to the direct method. The use of impedance simplifies the calculation assumptions compared to those that must be introduced into a model using the direct method.

In our work, the latter method was used to study the influence of changes in soil behavior under seismic excitation on the seismic response of a building (frequency, damping ratio, Shear modulus, displacement...).

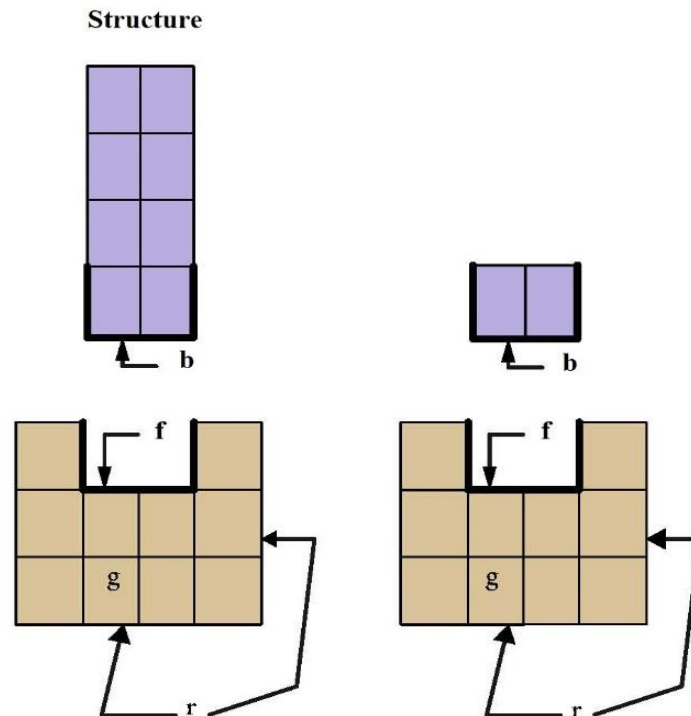


Fig. I.6. The substructure method model.

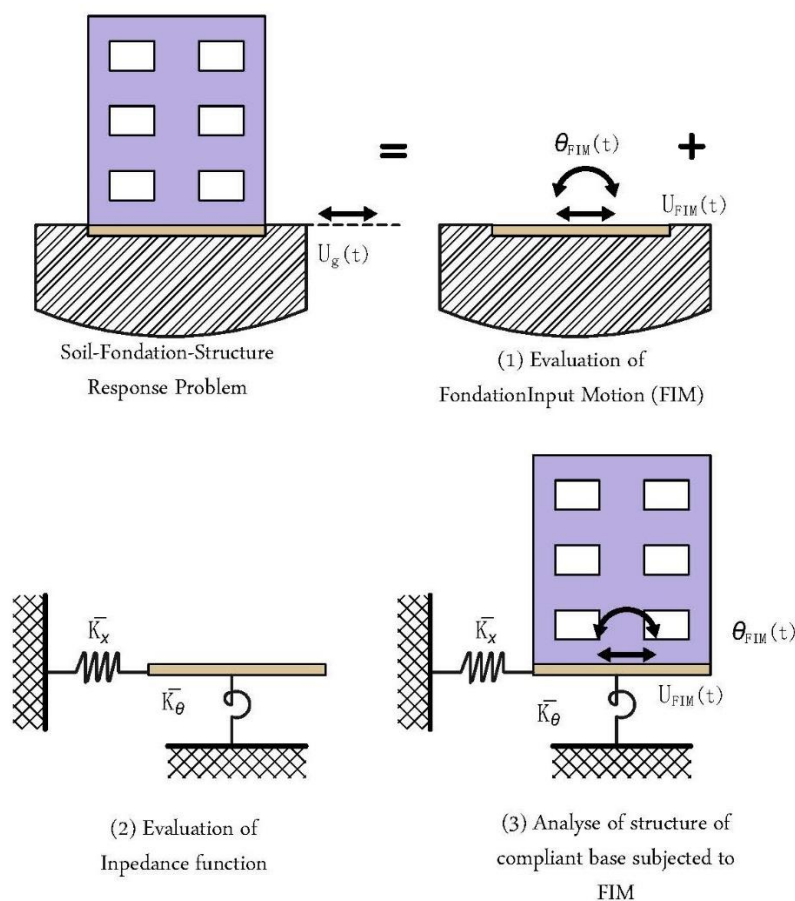


Fig. I.7. The most important steps of the substructure approach.

1.4.3. The hybrid method

The Hybrid Method is the third major family of methods used to assess the SSI phenomenon. This method lies between the direct method and the substructure method. The hybrid method was developed to overcome the disadvantages of the previous methods, although it also has its drawbacks. This method is a combination of the direct and substructure methods, taking advantage of each method's advantages (Chatzigogos et al., 2009). This method divides the problem into two subdomains. The first semi-infinite domain, called the far field, is formed only by the soil and is far enough away from the foundation that it is not affected by the SSI. For these reasons, this field is considered elastic (linear) and the methods adapted to linear problems (dynamic impedance) are used to model it. Thus, it is in this field that the energy dissipated due to radiative damping can be considered (**Fig. I.8**). The second finite field, called the near field, is formed by a surface foundation and a finite volume of the underlying soil. This field includes all the heterogeneities and nonlinearities of the system, which are composed of two parts: the material nonlinearities (plasticity of the soil) and the

geometric nonlinearities (due to foundation movement). It is integrated in the model of the superstructure and can be treated by a direct method (the finite element method) and also the concept of the macro-elements can be used (Cremer et al., 2001). Thus, this method reduces the computational time compared to the direct method. The difficult part of the hybrid method is the definition of the boundary between the near and far fields. Like the direct method, this method provides an accurate model of the SSI because it takes into account the nonlinearity in the near-field ground. This type of method requires sophisticated modeling. (Halabian & El Naggar, 2002; Sayyadpour et al., 2016)

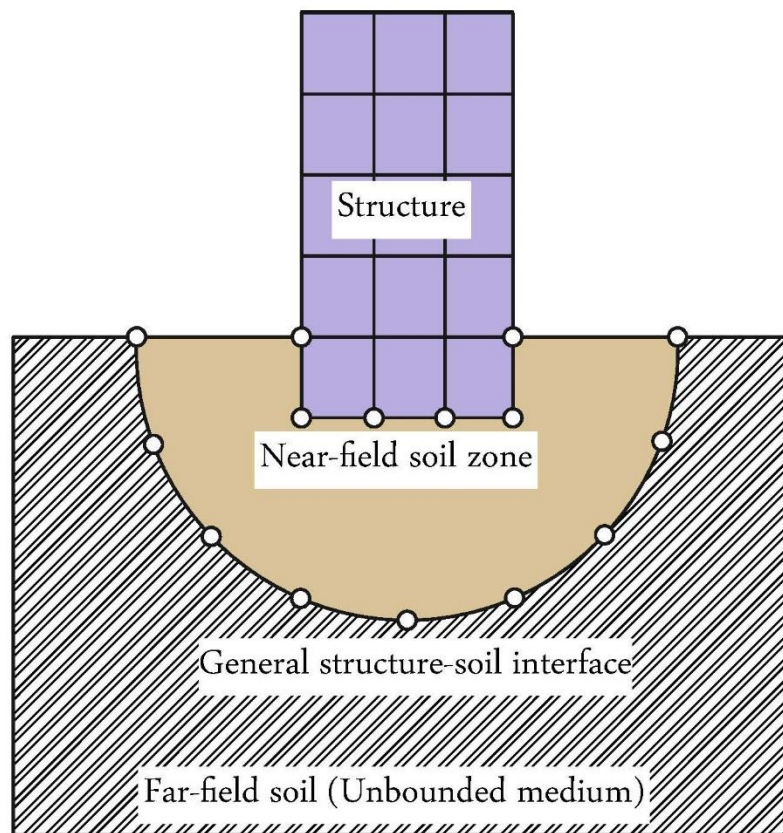


Fig. I.8. The soil-structure system considered in hybrid methods.

I.5. IMPEDANCE FUNCTIONS

From the previous sections, it is clear that the dynamic impedance of the foundation is an essential parameter for the representation of the SSI and for obtaining the response of the soil-foundation-structure system. the dynamic response of foundations is an important research topic because it affects the safety and reliability of the structures built on them. When a

structure is subjected to dynamic loads, such as earthquake or wind loads, the foundation can deform and vibrate, which can cause damage or failure of the structure. Therefore, understanding the dynamic behavior of foundations is critical to ensuring the safety and longevity of structures. Many studies have been conducted on this topic since the early 1970s, and researchers continue to investigate new methods for analyzing and designing foundations to withstand dynamic loads (Ahmad & Rupani, 1999; Assimaki & Kausel, 2002; Badreddine & Fillali, 2012; Bolisetti, 2015; Cavalieri et al., 2020; G. Gazetas, 1991; Ghandil et al., 2016; Guellil et al., 2020; Jaya & Meher Prasad, 2002; Jayalekshmi et al., 2014; Masaeli & Ahmadi, 2021; Sbartai, 2018; Stewart et al., 2003; Tahar Berrabah et al., 2012; Tileylioglu et al., 2011; Veletsos & Meek, 1974; Wolf & Preisig, 2003). Calculating the impedance functions of a foundation is an important issue in geotechnical engineering (Liu et al., 2020; Zhang and Wolf, 1998), its main role is to couple or facilitate the connection between the soil and the structure that allows the two subdomains to interact. (Petridis et al., 2018; Ronak et al., 2021)

In simple terms, the impedance of a foundation is equal to the reaction exerted on the massless foundation when it is subjected to unit harmonic displacements directed along one of its degrees of freedom (**Eq. (I.2)**) (Pecker, 2007). Thus, the impedance is the quotient of a force applied directly to the foundation (which is equal to the soil reaction) and the resulting displacement. (Pena and Guzman 2014).

$$S = F/u \quad (\text{I.2})$$

According to (G. Gazetas, 1991), the complex dynamic impedance S of the foundation is expressed as follows:

$$S = K + i\omega C \quad (\text{I.3})$$

Where the real component K is the dynamic stiffness, which reflects the stiffness and the inertia of the system (soil - foundation). The imaginary component ωC of the dynamic impedance is the circular frequency ω multiplied by the damping coefficient C , which expresses the radiation and material damping of the system (**Eq. (I.3)**). Radiation and material damping result from waves propagating away from the foundation and energy dissipation due to the effect of hysteretic material in the soil, respectively.

As shown in **Fig. I.9**, the impedance can be represented by a set of springs and dampers. In the general case, there is dynamic impedance of the foundation for translational (horizontal or vertical), rocking, and torsional modes. There is also coupled horizontal rotation-

displacement impedance. At this point, a rigid foundation has six degrees of freedom, so the impedance matrix has the dimension (6×6) . The different degrees of freedom are coupled and the impedance matrix is full if the foundation has any shape at all. If the foundation has symmetries, some off-diagonal coupling terms disappear. In the case of the circular foundation, there are 4 degrees of freedom: horizontal and vertical translations, rotation about a horizontal axis, and rotation about a vertical axis. The vertical translation and the rotation around a vertical axis are completely uncoupled from the other degrees of freedom; on the other hand, the horizontal displacement and the rotation around a horizontal axis are coupled in all theories; but for the surface foundation the coupling term is negligible and it is allowed to consider that the impedance matrix is a diagonal matrix of dimension (4×4) .

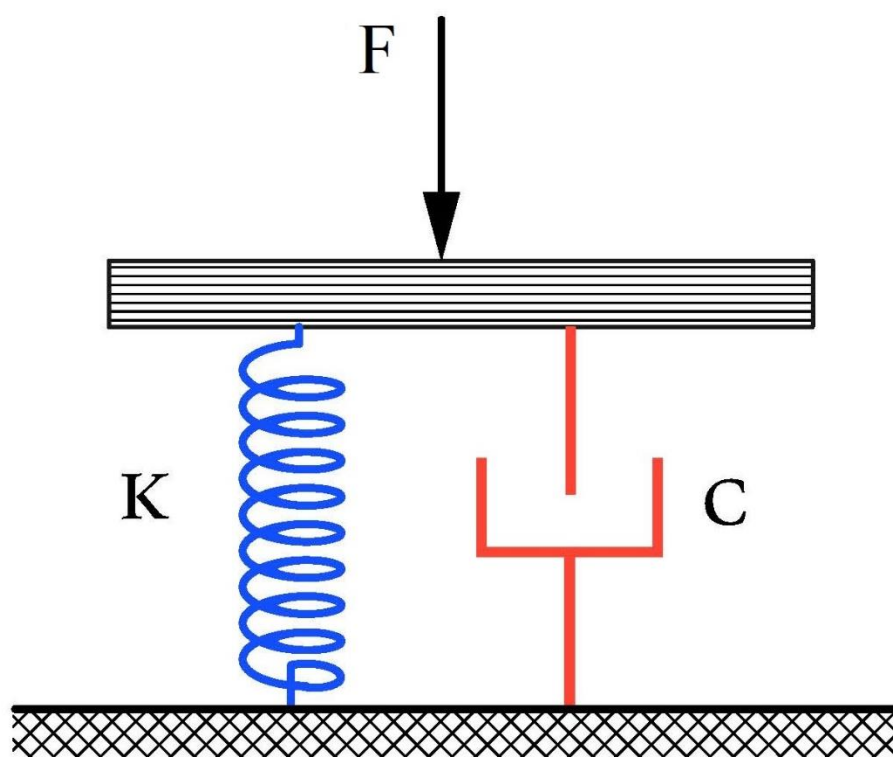


Fig. I.9. Vertical impedance of a simple oscillator.

The impedance functions are an important parameters, especially when selecting the mathematical model to be used for the analysis, and it can be affected by several factors, including: (i) the shape of the foundation, whether it is circular, rectangular, or arbitrary; (ii) the type of soil profile, such as a deep layer, a multi-layer soil profile, or layers over bedrock; and (iii) the embedment of the foundation, such as whether it is a surface foundation, an embedded foundation, or a pile foundation.

The dynamic response of a rigid, massless foundation has been the subject of numerous studies over the past three decades. Horace Lamb, (1904) studied the vibrations of a semi-

infinite linear elastic body subjected to a concentrated harmonic load. In 1936, Reissner, (1936) analyzed the response of a disk placed on the surface of an isotropic and semi-infinite elastic body. This analysis revealed the existence of energy dissipation by radiation as if the propagation medium had some damping. Based on these results, Sung, (1953) extended Reissner's work to the motion of the six degrees of freedom of the foundation. The idea of treating the behavior of the soil-foundation system, in vertical translation, as a simple oscillator of constant stiffness and damping was introduced by Lysmer, (1965). This approach is known as the "Lysmer analogy". The work of Veletsos & Wei, (1971) on the dynamic analysis of the flexibly mounted system was a significant contribution to the field of structural engineering. They introduced the concept of a massless disk as a way to simplify the analysis of flexible foundations. By modeling the foundation as a disk, they were able to calculate the dynamic response of the system with greater accuracy and efficiency.

We also note the important contribution of Gazetas (B. G. Gazetas, 1992; G. Gazetas, 1983; G. Gazetas & Stokoe, 1991). In his research work on soil-structure interaction, and in particular on the determination of impedance functions, he provides a set of graphs and tables for the calculation of impedance functions of certain dimensionless parameters and valid for a foundation of any shape on the surface or buried resting on a homogeneous semi-infinite medium or on a soil mass resting on a bedrock. It also provides algebraic formulas and dimensionless curves corresponding to an unburied surface foundation resting on a heterogeneous half-space. These results are based on simple physical models calibrated by the results of the boundary element formulation. They make use of all previous work related to the calculation of impedance functions. The case of strip footings on a semi-infinite elastic, homogeneous and isotropic medium is also treated. The impedance functions have been developed by an analytical method of integral equations solved numerically. (Mylonakis & Gazetas, 2000)

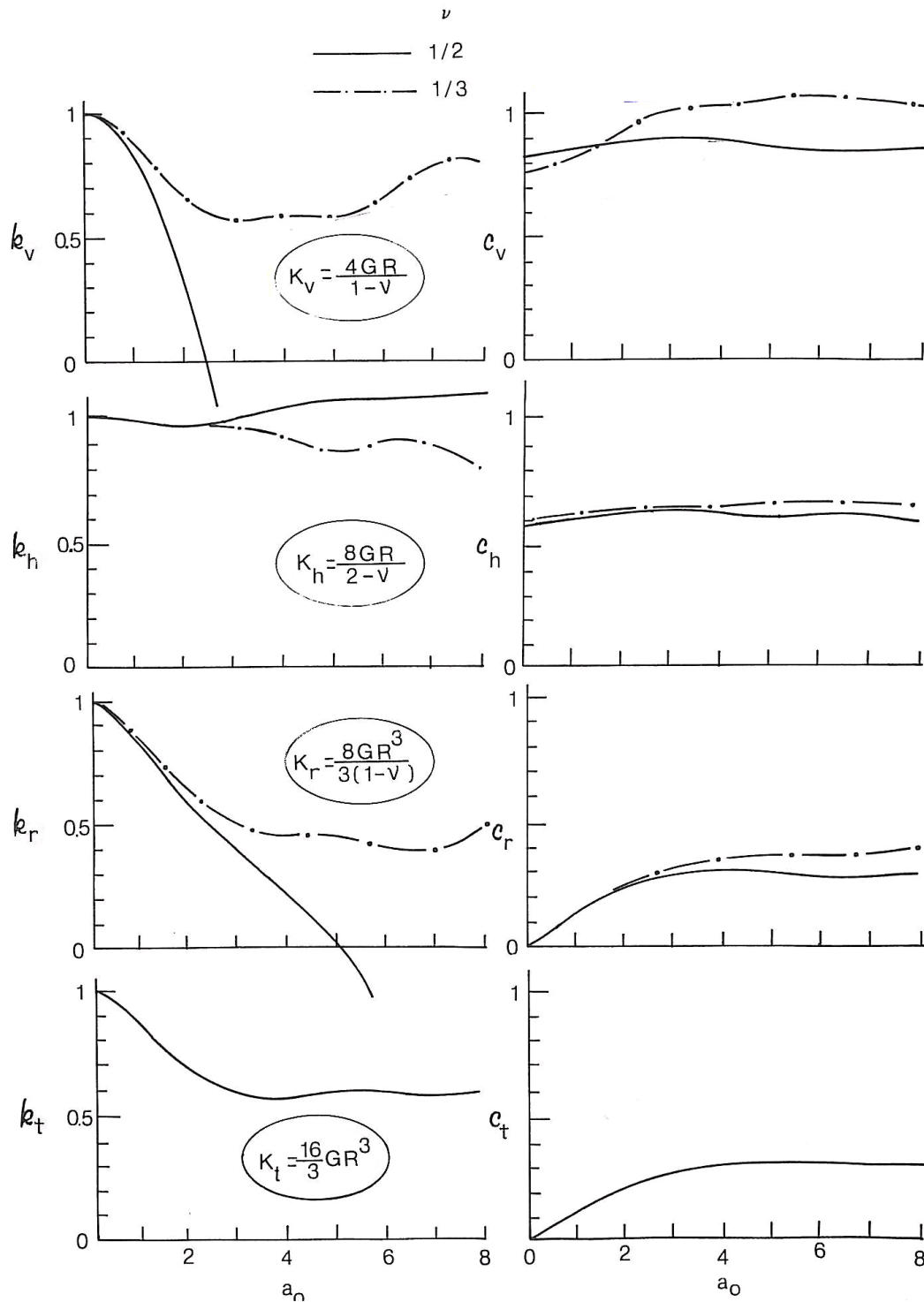


Fig. I.10. Impedance functions of rigid circular foundations on homogeneous half-space. (G. Gazetas, 1983)

I.6. SOIL-STRUCTURE INTERACTION IN SEISMIC CODES:

In the majority of current building codes, the design calculations of structures are performed by neglecting the soil-structure interaction (SSI); the dynamic response is obtained

by assuming that they are embedded at their base. This assumption has been adopted by the codes in the belief that the SSI always plays a beneficial role in reducing the inertial forces acting on the structures. This assumption proves to be correct for the majority of buildings and seismic environments, but it results in a design that is often too conservative and not in line with the performance-based seismic design approach. Moreover, post-earthquake observations have shown that the SSI can be detrimental for some buildings built on unconventional soils (Mylonakis & Gazetas, 1998). One of the main reasons for not considering the SSI in engineering studies is the complexity of the methods used in the analyses, since they require a good definition of the soil parameters under the foundation of the structure to be studied, which is very difficult and very expensive. However, seismic codes try to approach this problem in a simplified way. In order to optimize the design of buildings or to predict their seismic behavior in a more realistic way, international building codes are beginning to introduce clauses that allow the consideration of SSI in the design phase. Eurocode 8 (EN-1998-5) requires the study of the effects of dynamic soil-structure interaction in the following cases:

- ❖ Structures where P- Δ (2nd order) effects play a significant role, such as slender structures, where the eccentricity of the weight of the masses with respect to the vertical axis induces an additional bending moment;
- ❖ Structures with massive or deep foundations, such as bridge piers, silos or similar industrial structures;
- ❖ Narrow and thin structures such as towers and chimneys covered by EN 1998-6: 2004;
- ❖ Buildings supported on very soft soils with average shear wave velocity V_s less than 100m/s, such as S1 soils.

I.7. CONCLUSION

The phenomenon of soil-structure interaction is an essential field of study in civil engineering. It refers to the complex relationship that exists between the soil and the structures built on it. It can have adverse or beneficial effects on structures. Understanding this interaction and considering the geotechnical characteristics of the soil in the design of structures is critical to the design and construction of durable and safe structures.

In order to design and construct durable and safe structures, it is essential to understand this interaction and to consider the geotechnical characteristics of the soil in the design of structures. As we continue to increase our knowledge in this area, we will be able to design

structures that are more resistant and better adapted to the geotechnical environment in which they are located.

This chapter is dedicated to a bibliographical analysis of the soil-structure interaction phenomenon and its two components that occur simultaneously between the structure, the foundation and the soil: Kinematic interaction and Inertial interaction, as well as to their different analysis methods and to the dynamic impedance of the foundation, which is an essential parameter to represent the SSI and to obtain the response of the soil-foundation-structure system.

Finally, a general view on the soil-structure interaction in seismic codes and the cases required by the Eurocode 8 (EN-1998-5) for taking into account its effects in the studies.

A detailed study of the linear and nonlinear behavior of the soil and its criteria is presented in the following chapter.

CHAPTER II: DYNAMIC PROPERTIES OF SOILS

II.1. INTRODUCTION

The determination of shear modulus and damping in particular, and soil properties in general, highlights the complexity of describing the behavior of this material. In the literature, soil behavior models range from simple linear elastic models to more complex nonlinear elastoplastic models (Pitilakis et al., 2005). The approach generally taken to determine soil behavior laws is to derive simplified concepts from experimental data that express the essential characteristics of soil behavior. These concepts are then assembled into a model based on the fundamental theories of continuum mechanics.

Although soil can be approximated as a linear material in many geotechnical analyses, strong seismic excitation generates additional deformations that can induce nonlinear behavior (de Silva et al., 2018; Halabian & El Naggar, 2002). For example, high stresses and strains can lead to variations in stiffness and strength, as well as elastoplastic behavior. These nonlinearities can affect the response of the soil and the structures built on it.

In the process of designing a soil-foundation-structure system subjected to earthquakes, the behavior of the soil must be considered with the best possible prediction to represent its actual behavior (as a nonlinear constitutive model). Soil nonlinearity has a large effect on the dynamic response of the system and is more appropriate for simulating real soil-structure interactions. (Pecker et al., 2014; Wood, 2014)

Sreya Dhar, Ali Güney Özcebe, Kaustubh Dasgupta, Arindam Dey, (2016) find that due to soil nonlinearity, there were changes in the PGA and maximum shear strain profile of the studied column between the FF (free field) and SFB (soil-foundation-bridge) models. Due to the high level of soil nonlinearity under the foundation, it was found that the seismic demand on the superstructure was significantly modified, with additional kinematic effects due to residual displacements of the bridge foundations.

According to the results of a numerical study by Luo et al., (2016) using a 3D finite element analysis of the SPSI system based on linear and nonlinear equivalent models, the seismic soil-pile-structure interaction can be significantly affected by soil nonlinearity, and the traditional linear equivalent soil model underestimates the structural acceleration response under seismic excitation.

In practice, the use of a computational code based on finite element or boundary element methods to account for soil nonlinearity is reserved for very specific structures

(nuclear power plants, dams, etc.). To this end, the researchers focused on simplified methods for numerical modeling of the SSI problem, taking into account the nonlinear behavior of the soil. (Fatahi & Tabatabaiefar, 2014; Sameti & Ghannad, 2016)

Robert et al., (2015) develops a general strategy for studying nonlinear dynamic soil-structure interaction problems in the context of seismic vulnerability analysis of buildings. Thus, realistic finite element models are developed and applied to nonlinear dynamic soil-structure interaction problems. The models cover a wide range of soil conditions and building typologies exposed to different seismic databases. A modeling strategy has been developed and validated to significantly reduce the numerical cost.

Sekhri, (2021) has numerically studied the global soil-pile-structure interaction problem under lateral loading and the soil-pile-structure and pile group interaction under dynamic loading using the ABAQUS code with consideration of soil nonlinearity by the "linear equivalent" method. His results confirm the reliability of this method, which provides a good fit for soil-pile-structure interaction problems.

The key step in the response of the soil-structure system is to study the behavior of the soil under cyclic loading and the resulting movement. Thus, a soil behavior law is defined by the relationship between stresses and strains due to imposed loads. The choice of soil behavior type is strongly dependent on the amplitude of the load (strain). The key parameter describing soil behavior is the amplitude of deformation. (Anastasopoulos & Kontoroupi, 2014; Johansson & Kaynia, 2021)

Soil behavior models and analysis methods as a function of shear strain are presented in the following table (**Table II.1**).

Table II.1: Soil Behavior Model and Analysis Method as a Function of Cyclic Deformation Amplitude According to Davidovici (1985).

Shear deformation	Less than 10^{-5}	Between 10^{-5} and 10^{-4}	Greater than 10^{-3}
Behavioral Law	Linear	Hysteretic Model	Highly nonlinear
Soil Representation	Linear Elastic	Viscoelastic	Incremental laws
Analysis Method	Linear	Equivalent Linear	Step-by-step integration

II.2. LINEAR SOIL BEHAVIOR

The linear elastic behavior of soil refers to the way a material deforms when subjected to external forces. In the case of soil, it describes the linear relationship between applied stresses and resulting deformations as long as the elastic limit of the material is not exceeded.

According to linear elastic behavior, when stress is applied to soil, it deforms reversibly and in proportion to the applied stress. This means that if you double the applied stress, the resulting deformation will also be doubled. Once the load has been released, the soil returns to its original shape without being permanently deformed.

This linear elastic behavior is a simplification used to model soil in many geotechnical engineering calculations. It is valid for small deformations and for soils that do not undergo significant changes in their internal structure when subjected to stress. However, it is important to note that some soils, such as clay soils, may exhibit non-linear elastic behavior due to the presence of consolidation, creep or particle interaction phenomena.

The concept of linear elasticity is illustrated in the following figure:

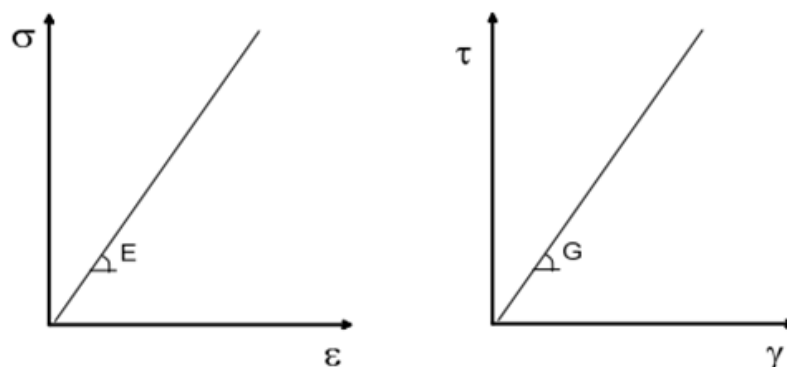


Fig. II.1. Illustration of Linear Behavior. (Davidovici, 1985)

In this figure, the shear modulus is defined by the constant G , which represents the behavior of the soil and is written by the following relationship:

$$G = \frac{\tau}{\gamma} \quad (\text{II.1})$$

where:

- τ is the cyclic shear stress,
- γ = cyclic shear strain.

Linear elastic behavior is generally represented by the following phenomena

- Large deformation amplitudes remain elastic.
- The overall safety factor is sufficiently high, or the loading is not very high.
- Local failures do not control the behavior in the region of interest.
- Low-amplitude seismic loads, such as those generated by geophysical testing.

II.3. NON-LINEAR SOIL MODEL

Nonlinear soil behavior refers to soil response that does not follow a linear relationship between applied stresses and resulting deformations. In contrast to linear elastic behavior, soils exhibiting nonlinear behavior may undergo permanent or irreversible deformation when subjected to loading.

During an intense seismic event, nonlinear ground behavior can play an important role, where the ground can undergo significant deformation and reach stress levels that exceed the elastic limit. This results in complex nonlinear responses due to the dynamic forces and accelerations induced by the earthquake. (Jia, 2018)

Nonlinear soil behavior is generally characterized by the decrease in the normalized shear modulus G/G_{max} and the increase in its damping ratio ξ/ξ_{max} as a function of shear strain γ (**Fig. II.2**). These two main parameters help to describe the behavior of the soil between low and high strains.

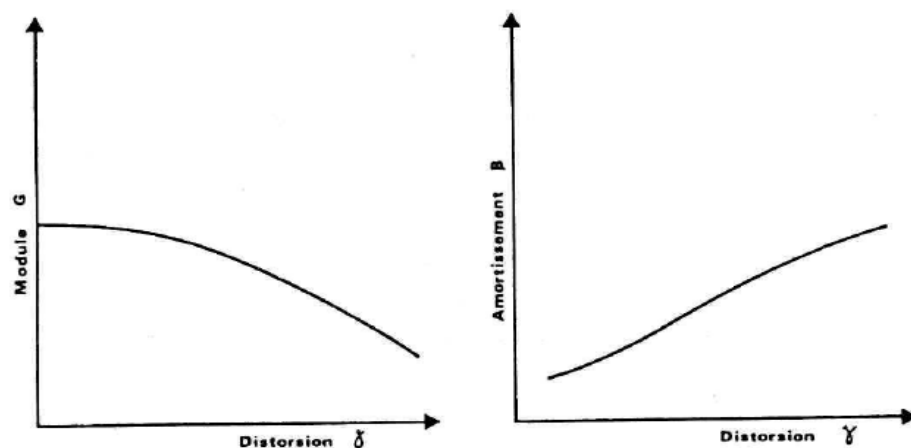


Fig. II.2. Variations in shear modulus and damping as a function of shear strain.

(Davidovici, 1985)

II.3.1. Nonlinear soil models under cyclic loading

The nonlinear stress-strain relationship can be more accurately represented by nonlinear cyclic models that translate the actual stress history described during cyclic loading tests. These models are based on the rules of Masing (1926), which suggest that the shape of the initial stress-strain curves follows the law $\tau = F_{bb}(\gamma)$ and can be represented by two parameters, the initial shear modulus and the shear strength.

$$F_{bb}(\gamma) = \frac{G_{max}\gamma}{1 + \left(\frac{G_{max}}{\tau_{max}}\right)|\gamma|} \quad (\text{II.2})$$

G_{max} and τ_{max} can be measured directly or calculated from empirical correlations.

II.3.1.1. Hyperbolic model of Masing

This model belongs to the family of models that use two parameters to define the stress-strain relationship (Kondner and Zelasko, 1963; Duncan and Chang, 1970), following the rules established by Masing (1926) for the construction of the skeletal curve and the hysteresis loop.

The stress-strain relationship for this model is defined by the following equation:

$$\tau_{max} = \frac{G_{max}\gamma}{1 + \left(\frac{\gamma}{\gamma_r}\right)} \quad (\text{II.3})$$

The secant modulus G can be derived from **Eq. (II.3)** in the following form:

$$\frac{G}{G_{max}} = \frac{1}{1 + \left(\frac{\gamma}{\gamma_r}\right)} \quad (\text{II.4})$$

The values of the G/G_{max} ratio calculated by **Eq. (II.4)** are shown in **Fig. II.3** as a function of the ratio $\frac{\gamma}{\gamma_r}$. Note that the secant shear modulus is halved when the shear strain becomes equal to the reference unit strain.

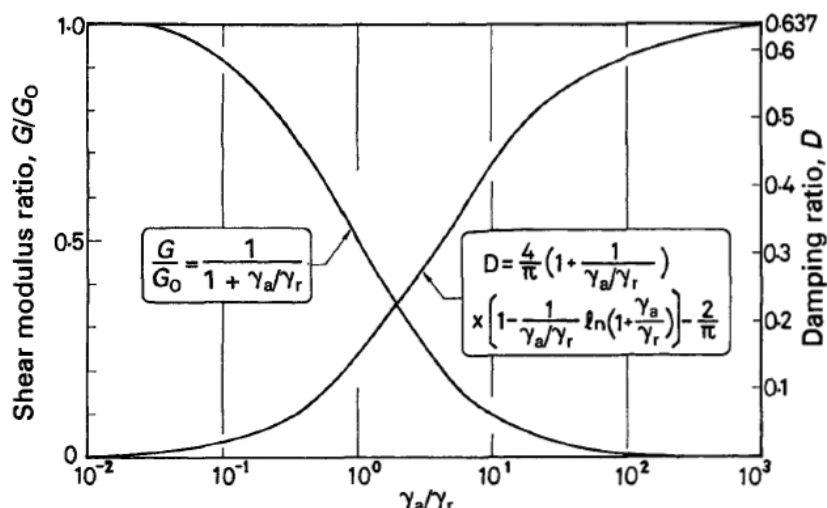


Fig. II.3. Shear modulus and damping fraction of the hyperbolic model. (Ishihara, 1996)

The expression for the damping fraction of the model can be derived by applying the rules of Masing (1926) to the skeletal curve given by **Eq. (II.3)**.

$$D = \frac{4}{\pi} \left[1 + \frac{1}{\gamma_a/\gamma_r} \right] \left[1 - \frac{\ln(1 + \gamma_a/\gamma_r)}{\gamma_a/\gamma_r} \right] - \frac{2}{\pi} \quad (\text{II.5})$$

Note that as the ratio $\frac{\gamma}{\gamma_r}$ becomes infinite, the value of D tends to $2/\pi=0.637$.

The damping fraction D can be expressed as a function of the ratio G/G_{max} by substituting **Eq. (II.4)** into **Eq. (II.5)**:

$$D = \frac{4}{\pi} \frac{1}{1 - G/G_0} \left[1 + \frac{G/G_0}{1 - G/G_0} \ln \left(\frac{G}{G_0} \right) \right] - \frac{2}{\pi} \quad (\text{II.6})$$

The following figure shows the calculated values of **Eq. (II.6)**:

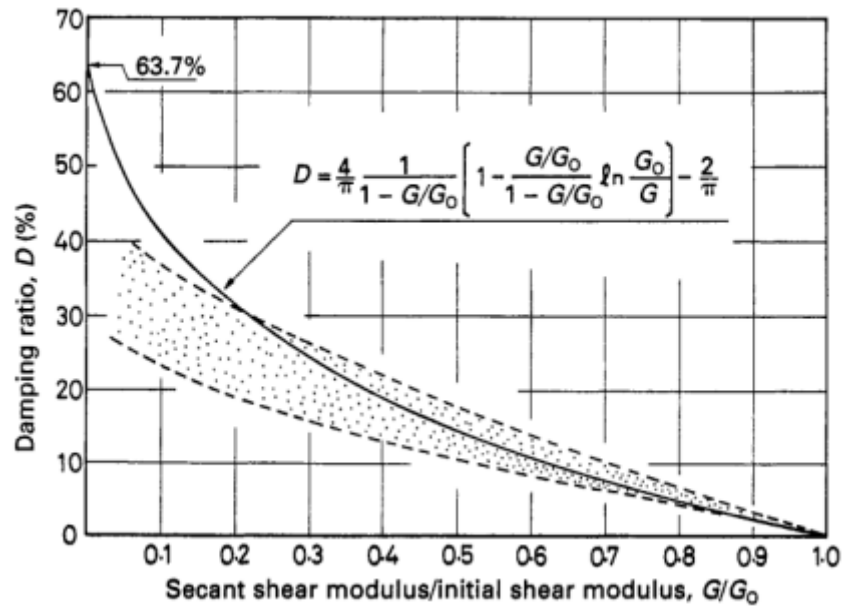


Fig. II.4. Relationship between shear modulus and damping fraction (Ishihara, 1996)

II.3.1.2. Hyperbolic model of Hardin and Drnevich

Hardin and Drnevich (1972b) proposed a model based on the rules proposed by Masing (1926), in which the hyperbolic expression proposed by Kondner (1963) is transformed into a relationship between shear stress τ and shear strain γ :

$$\tau = \frac{\gamma}{\frac{1}{G_{max}} + \frac{\gamma}{\tau_{ult}}} \quad (\text{II.7})$$

Where G_{max} is the maximum shear modulus and τ_{ult} is the maximum shear stress, which depends on the initial state of stresses in the soil and the manner in which they are applied. For a soil composed of horizontal layers, the ultimate shear stress is a function of the soil strength curve.

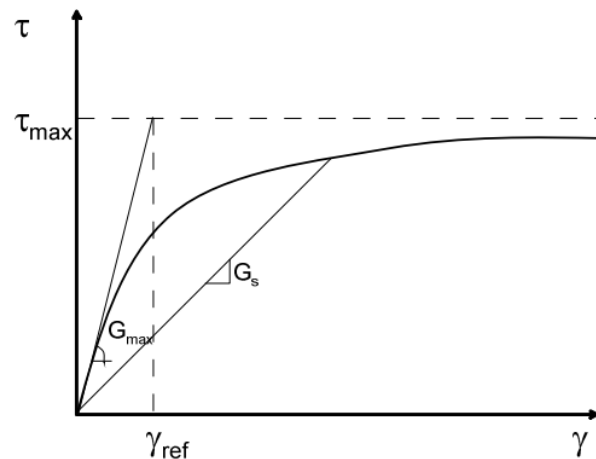


Fig. II.5. Hyperbolic stress-strain relationship (Hardin and Drnevich, 1972b)

II.4. METHODS FOR ANALYZING THE SEISMIC RESPONSE OF SOILS

Soil seismic response analysis is an important branch of geotechnical engineering that aims to understand how soils respond to seismic vibrations. This is essential for the design and stability assessment of structures in seismic zones. When the magnitude of the cyclic shear deformation is less than 10^{-4} , the cyclic behavior of soils can be represented with reasonable accuracy by a constitutive model based on the classical theory of linear viscoelasticity. The response of soils with nonlinear behavior is solved by several methods. The choice of the method depends on the value of the deformation (One-Dimensional Linear Analysis, Temporal Nonlinear Analysis, Equivalent Linear Analysis,) (**Table II.1**). (Abate & Massimino, 2017; Assimaki & Kausel, 2002)

II.4.1. Equivalent Linear Analysis

Due to the complexity of seismic ground response, several researchers have proposed an equivalent linear method for calculating the response of a one-dimensional, horizontally layered soil profile subjected to vertical propagation. It can approximate the nonlinear behavior of soils under cyclic or seismic loading by equivalent simple linear laws. (Moghaddasi et al., 2011; Pitilakis & Clouteau, 2010)

The equivalent linear method is an iterative procedure in which, at each iteration, for each soil layer (**Fig. IV.1**), the changes in the dynamic parameters of the soil are evaluated. These are reflected in the decrease of the shear modulus ratio, the increase of the damping percentage, the displacements, velocities, accelerations and stresses for each soil layer,

knowing that the soil profile is subjected to the seismic accelerogram applied at the bedrock level.

The equivalent linear method is the most widely used method in soil engineering practice because of its simplicity and ease of implementation and calculation speed, and is implemented in many calculation codes such as CALDYNASOIL, CYBERQUAKE, FLAC, SHAKE, ...

The principles and stages of analysis of this approach are as follows:

➤ **Step 1:** *Estimation of soil physical parameters*

The first procedure in this method is to estimate the initial physical parameters for each homogeneous soil layer i (the maximum shear modulus G_{max} , density ρ , maximum critical damping ζ_{max}).

In this step, all soil parameters are determined by in-situ tests or low-strain laboratory tests.

➤ **Step 2:** *Select the number of soil layers to analyze*

In this step, we can limit the total number of layers to be used in the analysis. This number depends on the accuracy of the result.

Idriss and Seed (1968) proposed the graph shown in **Fig. II.6**, where ERS is the percentage error in concentrated mass analysis.

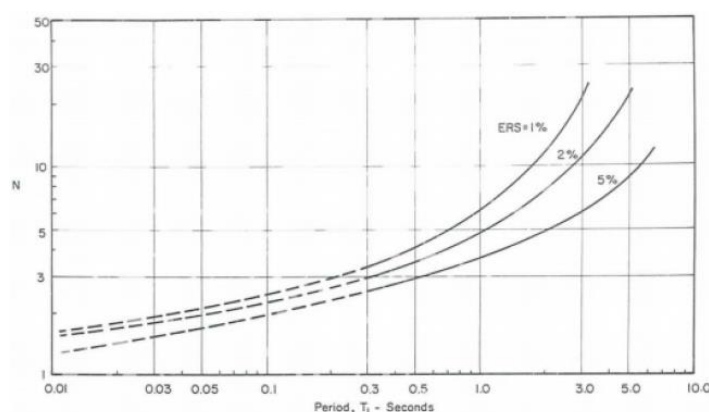


Fig. II.6. Number of Soil Layers vs. Calculation Accuracy.

T_1 : The fundamental period of each type of soil i composed of a homogeneous material.

$$T_{1(i)} = \frac{4h_i}{\sqrt{G_i}} \sqrt{\rho_i} \quad (\text{II.8})$$

Where:

- h_i : Thickness of layer i ,
- G_i : Shear modulus of layer i ,
- ρ_i : Density of layer i .

Finally, the total number of layers, N , is the sum of all the layers needed to model all the soil types that make up the N_m deposit:

$$N = \sum_1^{N_m} N_i \quad (\text{II.9})$$

- N_m is the number of different materials that make up the soil deposit.
- **Step 3:** Calculate mass, stiffness, and damping matrices.

In this calculation method, the soil layer is modeled by concentrated masses connected by spring and viscous damping elements (**Fig. IV.1**).

The soil mass is calculated for each layer using the formulas:

$$m_1 = \frac{\rho_1 h_1}{2} \quad (\text{II.10})$$

$$m_i = \frac{(\rho_{i-1} h_{i-1} + \rho_i h_i)}{2} \quad i = 2, 3, \dots, N \quad (\text{II.11})$$

Where: m_i is the elementary mass of layer i , ρ_i is its density.

The mass matrix, $[m]$, is a diagonal matrix of the form:

$$[m] = \begin{bmatrix} m_1 & 0 & 0 & \dots & 0 \\ 0 & m_2 & 0 & \dots & 0 \\ 0 & 0 & m_3 & \dots & 0 \\ \dots & \dots & \dots & \dots & 0 \\ 0 & 0 & 0 & 0 & m_N \end{bmatrix}_{N \times N} \quad (\text{II.12})$$

The stiffness for each soil layer is related to the shear modulus G_i and the sublayer height h_i by the following equation:

$$k_i = \frac{G_i}{h_i} \quad (\text{II.13})$$

The total stiffness of the system is written in matrix form as follows:

$$[k] = \begin{bmatrix} k_1 & -k_1 & 0 & \dots & 0 \\ -k_1 & k_1 + k_2 & -k_2 & \dots & 0 \\ 0 & -k_2 & k_2 + k_3 & \dots & 0 \\ \dots & \dots & \dots & \dots & \dots \\ 0 & 0 & 0 & 0 & -k_{N-1} \\ 0 & 0 & 0 & -k_{N-1} & k_{N-1} + k_N \end{bmatrix}_{N \times N} \quad (\text{II.14})$$

For the total damping matrix, the following form of expression is given:

$$[c] = \begin{bmatrix} c_1 & -c_1 & 0 & \dots & 0 \\ -c_1 & c_1 + c_2 & -c_2 & \dots & 0 \\ 0 & -c_2 & c_2 + c_3 & \dots & 0 \\ \dots & \dots & \dots & \dots & \dots \\ 0 & 0 & 0 & 0 & -c_N \\ 0 & 0 & 0 & -c_N & c_{N-1} + c_N \end{bmatrix}_{N \times N} \quad (\text{II.15})$$

➤ **Step 4:** Calculate dynamic response.

Solve the equations governing the motion of all soil layers (e.g., using a modal dynamic analysis method), taking into account the dynamic equilibrium for each layer:

$$[m] (\ddot{x}) + [c] (\dot{x}) + [k] (x) = - (m) \ddot{x}_r \quad (\text{IV.16})$$

Where (x) ; (\dot{x}) ; (\ddot{x}) = vectors of displacements, velocities and horizontal accelerations of each layer with respect to the rock; (m) a vector containing the mass of each soil layer; \ddot{x}_r = accelerogram at the rock level.

➤ **Step 5:** Calculation of the maximum shear unit deformations

For each layer i , the maximum shear unit deformations, $\gamma_{max}(i)$, are calculated from the maximum inter-layer displacements:

$$\gamma_{max}(i) = \frac{|x_i - x_{i+1}(t)|_{max}}{h_i} \quad (\text{IV.17})$$

➤ **Step 6:** Update of the stiffness and the effective equivalent critical damping fraction

Update the stiffness and the equivalent damping, from the maximum shear unit deformations calculated in step 5. In general, a fraction of the maximum values of 2/3 is used, because the maximum deformation levels are reached only once during the dynamic response.

Among the three models of nonlinear soil behavior integrated in the code CALDYNSOIL (Sbartai & Fillali, 2012), in this study we choose the model of behavior of Massing (1926), represented by the following relation:

$$\tau = \frac{\gamma}{\frac{1}{G_{max}} + \frac{\gamma}{\tau_{ult}}} \quad (\text{IV.18})$$

Where:

- τ is the shear stress.
- γ is the shear strain.
- τ_{ult} is the ultimate shear stress.

By dividing the **Eq. (IV.18)** by γ , we obtain the effective shear modulus of the soil G , according to the unitary deformation in shear γ_r by:

$$\frac{G}{G_{max}} = \frac{1}{1 + \frac{\gamma}{\gamma_r}} \quad (\text{IV.19})$$

Where $\gamma_r = \tau_{ult}/G_{max}$, is the unit deformation of the reference.

For the critical damping coefficient, $\xi_g/\xi_{g\ max}$, Massing (1926) proposed the relationship between critical damping and shear modulus as:

$$\frac{\xi_g}{\xi_{g\ max}} = \left(1 - \frac{G}{G_{max}}\right) \quad (\text{IV.20})$$

Where: $\xi_{g\ max}$ is the maximum critical damping (initial value).

- **Step 7: Stiffness and damping convergence**

Steps 3 through 7 are repeated until the stiffness and damping converge. In general, only a few iterations are sufficient to achieve convergence.

This method has been integrated into the CALDYNASOL calculation software (Kamel Filali, 2018), which is intended for dynamic calculations by equivalent linear analysis with concentrated masses, based on three hyperbolic laws, Hardin & Drnevich (1972), Ramberg &

Osgood (1943) and Masing (1926), to model the nonlinear behavior of the soil. This code can be used to estimate:

- The stress generated by dynamic loading
- The seismic response of the soil deposit
- The liquefaction potential using a variety of methods available in the literature.

The advantage of this program is that it doesn't take much time to perform the calculations and the results are very accurate.

In the present work, the CALDYNASOL calculation software (Kamel Filali, 2018) was used to determine the nonlinear dynamic parameters of the soil at different levels of seismic deformation in order to integrate them into the analysis of the interaction of the soil structure system with the nonlinear soil behavior.

II.5. CONCLUSION

It is important to note that many factors, such as the geological and geotechnical characteristics of the site, the magnitude and duration of the shock, and the distance from the source of the earthquake, affect the response of the ground to a seismic shock. Geotechnical studies and seismic analyses are performed to understand and account for these effects in the design of earthquake-resistant structures.

The nonlinearity of the soil during an earthquake plays an important role in the dynamic response of the soil-structure system. It is important to consider the nonlinear behavior of the soil when modeling soil-structure interaction (SSI) problems. This is necessary to obtain results that are very close to reality with respect to the response of structures, especially when subjected to high seismic loads. Two approaches can be used: a fully nonlinear analysis or an equivalent linear analysis.

This chapter presents a review of the literature on the dynamic properties of soils, their behavioral laws, and methods for analyzing the seismic response of soils.

***CHAPTER III: ANALYTICAL ANALYSIS WITH
VISCOELASTIC SOIL BEHAVIOR***

III.1. INTRODUCTION

The risks associated with seismic loads and ground motions have created the need for a rigorous dynamic analysis that takes into account the phenomenon of interaction between the structure and the soil supporting it, which is an essential phenomenon in the dynamic analysis of structures.

When structures are built on or in the ground, they interact with the surrounding soil, which can have a significant impact on their dynamic behavior, and this impact can be beneficial or detrimental depending on the type of soil, the seismic loading, the characteristics of the structure and several other factors that enter into its effect.

The basic objective of this chapter is to study and analyze the dynamic response of structures during earthquakes, considering the effect of soil-structure interaction. To this end, an analytical analysis based on the dynamic equilibrium of the soil-structure system modeled by an analog model with three degrees of freedom is performed in this work to obtain the seismic response of the selected structure. In order to explore the sensitivity of the response of a soil-structure system to different soil and structure parameters, this chapter investigates the effect of adopting different impedance function types on the structural response of the soil-structure system using springs and dashpots with two frequency cases: independent and dependent frequencies.

Finally, new analytical nonlinear relationships are proposed between the displacements of the structure, the embedding ratio of the foundation and the dimensionless circular frequency of the excitation.

The slenderness ratio, the mass ratio, the shear wave velocity of the soil and some other parameters are the main parameters considered in this parametric study of the model.

III.2. SYSTEM AND METHOD OF ANALYSIS

III.2.1. Dynamic soil-foundation-structure model

For the dynamic analysis of the soil-foundation-structure interaction, a simplified rheological model was used, as shown in **Fig. III.1**, where the superstructure is represented in a simplified way as a single-degree-of-freedom system resting on a circular shallow foundation, which resting on a soil deposit. The structure is described by its mass m , a lateral

stiffness with a spring coefficient K , and a damper with a coefficient C placed at a height h of a rigid bar. The soil-foundation system is modeled by discrete elements including horizontal and rocking equivalent linear springs and viscous dashpots with frequency-independent (Eq. (III.16) to Eq. (III.19)) and frequency-dependent (Eq. (III.22) to Eq. (III.25)) coefficients, where the spring and damping coefficients are denoted as K_h and C_h in the horizontal direction and as K_r and C_r in the rotational direction. The mass m_0 of the foundation is neglected. The system is subjected to a horizontal displacement of the ground support of pulsation ω and an amplitude u_g (g for ground). The fixed base frequency and the damping ratio of the structure are given by $\omega_s = (K/m)^{0.5}$, and $\xi (= C\omega_s/2K)$ (Wolf 1985). In this study, only the inertial interaction needs to be considered. The coupled system oscillates in the horizontal and rocking directions, as the effects of these motions are more important than the vertical and torsional motions. (Durmuş and Livaoglu 2015)

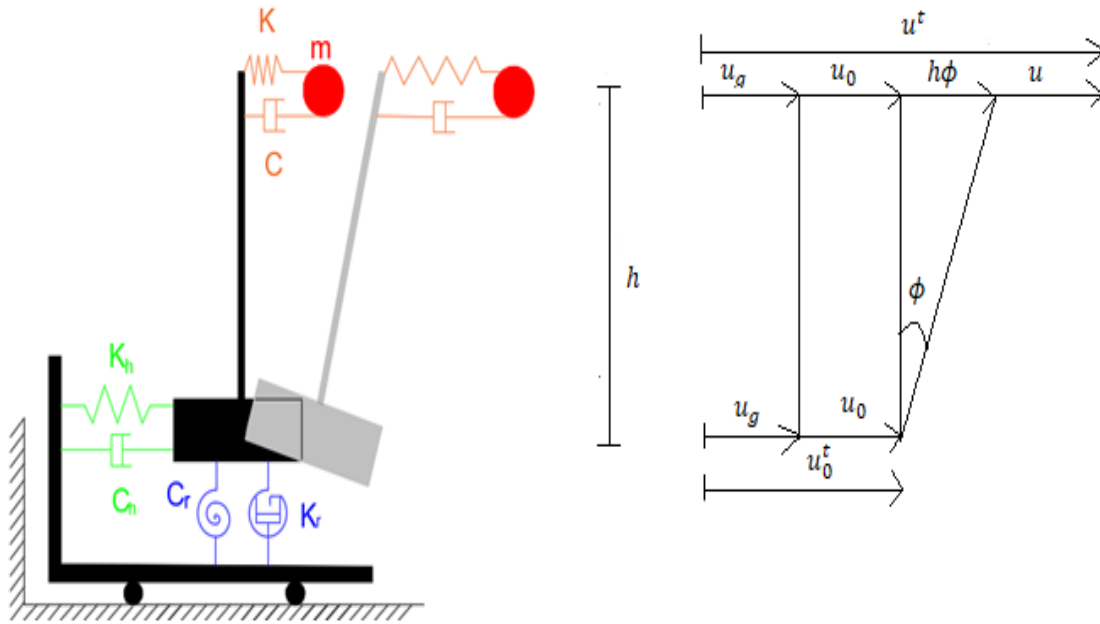


Fig. III.1. simplified soil-structure interaction model (for a single-degree-of-freedom structure).

System has three global degrees of freedom, the total lateral displacements of the mass with amplitude u^t and the base of the structure u_0^t can be divided into individual components as follows:

$$u^t = u_g + u_0 + h\phi + u \quad (\text{III.1})$$

$$u_0^t = u_g + u_0 \quad (\text{III.2})$$

Where:

- u_g : Amplitude of the horizontal excitation or free-field motion.
- u : Amplitude of the relative displacement of the mass and which is equal to the structural distortion.
- u_0 : Amplitude of the horizontal displacement of the foundation relative to the free-field motion.
- ϕ : Amplitude of the rotation of the foundation around a horizontal axis.
- P_h and M_r denote the horizontal-force and moment amplitudes of the soil, respectively, formulated as:

$$P_h = K_x(1 + i2\xi_x + i2\xi_g)u_0 \quad (\text{III.3})$$

$$M_r = K_\phi(1 + i2\xi_\phi + i2\xi_g)\phi \quad (\text{III.4})$$

Where:

- ξ_x : The viscous radiation damping ratio of the elastic soil in the horizontal direction.
- ξ_ϕ : The viscous radiation damping ratio of the elastic soil in the rocking direction.
- ξ_g : The hysteretic damping ratio of the soil.

Starting from scratch, the formulation of the dynamic equilibrium of the mass point and the horizontal and rocking equilibrium equations of the whole system (see **Fig. III.1**) can be established to obtain the equations of motion for this structure with a rigid basement by using **Eq. (III.3)** and **Eq. (III.4)** and introducing the following critical depreciation percentages leads to:

$$\xi = \frac{\omega C}{2K}; \quad \xi_x = \frac{\omega C_x}{2K_x}; \quad \xi_\phi = \frac{\omega C_\phi}{2K_\phi}; \quad C_h = C_x + \frac{2}{\omega}\xi_g K_x; \quad C_r = C_\phi + \frac{2}{\omega}\xi_g K_\phi \quad (\text{III.5})$$

$$\begin{cases} -\omega^2 m(u_0 + h\phi + u) + k(1 + 2\xi i)u = m\omega^2 u_g \\ -\omega^2 m(u_0 + h\phi + u) + k_h(1 + 2\xi_x i + 2\xi_g i)u_0 = m\omega^2 u_g \\ -\omega^2 mh(u_0 + h\phi + u) + k_r(1 + 2\xi_\phi i + 2\xi_g i)\phi = mh\omega^2 u_g \end{cases} \quad (\text{III.6})$$

By introducing the following notations:

$$m\omega_s^2 = k \quad m\omega_h^2 = k_h \quad mh^2\omega_\phi^2 = k_\phi \quad (\text{III.7})$$

Furthermore, by eliminating u_0 and ϕ from the three previous equations, we obtain:

$$\left(1 + 2\xi i - \frac{\omega^2}{\omega_s^2} - \frac{\omega^2}{\omega_h^2} \frac{1 + 2\xi i}{1 + 2\xi_x i + 2\xi_g i} - \frac{\omega^2}{\omega_r^2} \frac{1 + 2\xi i}{1 + 2\xi_\phi i + 2\xi_g i} \right) u = \frac{\omega^2}{\omega_s^2} u_g \quad (\text{III.8})$$

Now consider a simple oscillator with one degree of freedom of the same mass m , of its own pulsation $\tilde{\omega}$ and of damping $\tilde{\xi}$ subjected to a harmonic displacement \tilde{u}_g of the pulsation ω at its base (case of the structure embedded at its base).

The response of the oscillator is:

$$\left(1 + 2\tilde{\xi} i - \frac{\omega^2}{\tilde{\omega}^2} \right) u = \frac{\omega^2}{\tilde{\omega}^2} \tilde{u}_g \quad (\text{III.9})$$

The equivalent oscillator will have the same response as the structure shown in **Fig. III.1** when the following equation is satisfied:

$$\frac{1}{\tilde{\omega}^2} = \frac{1}{\omega_s^2} + \frac{1}{\omega_h^2} + \frac{1}{\omega_r^2} \Rightarrow \tilde{\omega}^2 = \frac{\omega_s^2}{1 + k/k_h + kh^2/k_r} \quad (\text{III.10})$$

It follows that the fixed-base frequency ω_s is always higher than the fundamental frequency of the soil-structure system, from the **Eq. (III.8)**, **Eq. (III.9)** and **Eq. (III.10)**, and in the resonance case $\tilde{\omega} = \omega$ the equivalent damping ratio becomes:

$$\tilde{\xi} = \frac{\tilde{\omega}^2}{\omega_s^2} \xi + \left(1 - \frac{\tilde{\omega}^2}{\omega_s^2} \right) \xi_g + \frac{\tilde{\omega}^2}{\omega_h^2} \xi_x + \frac{\tilde{\omega}^2}{\omega_r^2} \xi_\phi \quad (\text{III.11})$$

And

$$\tilde{u}_g = \frac{\tilde{\omega}^2}{\omega_s^2} u_g \quad (\text{III.12})$$

$$u_0 + h\phi + u = \omega_s^2 \left(\frac{1}{\tilde{\omega}^2} + 2(\xi - \xi_g) i \left(\frac{1}{\tilde{\omega}^2} - \frac{1}{\omega_s^2} \right) - \frac{2\xi_x i}{\omega_h^2} - \frac{2\xi_\phi i}{\omega_r^2} \right) u \quad (\text{III.13})$$

The dimensionless parameters given in **Eq. (III.14)** can be used to generalize the results obtained and to better evaluate the soil-structure interaction effect, where c_s is the shear wave velocity of the soil, r is the radius of the foundation, ρ is the mass density, and $G(= \rho c_s^2)$ is the shear modulus.

$$\bar{s} = \frac{\omega_s h}{c_s}; \bar{h} = \frac{h}{r}; \bar{m} = \frac{m}{\rho r^3} \quad (\text{III.14})$$

Since the judicious evaluation of the impedance function is a step that must be addressed, we aim to evaluate the differences that occur due to the effects of their form on the seismic response of structures. For this purpose, two expressions are used to estimate the stiffness and damping parameters of the soil-foundation interaction (static parameters: "frequency independent", dynamic parameters: "frequency dependent").

In real conditions, the stiffness and damping coefficient of the foundation depend on the frequency. Therefore, to illustrate the effect of SSI and the influence of its expression forms, the following frequency-independent and frequency-dependent approximate expressions are used to estimate the stiffness and damping coefficient of a rigid circular foundation of radius r (Wolf 1985; Wolf and Preisig 2003).

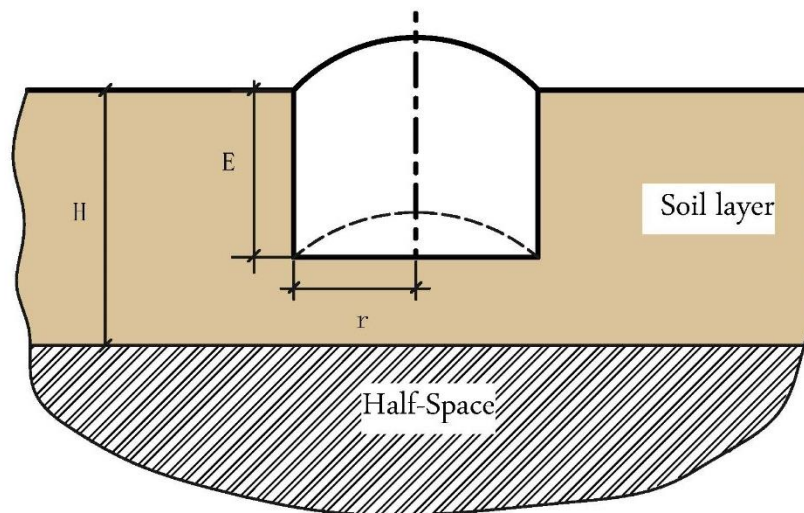


Fig.III.2. Schematic representation of a rigid cylindrical foundation embedded in a layer of soil over half the space.

The general form of the foundation impedance function can be described by the following equation:

$$K^d = K^s(k + ia_0c) \quad (\text{III.15})$$

Where:

- K^s : Static rigidity coefficient.

- k : Dimensionless spring coefficient.
- a_0 : Dimensionless frequency.
- c : Dimensionless damping coefficient.

III.2.2. Case of Frequency Independent Expressions:

$$K_x^s = \frac{8Gr}{2 - \nu} \quad (\text{III.16})$$

$$C_x = \frac{4.6}{2 - \nu} \rho c_s r^2 \quad (\text{III.17})$$

$$K_\phi^s = \frac{8Gr^3}{3(1 - \nu)} \quad (\text{III.18})$$

$$C_\phi = \frac{0.4}{1 - \nu} \rho c_s r^4 \quad (\text{III.19})$$

Where:

- K_x^s : Static stiffness coefficient in horizontal direction.
- K_ϕ^s : Static stiffness coefficient in rocking direction.
- C_x : Damping coefficient in horizontal direction.
- C_ϕ : Damping coefficient in rocking direction.

The expression of the frequency $\tilde{\omega}$ and the equivalent damping coefficient $\tilde{\xi}$ calculated in **Eq. (III.10)** and **Eq. (III.11)** using the dimensionless parameters mentioned above for a rigid surface base ($D = 0$) leads to:

$$\frac{\tilde{\omega}^2}{\omega_s^2} = \frac{1}{1 + \frac{\bar{m}\bar{s}^2}{8} \left[\frac{2 - \nu}{\bar{h}^2} + 3(1 - \nu) \right]} \quad (\text{III.20})$$

$$\tilde{\xi} = \frac{\tilde{\omega}^2}{\omega_s^2} \xi + \left(1 - \frac{\tilde{\omega}^2}{\omega_s^2} \right) \xi_g + \frac{\tilde{\omega}^3}{\omega_s^3} \frac{\bar{s}^3 \bar{m}}{\bar{h}} \left[0.036 \frac{2 - \nu}{\bar{h}^2} + 0.028(1 - \nu) \right] \quad (\text{III.21})$$

III.2.3. Case of Frequency-Dependent Expressions:

In the case of frequency-dependent expressions ($a_0 \neq 0$), stiffness K^d is now expressed in terms of a static part, K^s (see **Eq. (III.16)** and **Eq. (III.18)**), times a dynamic modifier, k ; the radiation dashpot coefficient is similarly expressed in terms of static stiffness and the product of a dimensionless frequency $a_0 (= \omega^r/c_s)$, times a dynamic modifier, c . The dimensionless spring and damping coefficients k_x , c_x , k_ϕ and c_ϕ are functions of a_0 evaluated at the resonance case $\tilde{\omega} = \omega$. (Pais, Kausel, and Eirgirreerirgl 1988)

$$k_x(\omega) = 1 \quad (\text{III.22})$$

$$c_x(\omega) = \frac{\pi[1 + (1 + \alpha)D/r]}{K_x^s/Gr} \quad (\text{III.23})$$

$$k_\phi(\omega) = 1 - \frac{0.35 a_0^2}{1 + a_0^2} \quad (\text{III.24})$$

$$c_\phi(\omega) = \frac{\pi \left[\frac{\alpha}{4} + D/r + \left(\frac{1 + \alpha}{2} \right) \frac{2}{3} (D/r)^3 \right] \frac{a_0^2}{b + a_0^2} + 0.84(1 + \alpha)(D/r)^{2.5} \frac{b}{b + a_0^2}}{K_\phi^s/Gr^3} \quad (\text{III.25})$$

Where:

- k_x : Dimensionless spring coefficients in the horizontal direction.
- k_ϕ : Dimensionless spring coefficients in the rocking direction.
- a_0 : Dimensionless frequency.
- c_x : Dimensionless damping coefficients in the horizontal direction.
- c_ϕ : Dimensionless damping coefficients in the rocking direction.

The same dimensionless parameters (**Eq. (III.14)**) are again used to describe the key parameters of this coupled system: the stiffness ratio of the structure and the soil \bar{s} , the mass ratio \bar{m} , and the slenderness ratio \bar{h} . In this case, the frequency $\tilde{\omega}$ of the soil-structure interaction system (**Eq. (III.10)**) is given by:

$$\frac{\tilde{\omega}^2}{\omega_s^2} = \frac{1}{1 + \frac{\bar{m}\bar{s}^2}{8} \left[\frac{2 - \nu}{\bar{h}^2 k_x (1 + D)} + \frac{3(1 - \nu)}{k_\phi (1 + 2.3D + 0.58D^3)} \right]} \quad (\text{III.26})$$

And $\tilde{\xi}$: the equivalent damping ratio (**Eq. (III.11)**) is given by:

$$\tilde{\xi} = \frac{\tilde{\omega}^2}{\omega_s^2} \xi + \left(1 - \frac{\tilde{\omega}^2}{\omega_s^2}\right) \xi_g + \frac{\tilde{\omega}^3 \bar{s}^3 \bar{m} c_s}{\omega_s^3 128 \bar{h} r} \left[\frac{(2 - \nu)^2}{\bar{h}^2 k_x^2 (1 + D)^2} c_x + \frac{9(1 - \nu)^2}{k_\phi^2 (1 + 2.3D + 0.58D^3)^2} c_\phi \right] \quad (\text{III.27})$$

Where:

- $D = E/r$: The embedment ratio
- $b = \frac{2}{1+D} = 2$ for a rigid surface base ($D = 0$).
- $\alpha = c_p/c_s$: The velocity ratio.
- c_p : The compression wave velocity.
- c_s : The shear wave velocity.
- ν is the Poisson's ratio of the soil.

Eq. (III.26) and **Eq. (III.27)** are the new analytical formulas that we propose to calculate the equivalent frequency and the equivalent damping of the soil-structure system based on frequency-dependent impedance functions.

If the shear wave velocity of the soil is equal to infinity ($\bar{s}=0$), it means that the base state of the structure is fixed, but if the stiffness ratio is infinite ($c_s = 0$), it shows that a relatively rigid structure rests on relatively soft soil. more discussion on this issue is provided in the results section.

III.3. PARAMETRIC ANALYSIS AND RESULTS

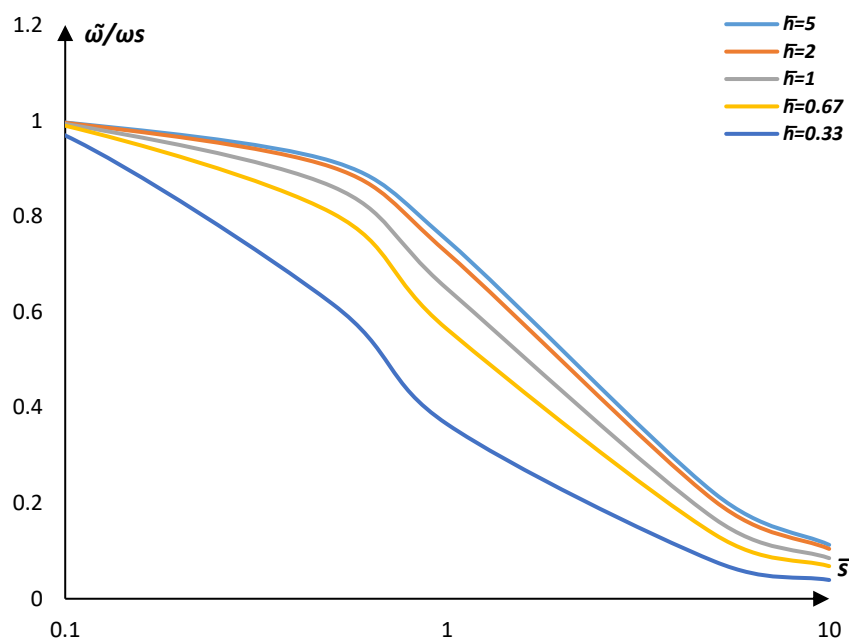
The problem considered in this work consists of a structure ($\xi = 0.025$) on a half-space, which is represented in a simplified way as an SDOF system in all of the SSI models. The soil properties are described by Poisson's ratio $\nu = 0.33$ and material damping $\xi_g = 0.05$. The superstructure and the soil were modeled linearly. This work aims to evaluate the influence of considering and neglecting the SSI and the effect of the impedance function form on the structural response of the soil-structure system by using springs and dashpots with two frequency cases: independent (static impedance function) and dependent frequencies (dynamic impedance function).

The slenderness ratio, the mass ratio, the shear wave velocity of the soil, and several other parameters are the essential parameters that are considered in this parametric analysis.

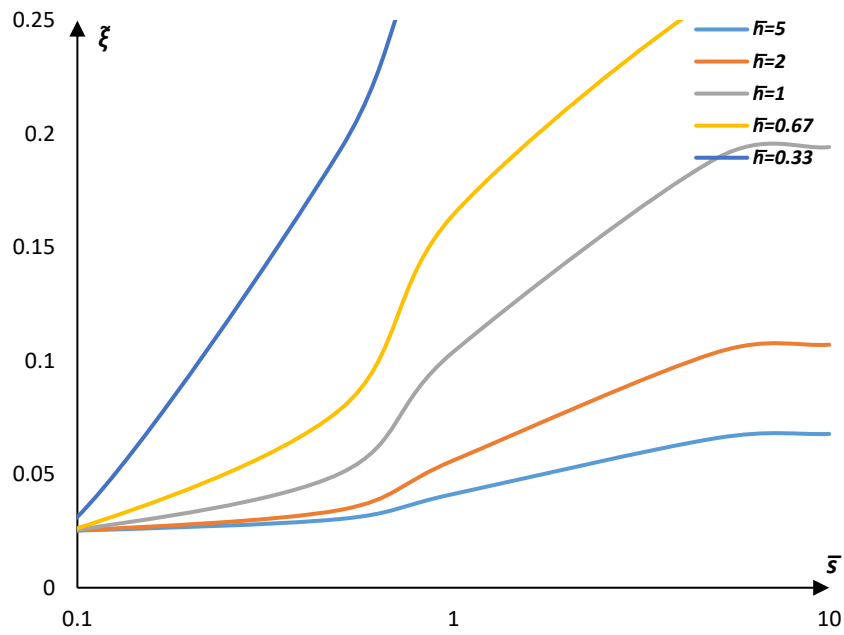
III.3.1. Natural frequency and damping of the soil-structure system

III.3.1.1. Frequency-independent impedance function case

The properties of the equivalent one-degree-of-freedom system $\tilde{\omega}/\omega_s$ and $\tilde{\xi}$ are plotted in **Fig. III.3(a)**, **(b)** and **Fig. III.4(a)**, **(b)** as a function of \bar{s} ($=0.1 \dots 10$), varying the slenderness ratio (\bar{h}) and the mass ratio (\bar{m}). We observe that the frequency ratio $\tilde{\omega}/\omega_s$ (**Fig. III.3(a)** and **Fig. III.4(a)**) decreases monotonically with the decrease of \bar{h} and the increase of \bar{s} and \bar{m} , respectively, while with respect to the effective damping ratio $\tilde{\xi}$ (**Fig. III.3(b)**), the increase of the latter with increasing of \bar{s} is evident, due to the effect of a large amount of radiation damping (mainly in the horizontal direction) applied over the whole range, it is found that $\tilde{\xi}$ is larger for squat structures (\bar{h} small) than for slender structures (\bar{h} large).

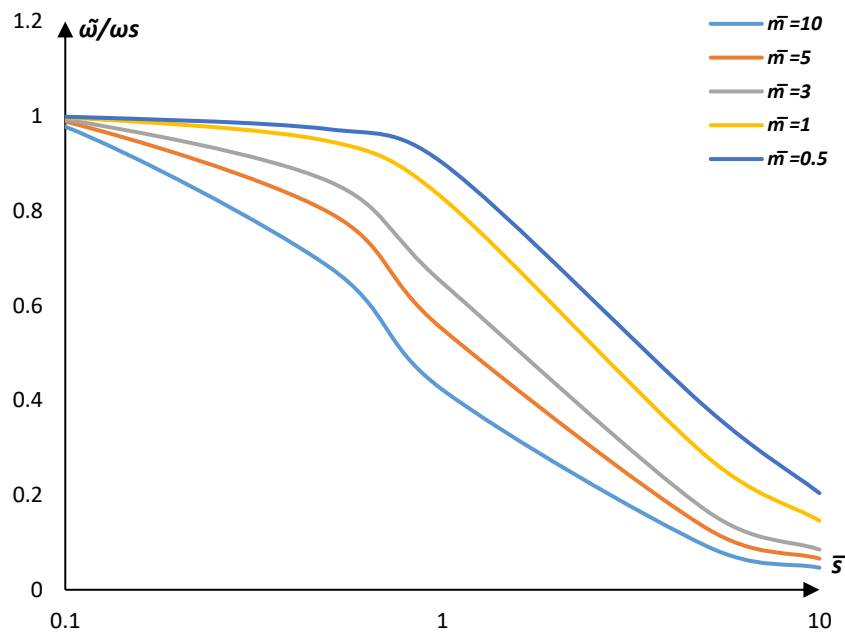


(a) Equivalent natural frequency.

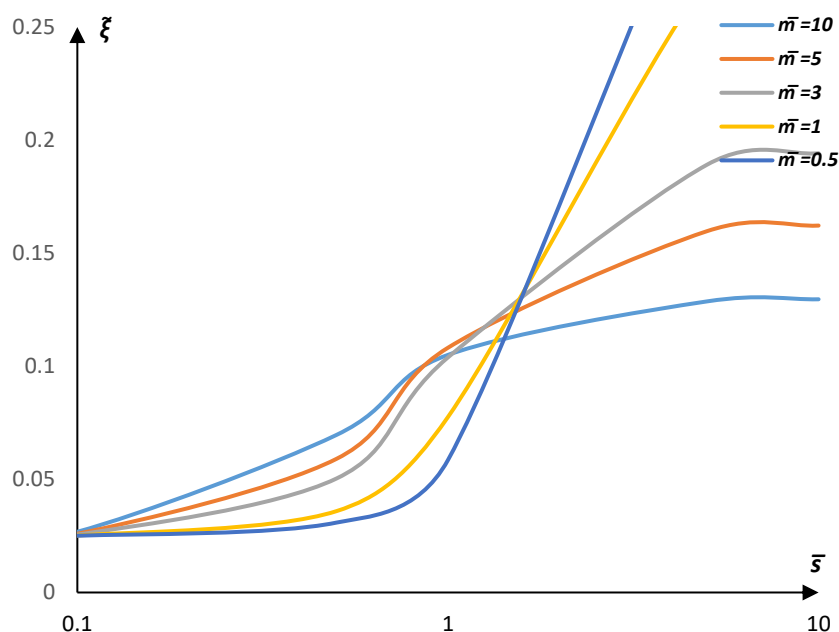


(b) Equivalent damping.

Fig. III.3. Properties of the equivalent one degree of freedom system ($\bar{m}=3$, $\nu=0.33$, $\xi=0.025$, $\xi_g=0.05$), varying slenderness ratio \bar{h} .



(a) Equivalent natural frequency.



(b) Equivalent damping.

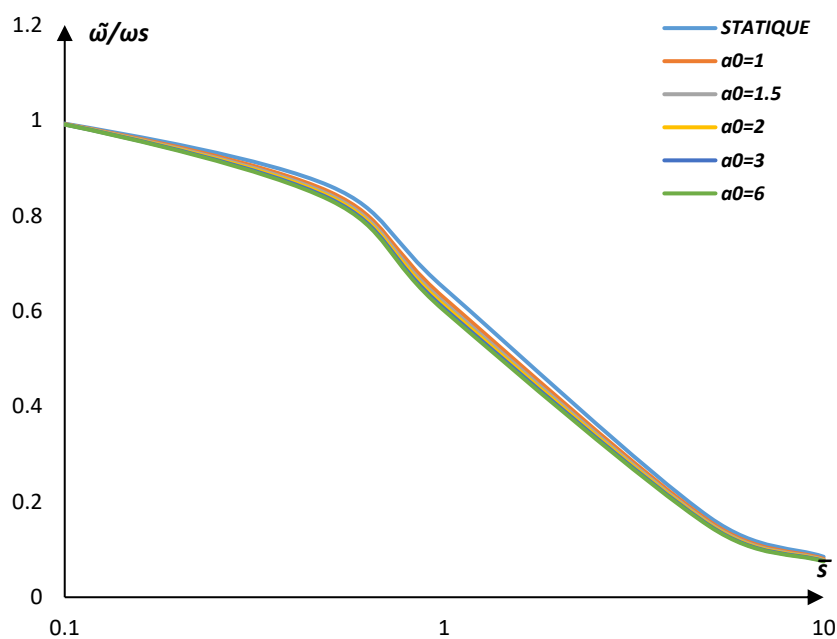
Fig. III.4. Properties of the equivalent one degree of freedom system ($\bar{h}=1$, $\nu=0.33$, $\xi=0.025$, $\xi_g=0.05$), varying mass ratio \bar{m} .

Interestingly, in contrast to the variation of \bar{h} , in the variation of \bar{m} , (**Fig. III.4(a)**), the magnitude of $\tilde{\xi}$ increases with increasing mass ratio (\bar{m}) in the lower frequency ratio range ($\bar{s} < 1$), and $\tilde{\xi}$ increases with decreasing of the mass ratio (\bar{m}) in the higher frequency ratio range ($\bar{s} > 1$) (softer soil). Since the slenderness ratio (\bar{h}) is large, the damping is small and this leads to an increase in displacement, increasing the mass ratio (\bar{m}) may lead to an increase or decrease in displacement, depending on the type of soil. In general, the change in the dynamic properties of the soil-structure system is due to the dominant role of the soil and its properties, the dominant role of the structure and its properties, and the interaction between them. (Lin, Wang, and Tsai 2008)

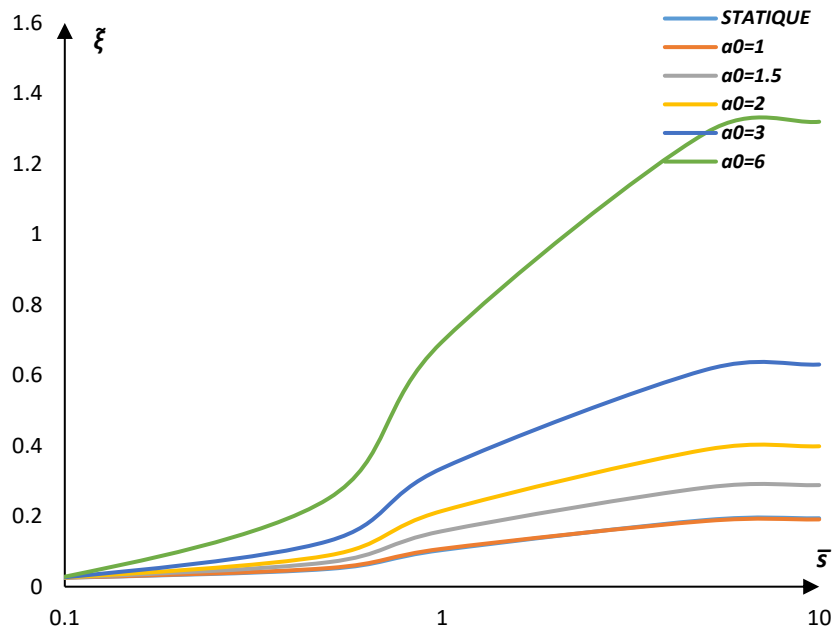
III.3.1.2. Frequency-dependent impedance function case

Similarly, for frequency-dependent expressions, the equivalent system parameters are plotted as $\tilde{\omega}/\omega_s$ and $\tilde{\xi}$ for $\bar{s} = (\omega_s h/c_s)$. In **Fig. III.5(a)**, **(b)**, we have also varied the dimensionless circular frequency $a_0 (=1, 1.5, 2, 3, 6)$. We observe that the combination of SSI effects and frequency-dependent impedance functions leads to an increased value of change in the results compared to the static case (the frequency-independent parameters). We note that the dimensionless circular frequency a_0 has a strong influence on the equivalent-damping

coefficient of the soil- structure system, but has little influence on the equivalent natural frequency of the system. However, similar trends are observed compared to the case of the frequency-independent expression (static impedance function) with different values, this similarity is due to the prevalent role of the soil in the structure response (Çelebi, Göktepe, and Karahan 2012). The influence of the embedment ratio of the foundation D on the properties of the equivalent system was also considered (see **Fig. III.6(a), (b)**). We find that the embedment ratio of the foundation D significantly influences the equivalent damping ratio and the equivalent natural frequency of the system (i.e., the structure and the soil). With its increase (D), we observe an increase in the equivalent damping coefficient and a decrease in the equivalent natural frequency of the system compared to the case of a surface rigid foundation ($D = 0$). This is due to the increase in the contact surface between the foundation and the ground, where the significantly increases the stiffness of the foundation. The results are similar to those obtained by (Ahmad and Rupani 1999) when studying the dynamic response to horizontal excitation of a rigid square footing in a two-layer soil profile by using an advanced BEM algorithm, where they find that when the embedment ratio, D/B , and the sidewalls to soil contact ratio, d/D , are both increased, the horizontal impedance generally increases.

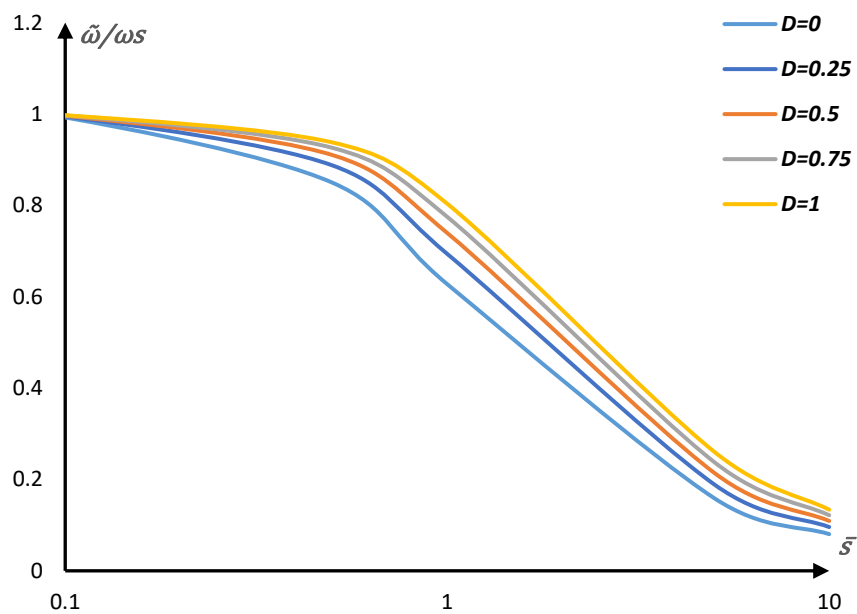


(a) Equivalent natural frequency.

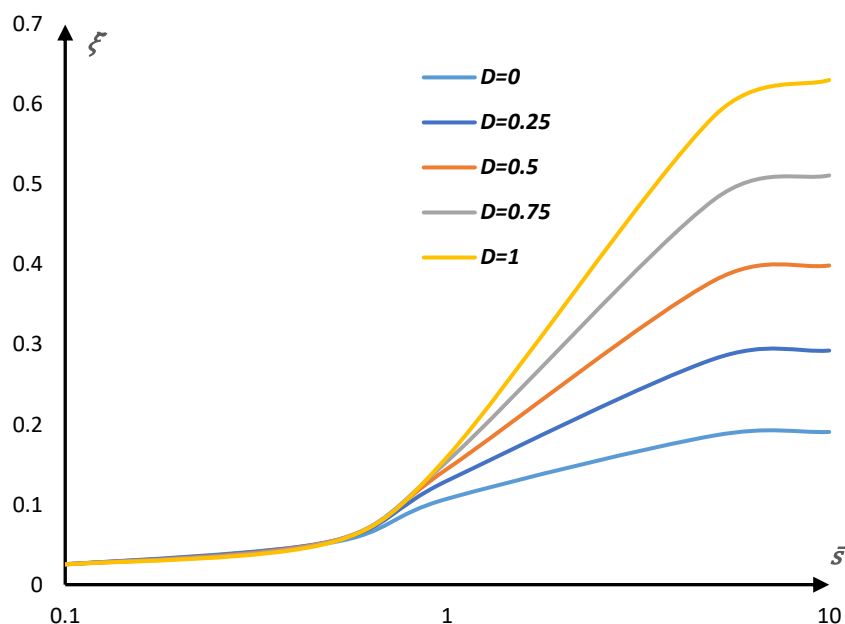


(b) Equivalent damping.

Fig. III.5. Properties of the equivalent one degree of freedom system ($\bar{m}=3$, $\bar{h}=1$, $\nu=0.33$, $\xi=0.025$, $\xi_g=0.05$, $D=0$), varying the dimensionless circular frequency α_0 .



(a) Equivalent natural frequency.



(b) Equivalent damping.

Fig. III.6. Properties of the equivalent one degree of freedom system ($\bar{m}=3$, $\bar{h}=1$, $\nu=0.33$, $\xi=0.025$, $\xi_g=0.05$, $a_0=1$), varying the embedment ratio D .

On the other hand, it has been shown that in all cases the increase of the adimensional frequency \bar{s} (c_s small, soft soil) (Garevski, M., & Ansal 2010) also significantly affects the two equivalent parameters ($\tilde{\omega}/\omega_s$ and $\tilde{\xi}$), where we observe a clear decrease of the frequency ratio, often deviating from the unit value, and a clear increase of the equivalent damping ratio. The nonzero value of the latter at a very low value of the soil stiffness ratio ($\bar{s}=0.1$) indicates the presence of hysteretic dissipation of the structure (assumed to be 2.5%), and for a significant soil-structure-interaction effect, the ratio $\tilde{\xi}$ essentially converges to the soil material-damping ratio $\xi_g = 0.05$. The few small undulations observed in the curves are the result of resonance phenomena in the soil-structure system.

From the above results, it can be summarized that the effect of SSI in this part is to shift the fundamental frequency of the system to lower frequencies (height period) and to increase the dissipated energy in the ground compared to the fixed base structure as the ground becomes softer (Farghaly and Ahmed 2013; Sobhi and Far 2021), and that the characteristics of the ground as well as the structure have a very important influence on this phenomenon. These results are consistent with those described in the literature on the SSI effect (Crouse and McGuire 2001; Forcellini, Mina, and Karampour 2022) and in major design codes

(FEMA 440, ATC-3-06). On the other hand, as widely observed by many researchers interested in studying the effects of soil-structure interactions on the impedance function and structural response of soil-foundation-structure (SFS) systems (Guellil et al. 2017; Massimino et al. 2019; Veletsos and Meek 1974), soil properties and structural parameters, especially shear wave velocity and layer thickness, structure height, and foundation radius, have a significant influence on the impedance function and, at the same time, on the response of the coupled system.

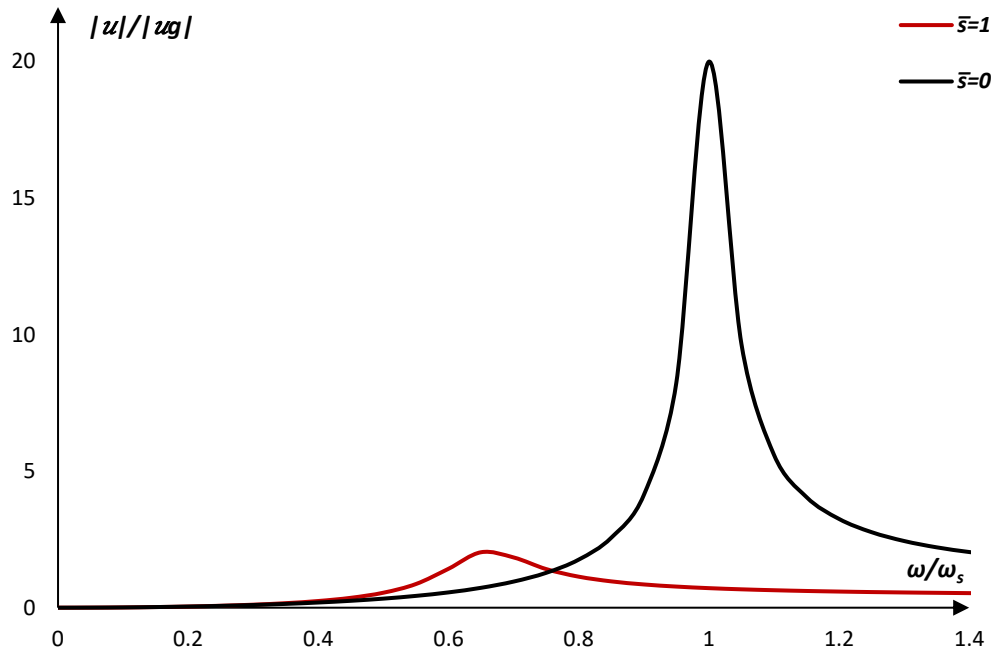
As a result, the change in the fundamental dynamic characteristics of the structure due to the SSI effect must be considered in the design of the structure to avoid the resonance effect, and the analysis will be more realistic.

III.3.2. Relative and absolute displacement of the structure

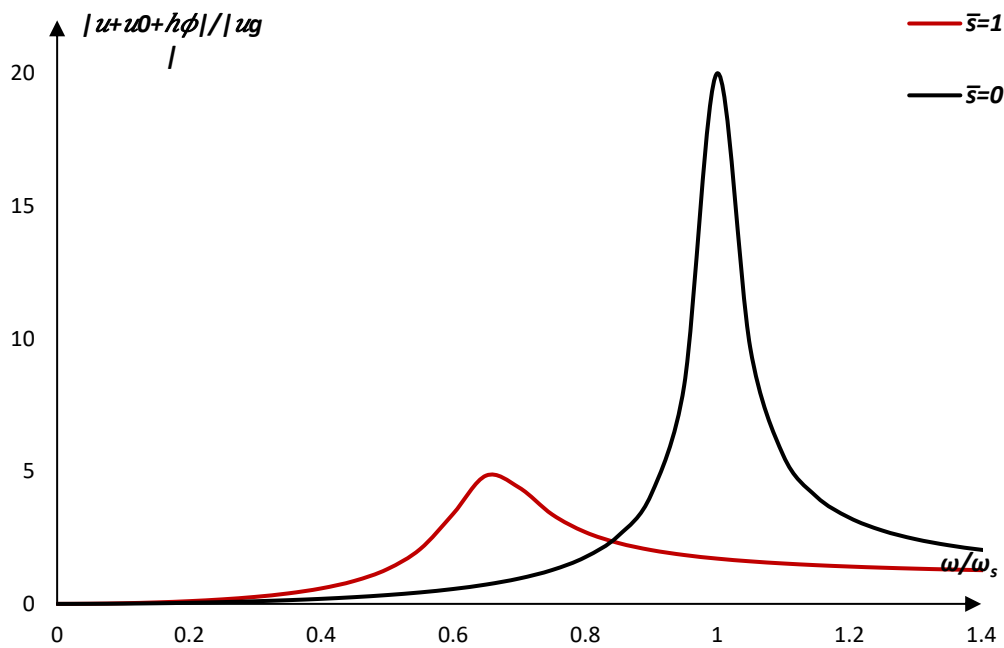
In the following **Fig. III.7** to **Fig. III.9**, the different dimensionless displacements of the structure for $\bar{s} = 1$ and $\bar{s} = 0$ are plotted as a function of the dimensionless excitation frequency $\omega/\omega_s (= 0, 0.2, 0.4, 0.6, 0.8, 1, 1.2, 1.4)$. This follows from **Eq. (III.9)**, **Eq. (III.12)** and **Eq. (III.13)** by using the two analytical "frequency independent" and "frequency dependent" expressions for the viscoelastic soil behavior. For the stiffness $\bar{s} = 0$ (rigid soil, $c_s = \infty$), i.e., we are in the case of a fixed base structure (or $\tilde{\xi} = \xi$, $\tilde{\omega} = \omega_s$ and $\tilde{u}_g = u_g$). However, the stiffness ($\bar{s} = 1$), which takes into account the soil-structure interaction is always different from that of the same structure on rigid soil.

III.3.2.1. Case of Frequency-Independent Impedance Functions

It is very interesting to observe how the displacement of the structure was strongly influenced by the presence of the soil, where the SSI here (see **Fig. III.7(a), (b)**) had a beneficial effect by again reducing the maximum response (Veletsos and Damodaran Nair 1974). Of course, this is due to an increase in the effective damping of the entire system, which is related to the effect of the soil-structure interaction. This brings us back to the basic function of the soil. However, it is important to emphasize that in several cases the SSI has been shown to have a detrimental effect (Karatzetzou and Pitilakis 2018; Rovithis et al. 2017). It's clear from **Fig. III.7(a), (b)** that the interaction effect is negligible for the extremely small and very large ω/ω_s ratios.



(a) Structural distortion.



(b) Displacement of the mass relative to free field.

Fig. III.7. Influence of soil-structure interaction as a function of excitation frequency ($\bar{m}=3$, $\bar{h}=1$, $\nu=0.33$, $\xi=0.025$, $\xi_g=0.05$, $D=0$) (a), (b).

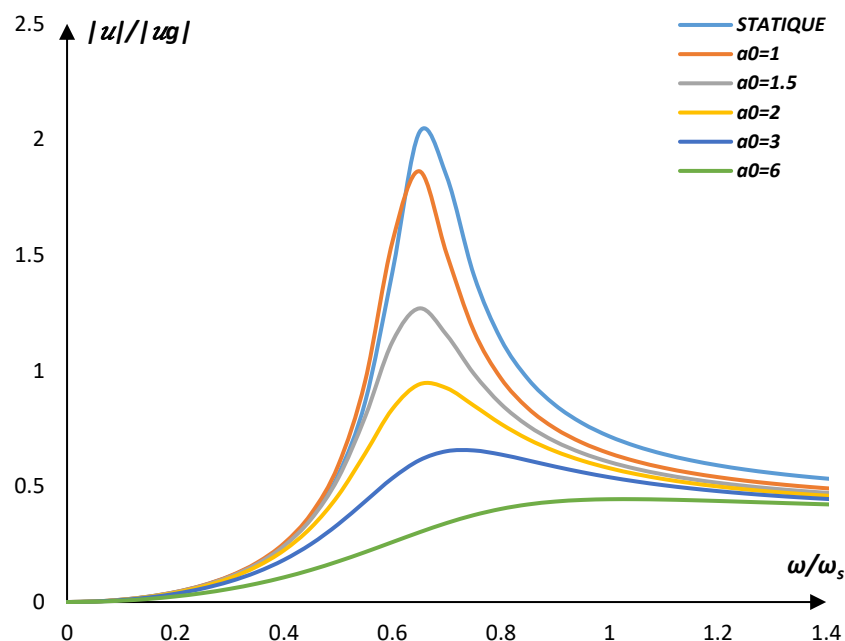
III.3.2.2. Case of frequency-dependent Impedance Function

In **Fig. III.8** and **Fig. III.9**, we have calculated the displacements using the form of the frequency-dependent expression, where we have varied the dimensionless circular

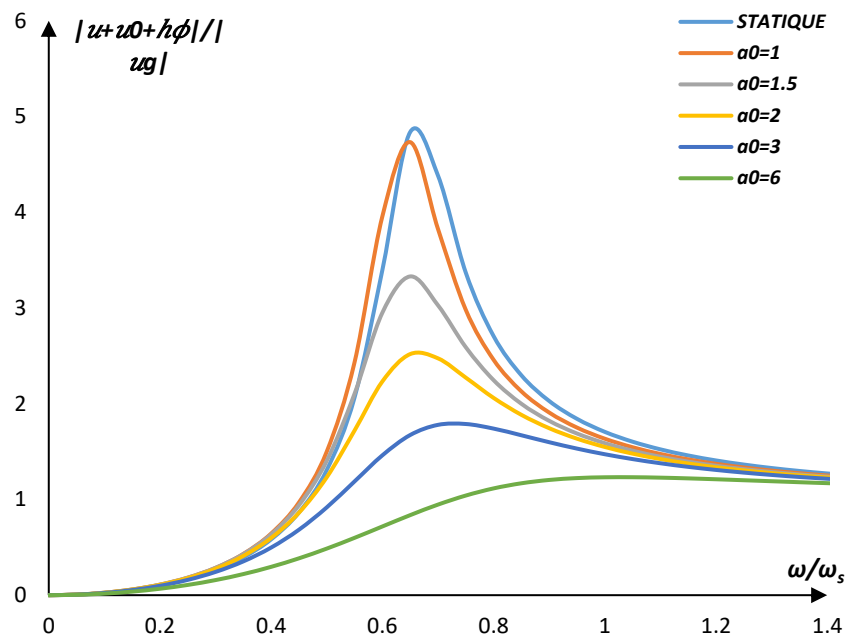
frequency $a_0 = (1, 1.5, 2, 3, 6)$ and the embedment ratio D of the foundation as a function of the excitation frequency ratio ω/ω_s for $\bar{s} = 1$.

We find that increasing in the value of the foundation embedment ratio, (D), not only reduces the structural distortion and increases the mass displacement (**Fig. III.9(a), (b)**), (Moghaddasi et al. 2011), but also shifts the frequency to the right. However, the effect of the dimensionless circular frequency, a_0 , is greater than the effect of the foundation embedment ratio, **Fig. III.8(a), (b)**, where it reduces structural distortion and mass displacement as the frequency content increases and expands. This general pattern is typical of and holds true for infinite domains. As the frequency increases, K^d decreases and C increases, which explains the decrease in displacements. (Wen, Hu, and Chau 2002)

Moreover, the frequency-dependent expressions seem to mainly affect the amplitude of the dynamic response of the structure compared to the case of the frequency-independent expressions (static impedance function), while the shape of the curves remains the same and the peak is at the same frequency, in other words, the damping in the system is greater when the frequency-dependent impedance function is considered (Far and Flint 2017; Maheshwari and Sarkar 2011; Zhang and Tang 2009). However, at low frequencies, the structural distortion and mass displacement are not different from the static case.

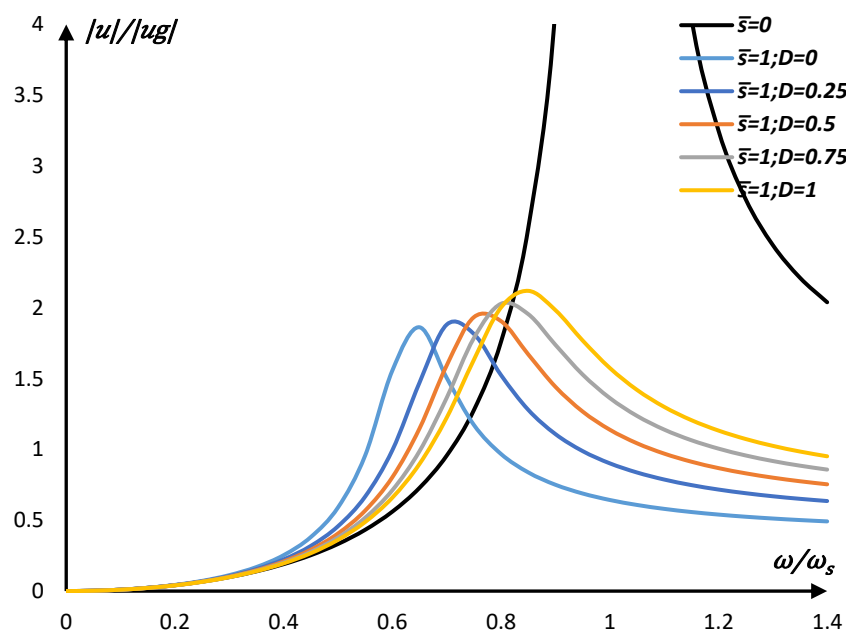


(a) Structural distortion.

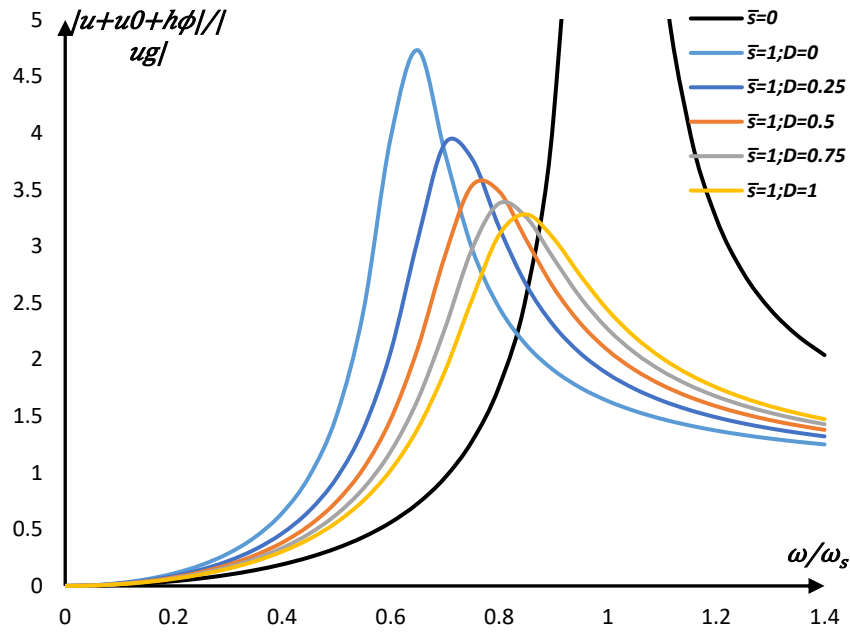


(b) Displacement of the mass relative to free field.

Fig. III.8. Influence of soil-structure interaction as a function of excitation frequency ($\bar{m}=3$, $\bar{h}=1$, $\nu=0.33$, $\xi=0.025$, $\xi_g=0.05$, $D=0$), varying a_0 .



(a) Structural distortion.



(b) Displacement of the mass relative to free field.

Fig. III.9. Influence of soil-structure interaction as a function of excitation frequency ($\bar{m}=3$, $\bar{h}=1$, $\nu=0.33$, $\xi=0.025$, $\xi_g=0.05$, $a_0=1$), varying D .

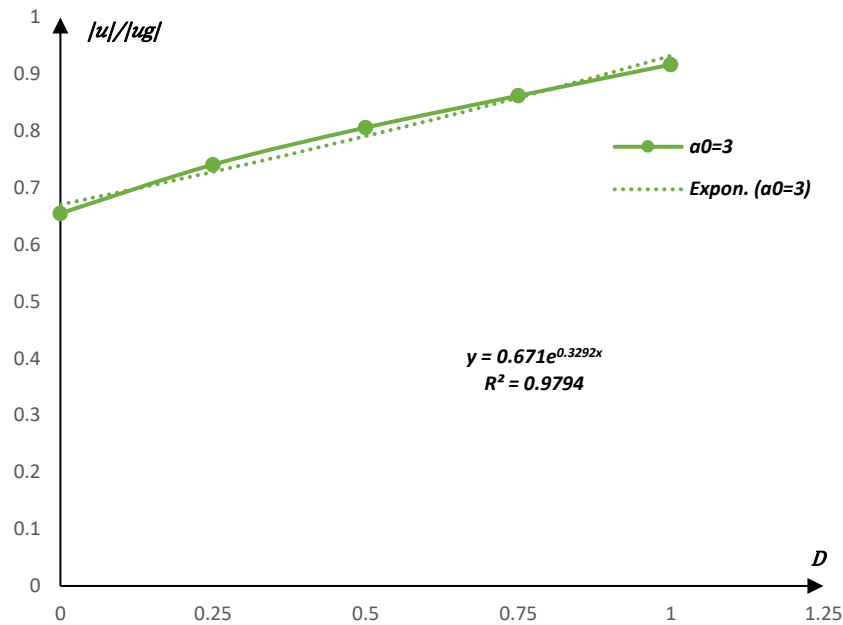
III.4. NEW ANALYTICAL NONLINEAR RELATIONSHIPS

Fig. III.10(a), (b) shows the maximum values of structural distortion and mass displacement for the dynamic case studied as a function of the embedment ratio of the foundation height D . It can be clearly observed that the soil structure interaction has a strong influence on the values of the peaks. The trend curves were also calculated by polynomial interpolation (dotted line) of the nonlinear function. The nonlinear relationships between the dimensionless displacement $|u|/|u_g|$ and the acceleration level D can be predicted with the following relationships:

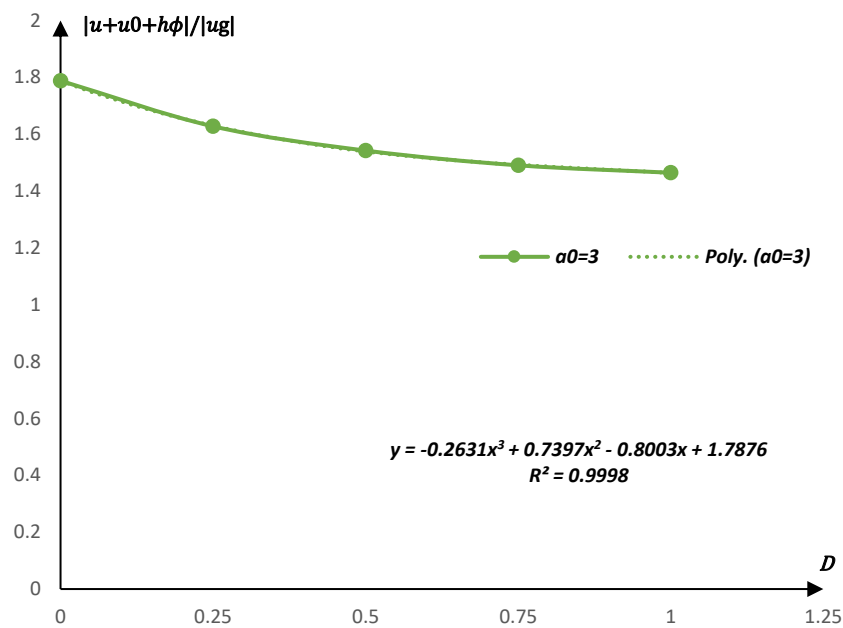
- For the dynamic impedance function:

$$|u|/|u_g| = 0.671 e^{0.3292 D} \quad (\text{III.28})$$

The goodness of statistical fit of the equation (**Eq. (III.28)**) is $R^2=0.9794$, the proposed formula (**Eq. (III.28)**) correctly predicts the results presented in this study.



(a) Structural distortion.



(b) Absolute displacement of the mass.

Fig. III.10. Max Displacement- the foundation embedment ratio D ($\bar{m}=3$, $\bar{h}=1$, $\nu=0.33$, $\xi=0.025$, $\xi_g=0.05$, $a_0=3$).

A nonlinear relation between $|u + u_0 + h\phi|/|u_g|$ and the embedment ratio of the foundation D can be assumed. The given relation is equal to:

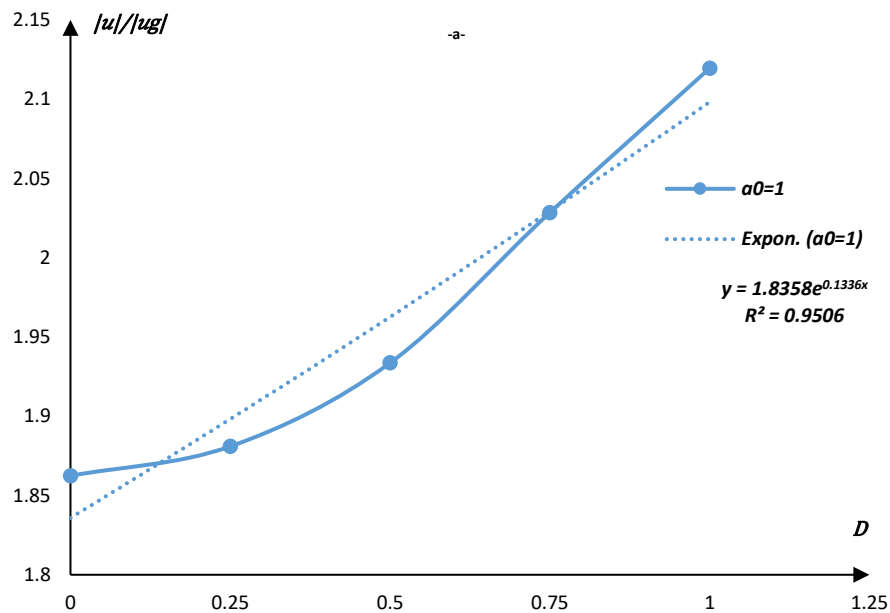
- For the dynamic impedance function:

$$|u + u_0 + h\phi|/|u_g| = -0.2631 D^3 + 0.739 D^2 - 0.8003 D + 1.7876 \quad (\text{III.29})$$

The statistical goodness of fit of the equation (Eq. (III.29)) is $R^2=0.9998$, the proposed formula (Eq. (III.29)) correctly predicts the results presented in this study.

It should be noted that the adjusted R^2 statistic is generally the best indicator of the quality of the fit when its value is closer to one. These curves describe the nonlinear behavior of the equivalent system, which makes it possible to determine the maximum value of the displacement at any desired level of the embedment ratio of the foundation D for $\alpha_0 = 3$.

For different ranges of the dimensionless frequency α_0 , we want to clarify how the anchorage height of the foundation D modifies the structural displacement u/u_g and the total displacement of the mass $u + u_0 + h\phi/u_g$. Thus, it can be seen from Fig. III.11(a) to (e) and Fig. III.12(a) to (e) that u/u_g and $u + u_0 + h\phi/u_g$ are not only a function of the foundation embedment ratio D itself, but also a function of α_0 . This has not been extensively discussed in the literature. Therefore, revised displacements u/u_g and $u + u_0 + h\phi/u_g$ are proposed here. They depend on both D and α_0 .



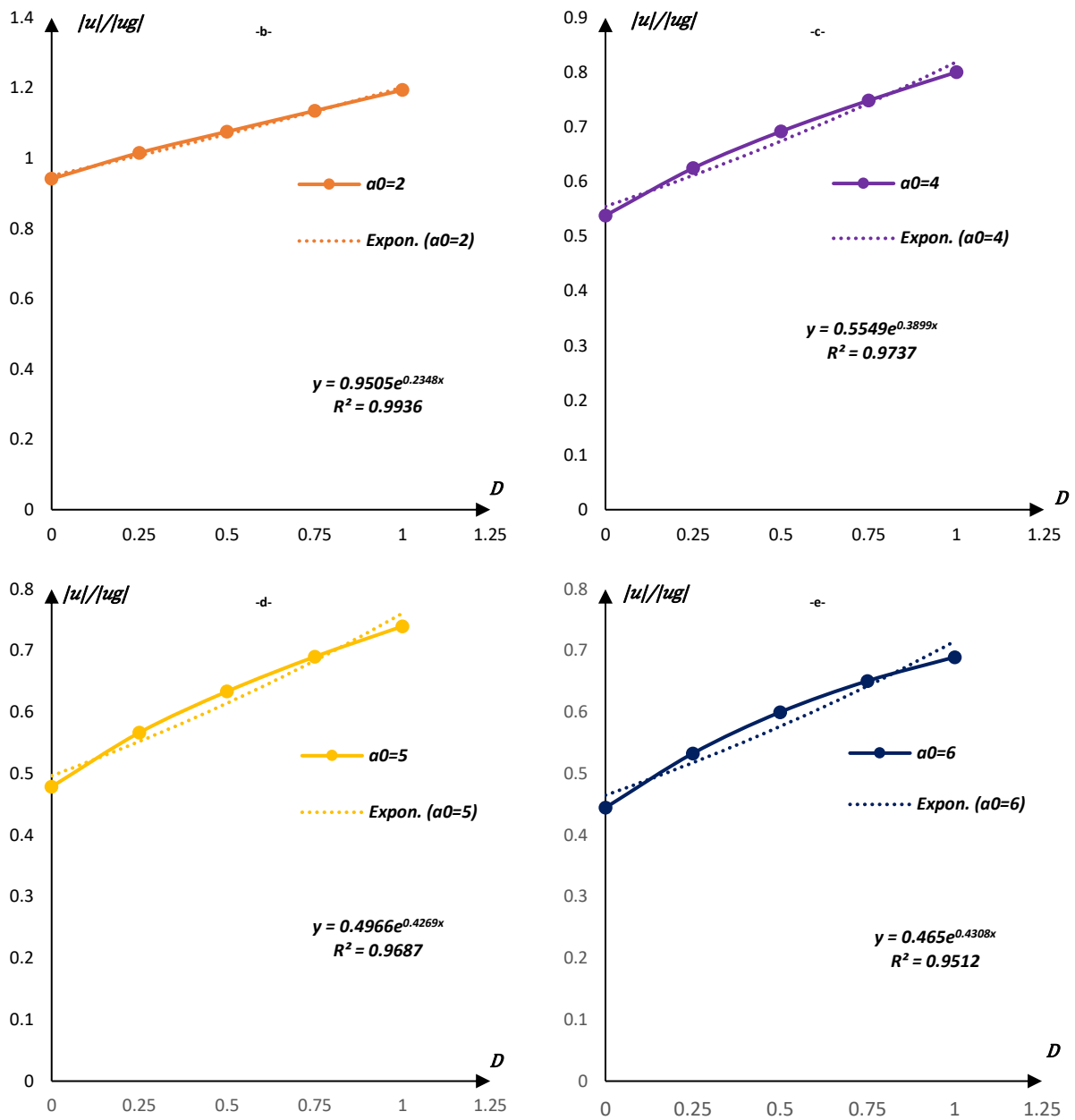
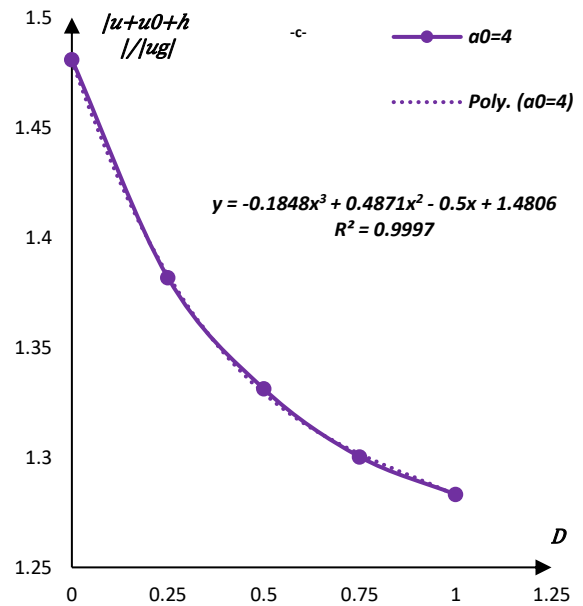
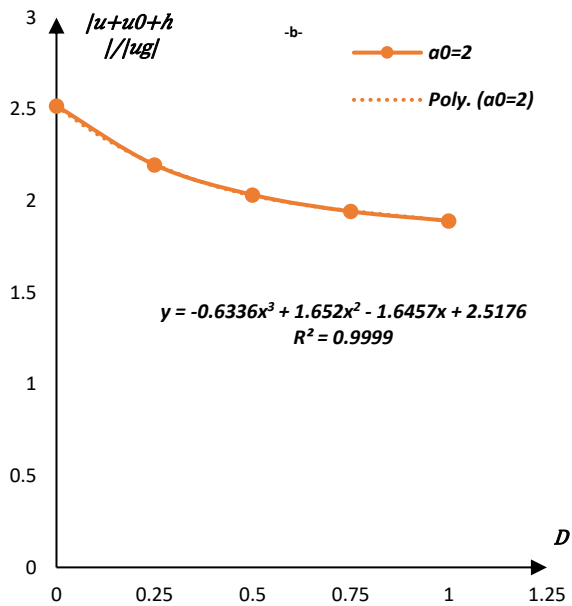
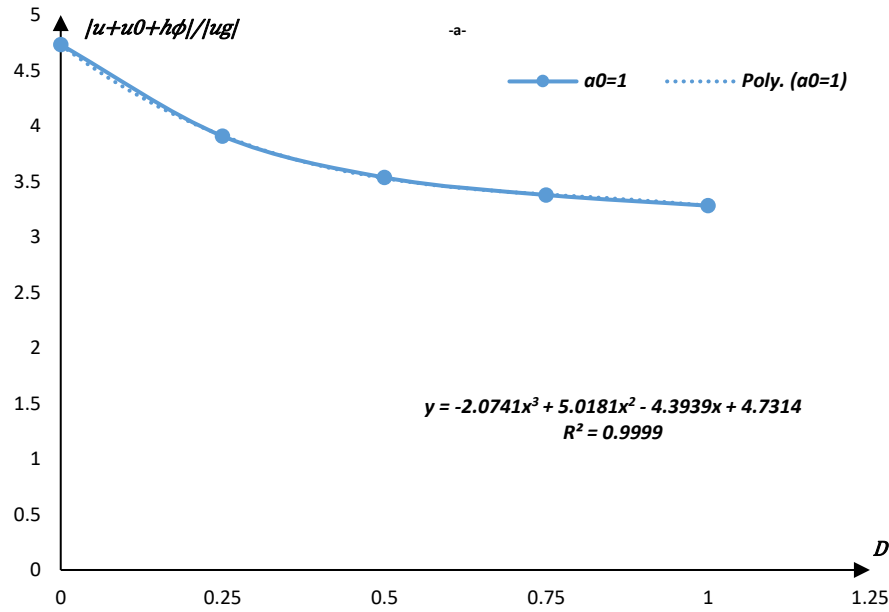


Fig. III.11. Max Structural distortion versus the foundation embedment ratio D ($\bar{h}=1, \bar{m}=3, \nu=0.33, \xi=0.025, \xi_g=0.05, a_0 (= 1, 2, 4, 5, \text{ and } 6)$).



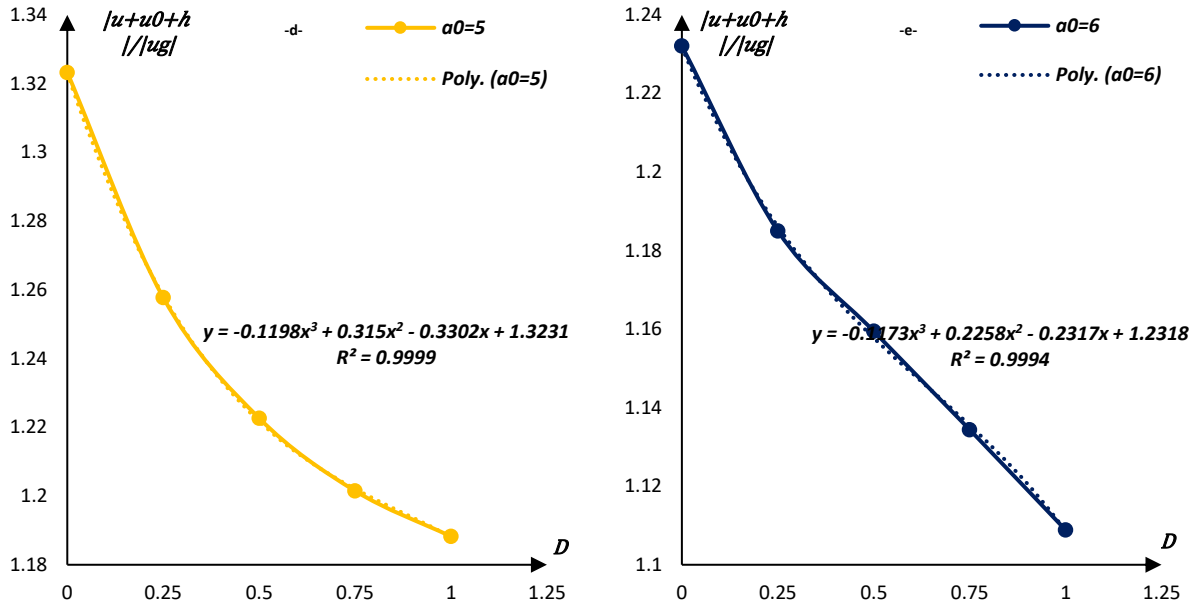


Fig. III.12. Max absolute displacement versus the foundation embedment ratio D ($\bar{h}=1, \bar{m}=3, \nu=0.33, \xi=0.025, \xi_g=0.05, a_0 (= 1, 2, 4, 5, \text{ and } 6)$).

From **Fig. III.11(a)** to **(e)**, the best-fit curve for the structural distortion correction versus the foundation embedment ratio D was an exponential function for each frequency in the form of:

$$\frac{|u|}{|u_g|} = b_0 \cdot e^{b_1 \cdot D} \tag{III.30}$$

The values of the coefficients b_0 , and b_1 were recorded for $a_0 = 1, 2, 3, 4, 5, 6$. **Fig. III.13** shows the values of b_0 and b_1 , thus simulating the dependence of $\frac{|u|}{|u_g|}$ on a_0 .

From the **Fig. III.13**, it is clear that b_0 and b_1 have been fitted with polynomial function, see **Table III.1**.

From **Fig. III.12(a)** to **(e)**, the best fit curve for the absolute displacement versus the anchorage height of the foundation D was a polynomial function for each frequency in the form of:

$$\frac{|u + u_0 + h\varphi|}{|u_g|} = b_2 D^3 + b_3 \cdot D^2 + b_4 \cdot D + b_5 \tag{III.31}$$

The values of the coefficients b_2, b_3, b_4 , and b_5 were recorded for $a_0 = 1, 2, 3, 4, 5, 6$. **Fig. III.14** shows the values of b_2, b_3, b_4 and b_5 , thus simulating the dependence of $\frac{|u+u_0+h\varphi|}{|u_g|}$ on a_0 . From the Fig. 13, it is clear that b_2 and b_3 follow a different trend and were given different polynomial functions, see **Table III.2**.

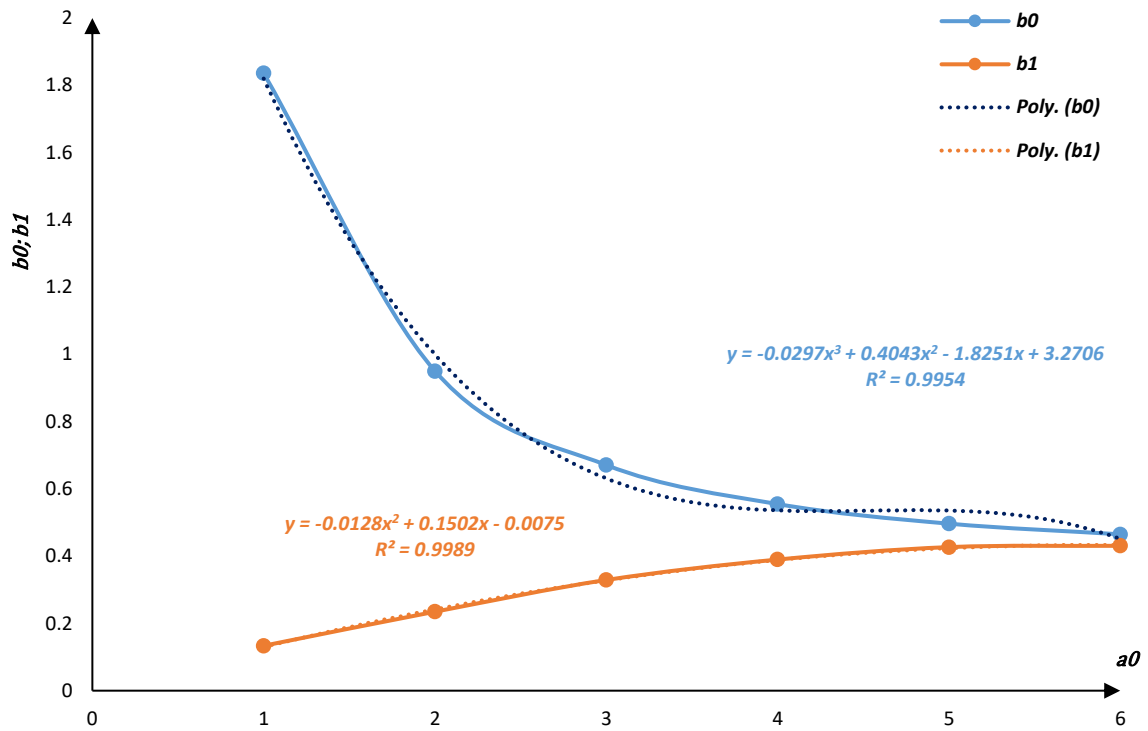


Fig. III.13. Variation of the coefficients b_0 and b_1 with a_0 .

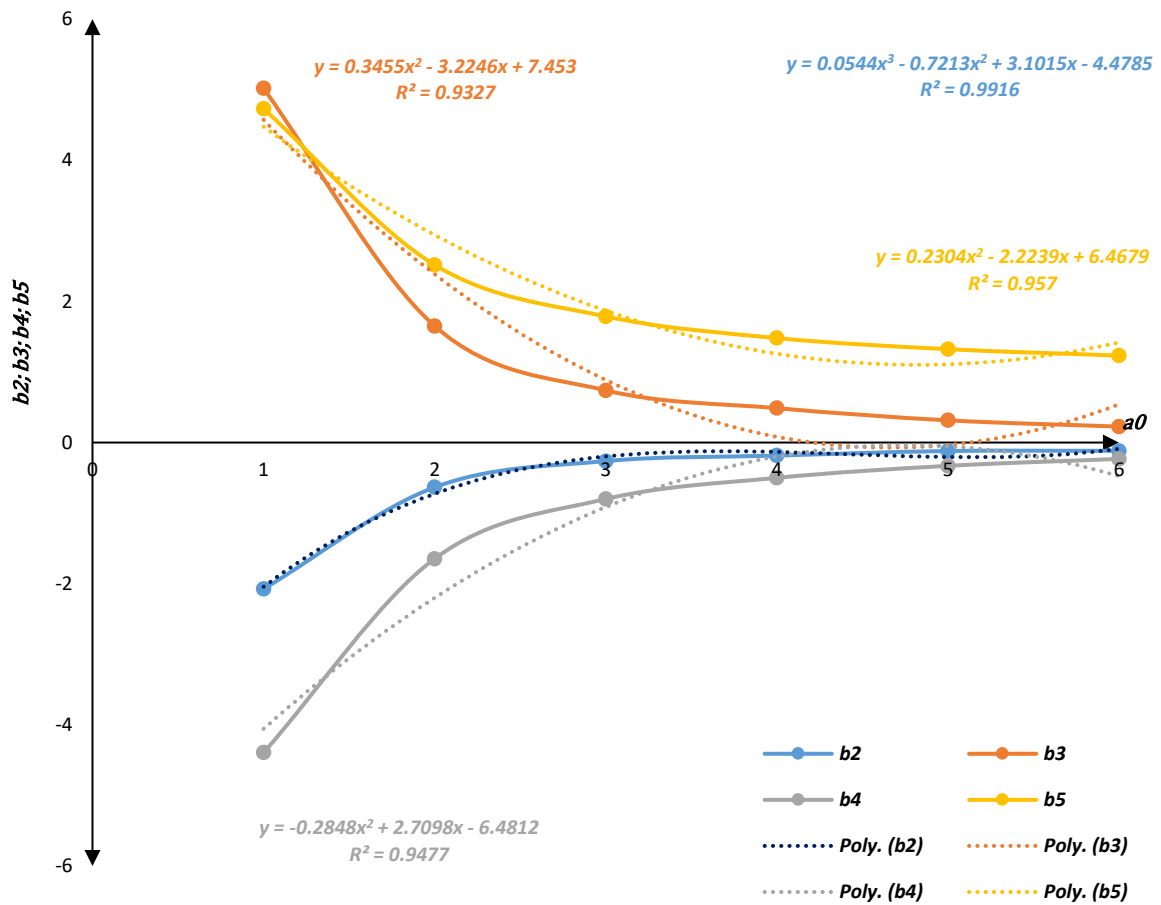


Fig. III.14. Variation of the coefficients b_2 , b_3 , b_4 and b_5 with a_0 .

Table III.1. The fitting functions of the b_0 and b_1 coefficients.

Coefficients	Fit Equations	R ²
b₀	$b_0 = -0.0297a_0^3 + 0.4043a_0^2 - 1.8251a_0 + 3.2706$	0.9954
b₁	$b_1 = -0.0128 a_0^2 + 0.1502 a_0 - 0.0075$	0.9989

Table III.2. The fitting functions of the b_2 , b_3 , b_4 and b_5 coefficients.

Coefficients	Fit Equations	R ²
b₂	$b_2 = 0.0544 a_0^3 - 0.7213 a_0^2 + 3.1015 a_0 - 4.4785$	0.9916
b₃	$b_3 = 0.3455 a_0^2 - 3.2246 a_0 + 7.453$	0.9327
b₄	$b_4 = -0.2848 a_0^2 + 2.7098 a_0 - 6.4812$	0.9477
b₅	$b_5 = 0.2304 a_0^2 - 2.2239 a_0 + 6.4679$	0.957

As a result, from the above analysis, the structural distortion and absolute displacement can be summarized by **Eq. (III.32)** and **Eq. (III.33)**:

$$\frac{|u|}{|u_g|} = (-0.0297a_0^3 + 0.4043a_0^2 - 1.8251a_0 + 3.2706) \cdot e^{(-0.0128 a_0^2 + 0.1502 a_0 - 0.0075) \cdot D} \quad (\text{III.32})$$

$$\begin{aligned} \frac{|u + u_0 + h\varphi|}{|u_g|} &= (0.0544 a_0^3 - 0.7213 a_0^2 + 3.1015 a_0 - 4.4785) \cdot D^3 \\ &+ (0.3455 a_0^2 - 3.2246 a_0 + 7.453) \cdot D^2 \\ &+ (-0.2848 a_0^2 + 2.7098 a_0 - 6.4812) \cdot D + (0.2304 a_0^2 \\ &- 2.2239 a_0 + 6.4679) \end{aligned} \quad (\text{III.33})$$

These new analytical nonlinear relationships between the relative and absolute displacement of the structure, the embedment ratio of the foundation and the dimensionless circular frequency of the excitation are proposed in order to consider this influence in a simple way in the calculation of the soil-structure interaction for different soil and structure types and for different seismic excitation frequencies.

III.5. CONCLUSION

This chapter performs an analytical analysis based on the dynamic equilibrium of the soil-structure system modeled by an analog model with three degrees of freedom to obtain the seismic response of the selected structure with viscoelastic soil behavior. To explore the sensitivity of the response of a soil-structure system to different soil and structure parameters, this chapter investigates the effect of adopting different impedance function types on the structural response of the soil-structure system using springs and dashpots with two frequency cases: independent and dependent frequencies.

Finally, new analytical nonlinear relationships are proposed between the displacements of the structure, the embedment ratio of the foundation and the dimensionless circular frequency of the excitation, in order to consider in a simple way this influence in the calculation of the soil-structure interaction for different soil types and seismic excitation frequency.

From the analyses presented in this chapter, we can conclude that

- The massive and/or higher structures, the soft soil and the excitation frequency are the main parameters where the SSI influence is more evident.
- This study shows the differences due to the influence of the form of the impedance function (static or dynamic).
- The dynamic responses of the structure under seismic motion, taking into account the soil-structure interaction, are highly dependent on: the type of soil (c_s), the characteristic of the structure (massive, slender, ...), the foundation embedding D , and the dimensionless excitation frequency (a_0), since its increase leads to a decrease in the displacement amplitude and an increase in the equivalent damping $\tilde{\xi}$.

In conclusion, a significant detrimental effect on the response and displacement performance of the structure is shown by the inclusion of the soil-structure interaction in the structural analysis in this work. This effect is characterized by an overestimation of the displacement of the structure and a strong dependence on the soil and structure properties. Ignoring the soil-structure interaction effect and the approximate representation of the impedance functions can lead to a behavior that is very different from the real one, and therefore can mislead the engineer's decision-making process and thus compromise the seismic safety of buildings.

Therefore, to ensure safety and structural integrity against seismic actions, it is strongly recommended that practicing engineers and engineering firms consider the effects of soil-structure interaction and properly address the dynamic characteristics of the soil in seismic analysis and building design.

***CHAPTER IV: ANALYTICAL ANALYSIS WITH
EQUIVALENT LINEAR SOIL BEHAVIOR***

IV.1. INTRODUCTION

For strong earthquakes, the behavior of the soil becomes nonlinear due to the degradation of its shear modulus G , which can have significant effects on the amplitude and the shape of the impedance function of the soil-foundation system as well as on the seismic response of the structures.

The study of the phenomenon of soil-structure interaction in nonlinear behavior is very complicated and requires sophisticated methods and tools. Unlike its study in the case of linear elastic soil behavior, where the soil parameters (especially the shear modulus G/G_{max} , the critical damping coefficient ξ/ξ_{max} and the shear wave variation V/V_{max}) are constant during the analysis, in nonlinear soil behavior all the values of the soil parameters are related by the amplitude of the excitation imposed on the soil. This behavior occurs when the soil is subjected to strong seismic level excitations.

Therefore, in the present work we have improved an approach that takes into account the nonlinearities of soil behavior in soil-structure interaction to solve this problem in a simple way using the equivalent linear method, where we have studied the influence of nonlinear soil behavior and the effect of the impedance function form using springs and dashpots with two frequency cases: independent and dependent frequencies (static impedance function, dynamic impedance function) on the seismic response of a coupled soil-structure system.

The problem considered in this study consists of a structure modeled as a single-degree-of-freedom system ($\xi = 0.025$) resting on shallow foundations. For the linear case, the soil properties are described by its Poisson's ratio $\nu = 0.33$, shear modulus $G = 1$, and material damping $\xi_g = 0.05$. In the case of nonlinear soil behavior and according to Eurocode 8 (2003), the consideration of the nonlinearity of the soil has been introduced in this work by taking into account the degradation of the soil shear modulus (G/G_{max}) and the amplification of the damping coefficient ratio ($\xi_g/\xi_{g max}$) as a function of the increase of the shear strain of the soil each time the earthquake is taken stronger. This part was processed by the Caldynasoil calculation code Sbartai & Filali (2012) and Filali & Sbartai (2017) to determine the nonlinear dynamic parameters of the soil at different levels of seismic deformation.

IV.2. SYSTEM AND METHOD OF ANALYSIS

IV.2.1. Methodology for calculating nonlinear soil behavior parameters

The nonlinear soil behavior is integrated into the analysis of the present model by the equivalent linear method and compared with the linear case. A seismic deformation variation is applied to the soil (weak, medium, and strong excitation). The behavior of the soil is thus described by curves giving the variation of the shear modulus ratio G/G_{max} and the critical damping ratio $\xi_g/\xi_{g max}$ as a function of each imposed deformation. This behavior is determined by the CALDYNASOIL calculation code of Sbartai and Filali (2012), which uses the equivalent linear method with concentrated masses and the hyperbolic models of Hardin and Drenevich (1972), Ramberg and Osgood (1943) and Massing (1926). This procedure is iterative and allows to estimate the seismic response of a soil profile consisting of horizontal layers, subjected to any seismic acceleration at the level of the substratum. Each layer is considered linear-elastic and modeled by a concentrated mass model. **Fig. IV.1** shows the simple mechanical model and the equivalent soil profile. The soil mass of this model is also concentrated above and below each layer.

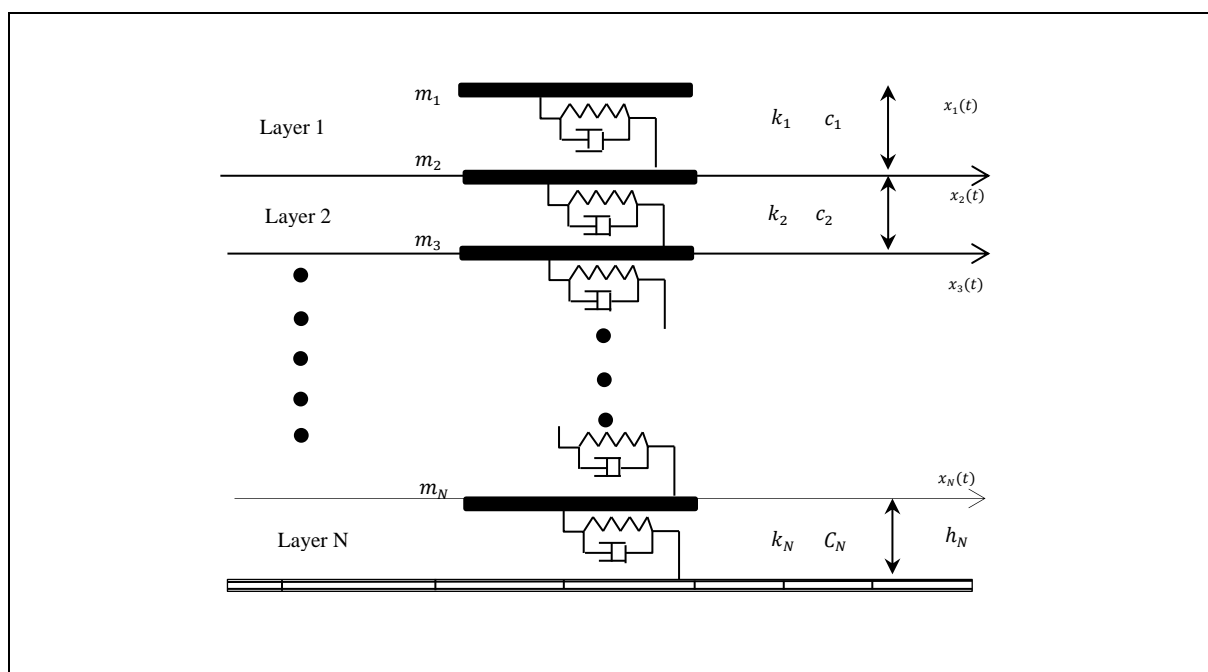


Fig. IV.1. Lumped Mass Model. (Filali and Sbartai 2017)

Where:

$$m_1 = \frac{\rho_1 h_1}{2}, \quad m_i = \frac{\rho_{i-1} h_{i-1} + \rho_i h_i}{2} \quad (i = 2, 3 \dots N) \quad (\text{IV.1})$$

m_i , and h_i are the concentrated mass, and the thickness of the soil layer i , respectively.

Briefly, the analysis steps of the equivalent linear concentrated mass method are as follows:

- **Step 1:** Estimate the initial physical parameters for each soil layer i (shear modulus G_{max} , mass density ρ , Poisson's ratio ν , hysteretic damping $\xi_{g_{max}}$. In this step, all soil parameters are determined by in-situ tests or laboratory tests with low deformation.
- **Step 2:** Select the number of soil layers to be analyzed.
- **Step 3:** Calculate the mass, stiffness, and damping matrices.
- **Step 4:** Solve the equations governing the motion of all soil layers (e.g., using a modal dynamic analysis method), taking into account the dynamic equilibrium for each layer:

$$[m] (\ddot{x}) + [c] (\dot{x}) + [k] (x) = - (m) \ddot{x}_r \quad (\text{IV.2})$$

Where (x) ; (\dot{x}) ; (\ddot{x}) = vectors of displacements, velocities and horizontal accelerations of each layer with respect to the rock; (m) a vector containing the mass of each soil layer; \ddot{x}_r = accelerogram at the rock level.

- **Step 5:** For each layer i , the maximum shear unit deformations, $\gamma_{max}(i)$, are calculated from the maximum inter-layer displacements:

$$\gamma_{max}(i) = \frac{|x_i - x_{i+1}(t)|_{max}}{h_i} \quad (\text{IV.3})$$

- **Step 6:** Update the stiffness and the equivalent damping, from the maximum shear unit deformations calculated in step 5. In general, a fraction of the maximum values of 2/3 is used, because the maximum deformation levels are reached only once during the dynamic response.

Among the three models of nonlinear soil behavior integrated in the code CALDYNSOIL (Sbartai and Fillali 2012), in this study we choose the model of behavior of Massing (1926), represented by the following relation:

$$\tau = \frac{\gamma}{\frac{1}{G_{max}} + \frac{\gamma}{\tau_{ult}}} \quad (\text{IV.4})$$

Where:

- τ is the shear stress.

- γ is the shear strain.
- τ_{ult} is the ultimate shear stress.

By dividing the **Eq. (IV.4)** by γ , we obtain the effective shear modulus of the soil G , according to the unitary deformation in shear γ by:

$$\frac{G}{G_{max}} = \frac{1}{1 + \frac{\gamma}{\gamma_r}} \quad \text{(IV.5)}$$

Where $\gamma_r = \tau_{ult}/G_{max}$, is the unit deformation of the reference.

For the critical damping coefficient, $\xi_g/\xi_{g\ max}$, Massing (1926) proposed the relationship between critical damping and shear modulus as:

$$\frac{\xi_g}{\xi_{g\ max}} = \left(1 - \frac{G}{G_{max}}\right) \quad \text{(IV.6)}$$

Where: $\xi_{g\ max}$ is the maximum critical damping (initial value).

- **Step 7:** Steps 3 through 7 are repeated until the stiffness and damping converge. In general, only a few iterations are sufficient to achieve convergence.

*The Equivalent Linear Method has been briefly described in this section; see **Chapter II** for more details.*

IV.2.2. Presentation of the calculation program

The calculation code **Caldynasoil** (2012) has been written in Matlab language and is intended for dynamic calculation of seismic response of soil deposits and evaluation of liquefaction potential of saturated sandy soils based on the equivalent linear calculation method with concentrated masses. The nonlinear soil behavior is modeled by three hyperbolic laws, Hardin & Drnevich (1972), Ramberg & Osgood (1943) and Masing (1926).

We have chosen the example of a seismic excitation of $PGA=0.3g$ on a sandy soil profile of height $H = 10m$, characterized by its dry density $\gamma_{sec} = 19.1\ k\ N/m^3$ and saturated density $\gamma_{sat} = 21.3\ k\ N/m^3$, shear wave velocity $c_s = 100\ m/s$, to illustrate how to find the dynamic properties of the soil using this calculation code. All soil parameters are displayed in the software interface, see **Fig.IV.2**.

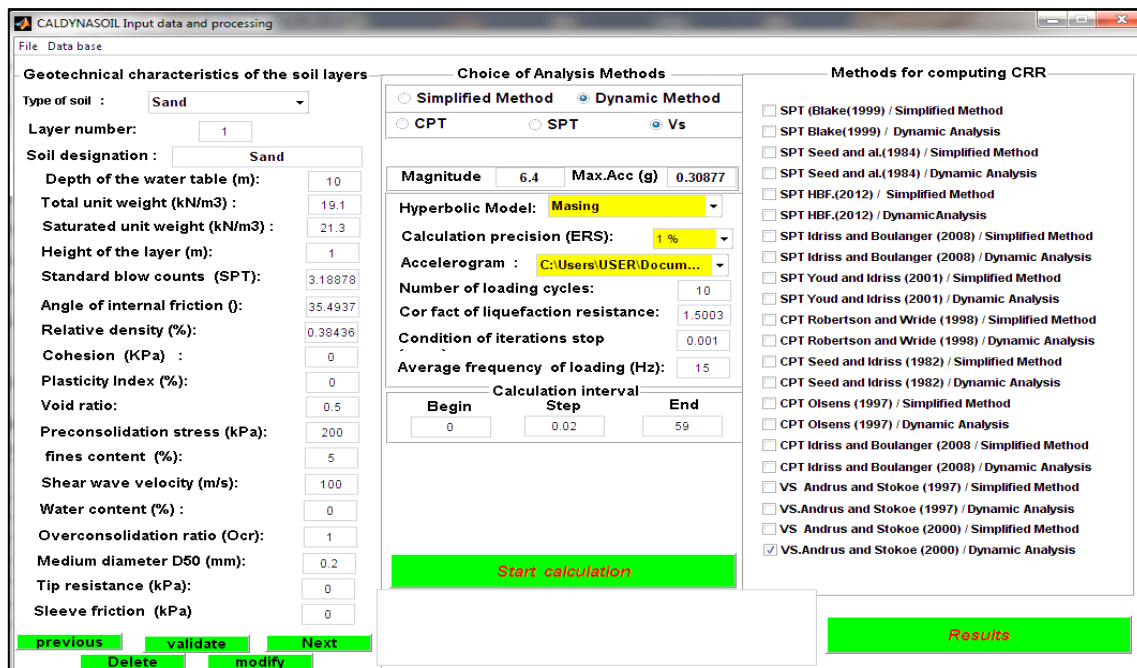


Fig. IV.2. Main interface of the Caldynasoil software. (Kamel Filali 2018)

This interface contains three main columns, as shown in **Fig. IV.2**, the first of which is dedicated to the input of all the geotechnical parameters of the initial soil profile. The second is dedicated to the selection of the analysis methods (either the simplified or the dynamic method), and also includes hyperbolic soil models, layer number accuracy (ERS) and, finally, the selection of the seismic accelerogram. The last column specifies the selection of the Cyclic Resistance Ratio (CRR) and Cyclic Stress Ratio (CRR/CSR or CRR/CSR_D) calculation methods.

In this example, we have chosen the dynamic calculation method to simulate the nonlinear behavior of the soil with the hyperbolic model of Masing (1926) and we have also checked Vs option, as shown in **Fig. IV.3**.

Choice of Analysis Methods

Simplified Method Dynamic Method

CPT SPT Vs

Magnitude: 6.4 Max.Acc (g): 0.30877

Hyperbolic Model: Masing

Calculation precision: Hardin et Drnevich

Accelerogram: C:\Users\USER\Documents\1.5003

Number of loading cycles: 10

Cor fact of liquefaction resistance: 1.5003

Condition of iterations stop: 0.001

Average frequency of loading (Hz): 15

Calculation interval

Begin	Step	End
0	0.02	59

Start calculation

Fig. IV.3. Analysis method selection.

Fig. IV.4 shows the calculation accuracy (ERS), which is set to 1% in this example.

Choice of Analysis Methods

Simplified Method Dynamic Method

CPT SPT Vs

Magnitude: 6.4 Max.Acc (g): 0.30877

Hyperbolic Model: Masing

Calculation precision (ERS): 1%

Accelerogram: C:\Users\USER\Documents\1.5003

Number of loading cycles: 10

Cor fact of liquefaction resistance: 1.5003

Condition of iterations stop: 0.001

Average frequency of loading (Hz): 15

Calculation interval

Begin	Step	End
0	0.02	59

Start calculation

Fig. IV.4. Calculation precision (ERS).

In this window (see **Fig. IV.5**), we have selected the accelerogram for our dynamic load selection, where we have chosen an earthquake with an acceleration of $Acc(g)=0.3g$.

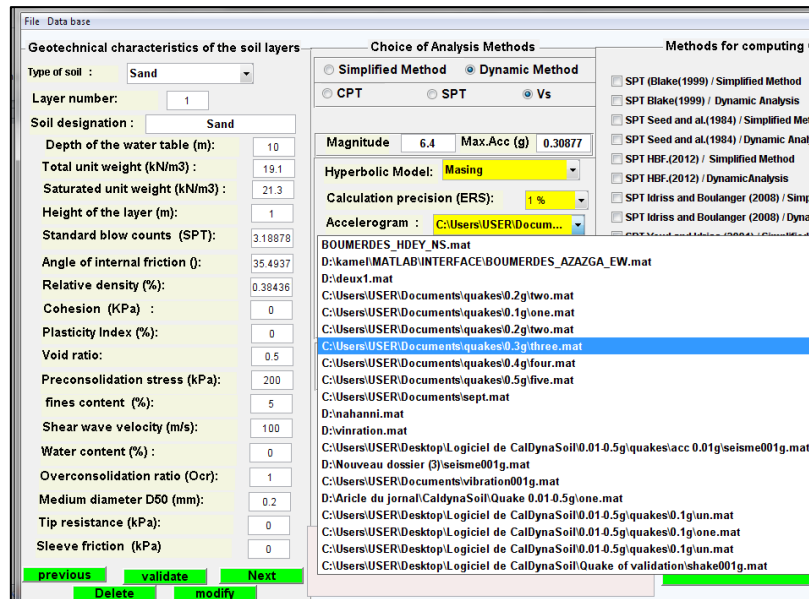


Fig. IV.5. Selecting the Seismic Acceleration.

To start the calculation, click on the "Start Calculation" button after selecting all geotechnical soil parameters, the appropriate analysis method and the earthquake (Fig. IV.6).

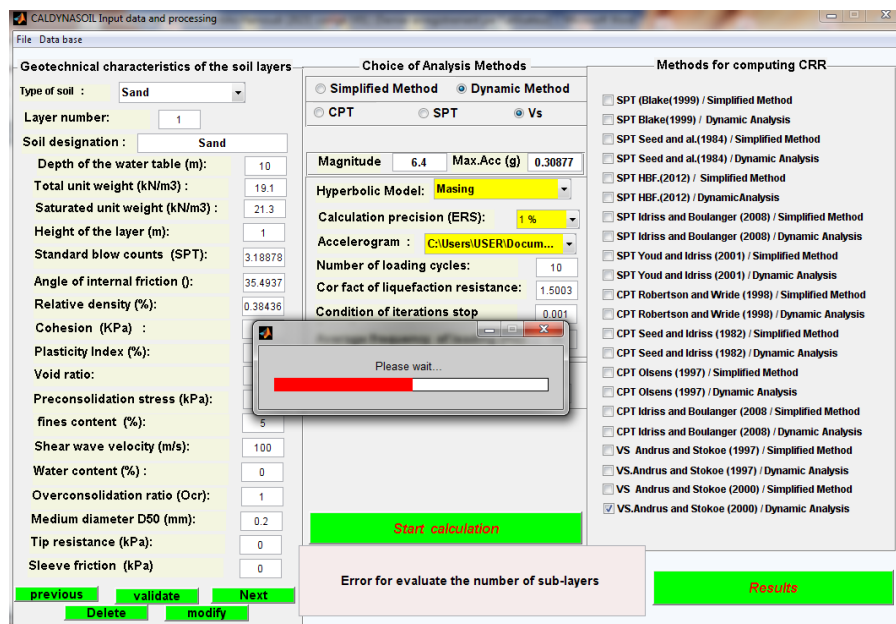


Fig. IV.6. Start Calculation Step.

At the end of the calculation step (Fig. IV.7), the following window appears, displaying the results of the analysis (number of calculation iterations, number of sublayers in the soil profile, dynamic soil parameters, etc.).

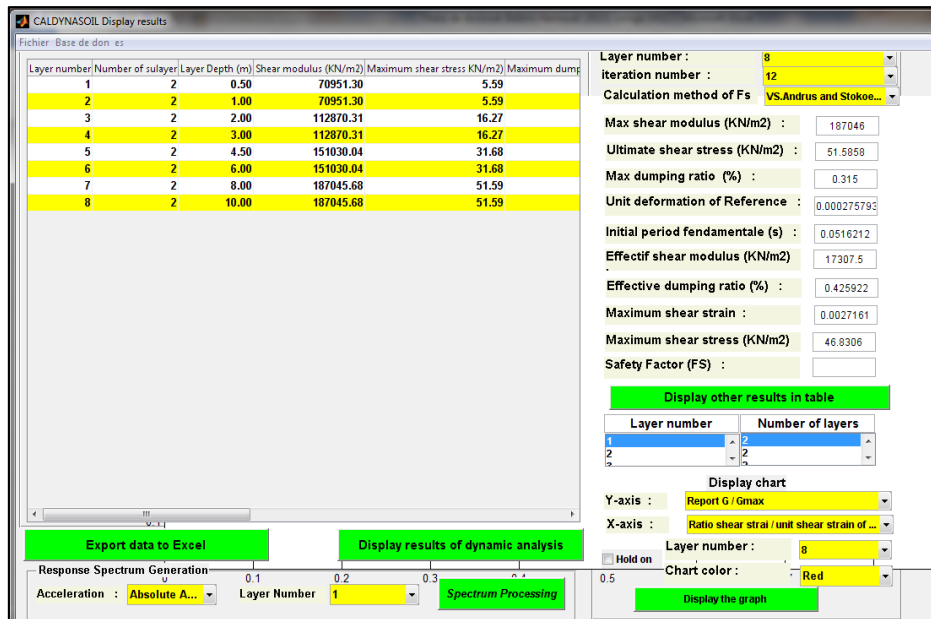


Fig. IV.7. Results window.

In the following Fig. IV.8, we can easily extract the curves of the decrease of the shear modulus G/G_{max} and the increase of the damping coefficient (ξ/ξ_{max}) and even their minimum and maximum values.

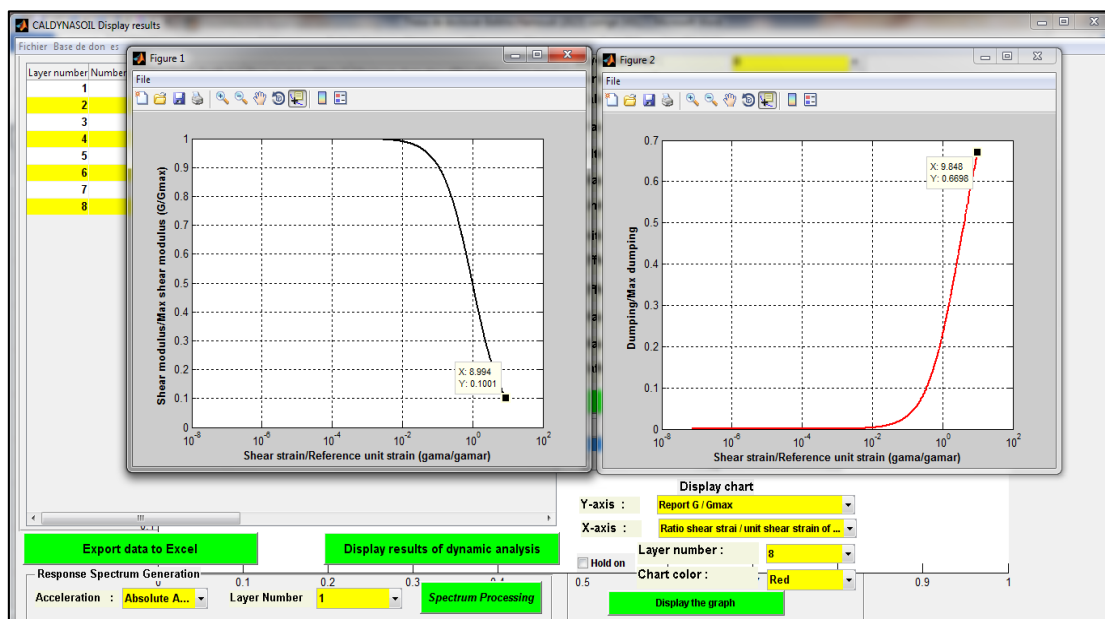


Fig. IV.8. Dynamic soil property values after analysis.

In this research work, we have chosen this calculation program to estimate the properties of nonlinear soil behavior to use it in the study of the seismic response of a soil-structure system with nonlinear soil behavior, because this calculation code gives good results of nonlinear soil behavior and it is not time-consuming to calculate. (Belkhir et al. 2022)

IV.2.3. Dynamic properties of nonlinear soil behavior

The soil profile (**Fig. IV.9**) is sandy with a height $H = 10m$, characterized by its density $\gamma = 19.1 k N/m^3$, shear wave velocity $c_s = 100 m/s$, and critical damping coefficient $\xi_{g\ max} = 0.05$. After applying the seismic accelerations of Loma Prieta-Diamond-0.10g, Nahanni-0.20-g, El-Centro-0.30g, Loma Preita-0.40g, Northridge-0.5g shown in **Fig. IV.10(a) to (e)** to this soil profile, we have obtained its nonlinear dynamic properties for each seismic excitation, where they are recorded in **Table. IV.1**. The two moduli (G/G_{max} , $\xi_g/\xi_{g\ max}$) are shown in **Fig. IV.11** to **Fig. IV.15** as a function of soil shear strain, and the peak ground acceleration PGA (= 0.1g to 0.5g). For the linear case, the soil properties are described by its Poisson's ratio $\nu = 0.33$, shear modulus $G = 1$, and material damping $\xi_g = 0.05$.

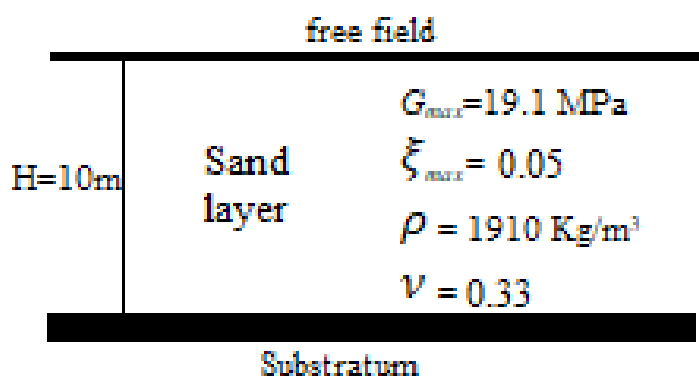
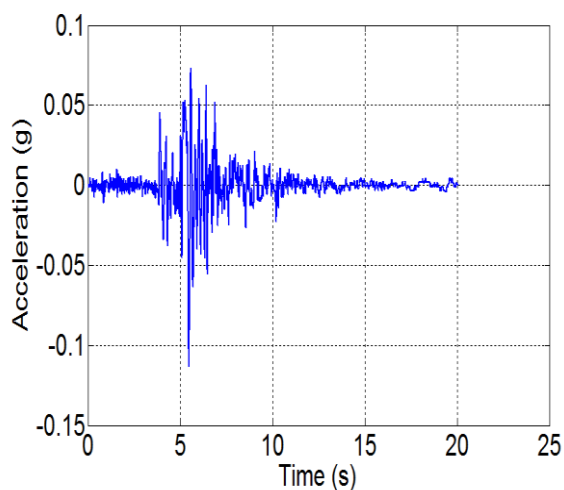
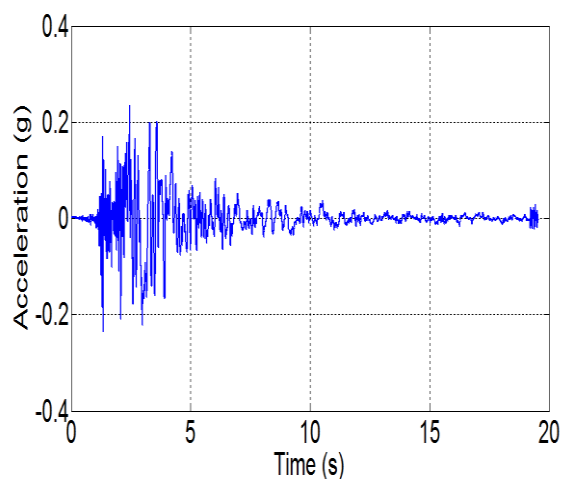


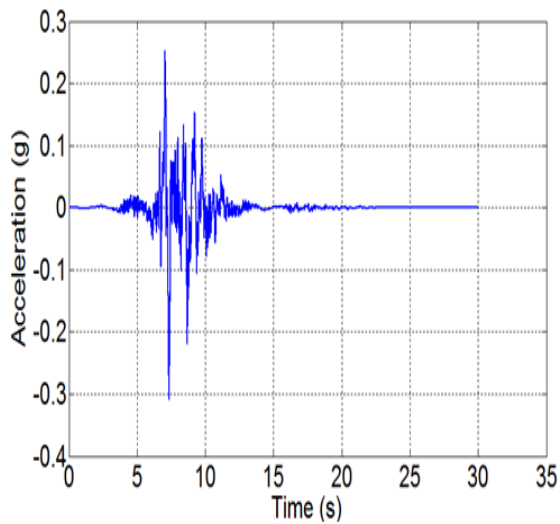
Fig. IV.9. Soil characteristics.



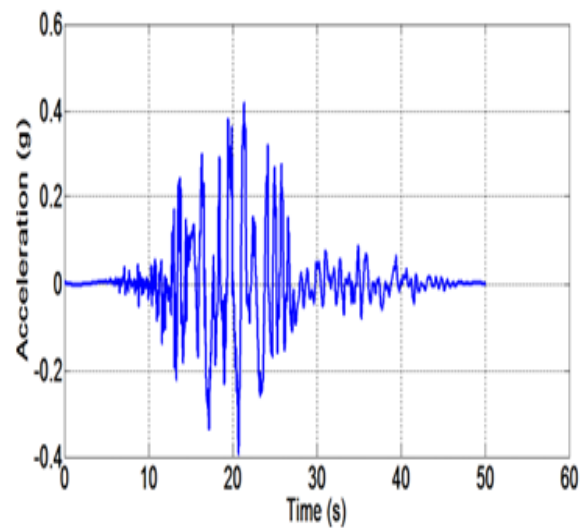
(a) The acceleration time histories of the Loma Prieta earthquake, "Diamond HTs" , 1989 (**0.1g**).



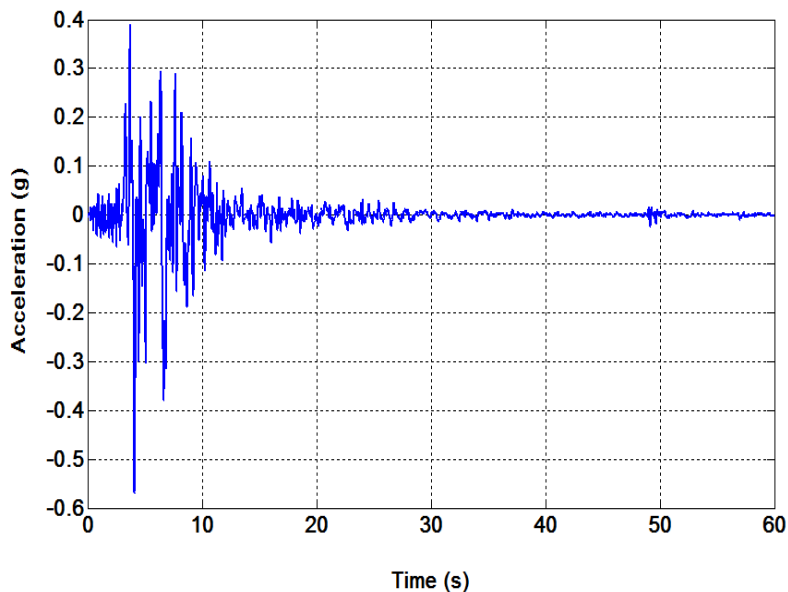
(b) The acceleration time histories of Nahanni, 1985 (**0.2g**).



(c) The acceleration time histories of the El-Centro, 1940 (**0.3g**)



(d) The acceleration time histories of the Loma Preita, 1989 (**0.4g**)



(e) The acceleration time histories of the Northridge ,1994 (**0.50g**)

Fig. IV.10. Seismic accelerations used in this study.

Fig. IV.11 to Fig. IV.15 show the effects of seismic accelerations imposed on the soil model. For a small seismic acceleration $PGA=0.1g$, the behavior of the soil is almost linear, because the amplitude of this deformation is very small, the value of the shear modulus is equal to $G/G_{max}=0.6$ and in the linear case it is equal to $G_{max}=1$ and the same remark is recorded in the soil damping coefficient $\xi/\xi_{max}=0.16$ and in the linear case it is equal to $\xi_{max}=0.05$. From the excitation of $PGA=0.2g$, the behavior of the soil enters the nonlinear

behavior, we see that the value of the shear modulus decreases and an increase in damping means that the soil loses its stiffness. The nonlinearity of the soil becomes more pronounced, especially for $PGA=0.3g$, 0.4 and $0.5g$, as shown in **Fig. IV.13**, **Fig. IV.14** and **Fig. IV.15**.

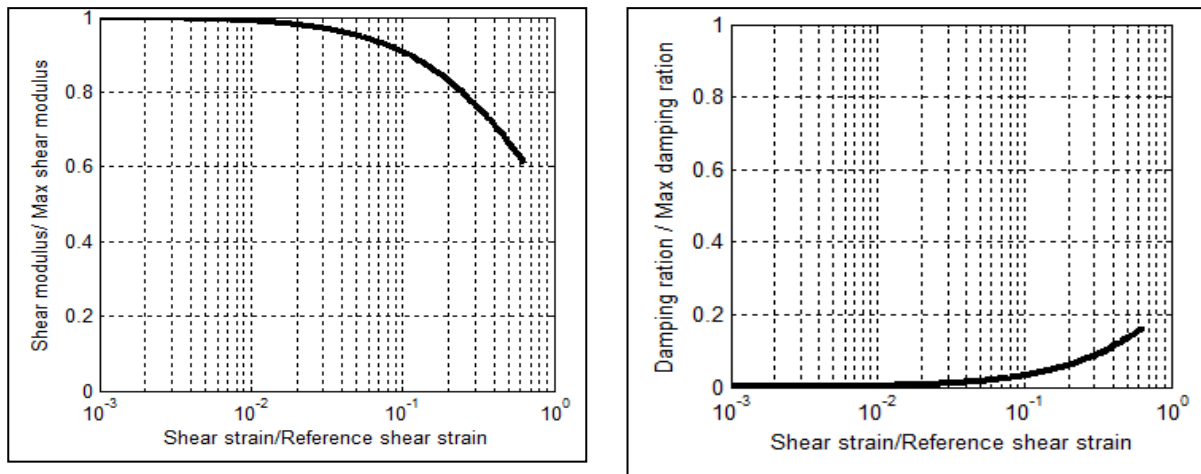


Fig. IV.11. Variation of shear modulus (G/G_{max}) and damping coefficient (ξ/ξ_{max}) as a function of shear strain (γ/γ_r) due to acceleration of "Diamond HTs" , 1989 (**0.1g**).

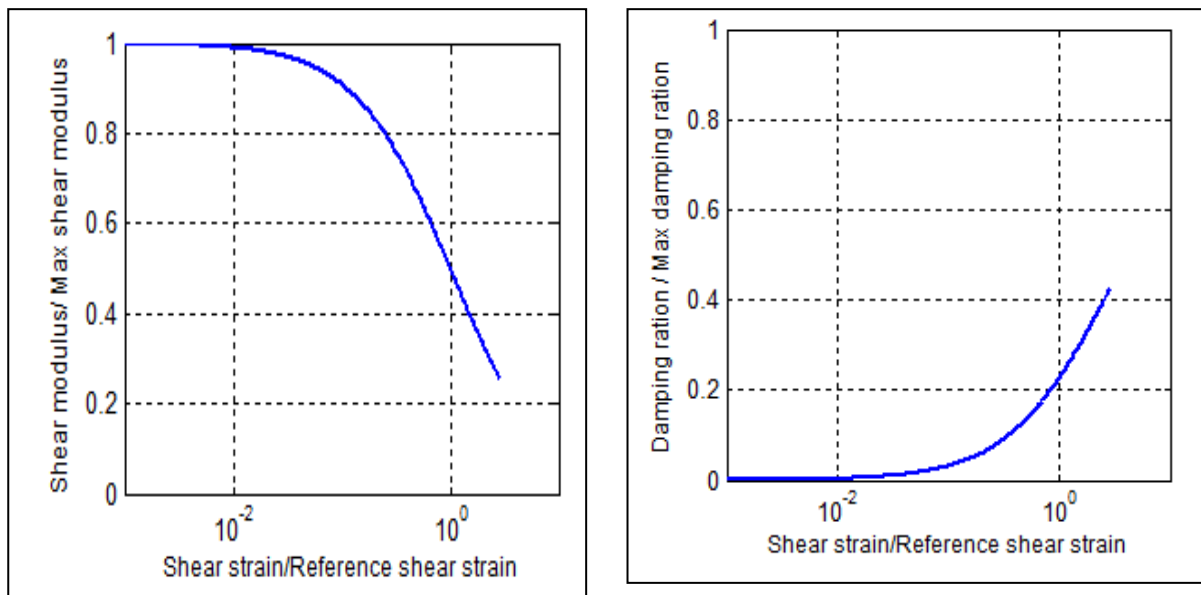


Fig. IV.12 Variation of shear modulus (G/G_{max}) and damping coefficient (ξ/ξ_{max}) as a function of shear strain (γ/γ_r) due to acceleration of of Nahanni, 1985 (**0.2g**).

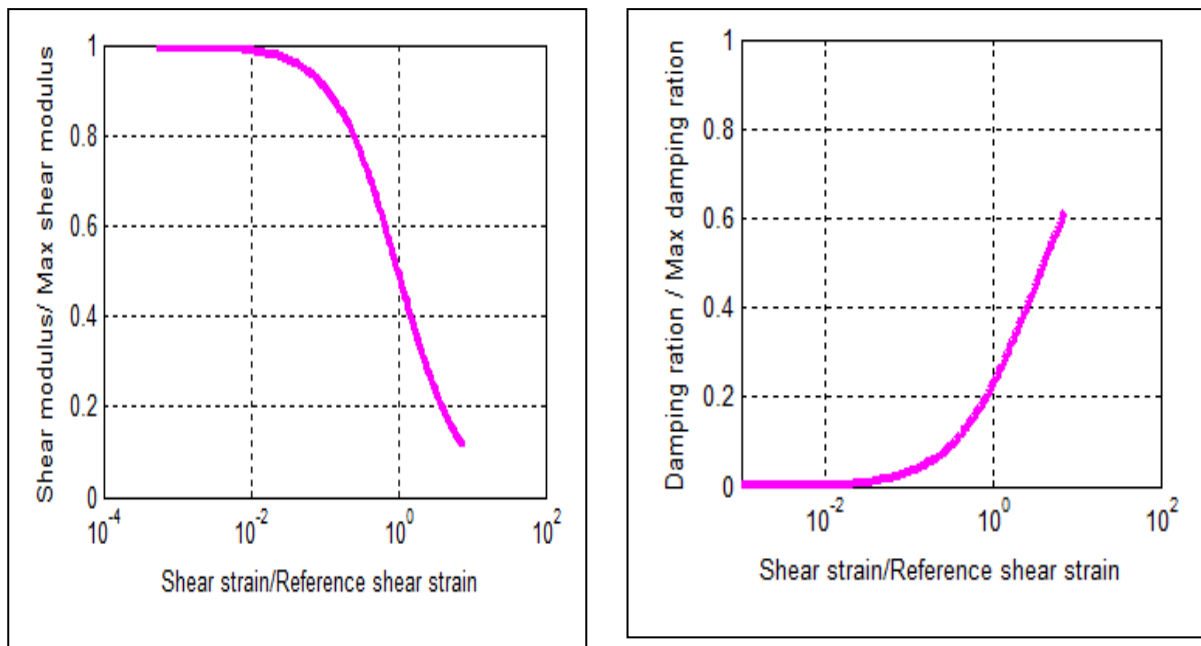


Fig. IV.13 Variation of shear modulus (G/G_{max}) and damping coefficient (ξ/ξ_{max}) as a function of shear strain (γ/γ_r) due to acceleration of the El-Centro, 1940 (**0.3g**).

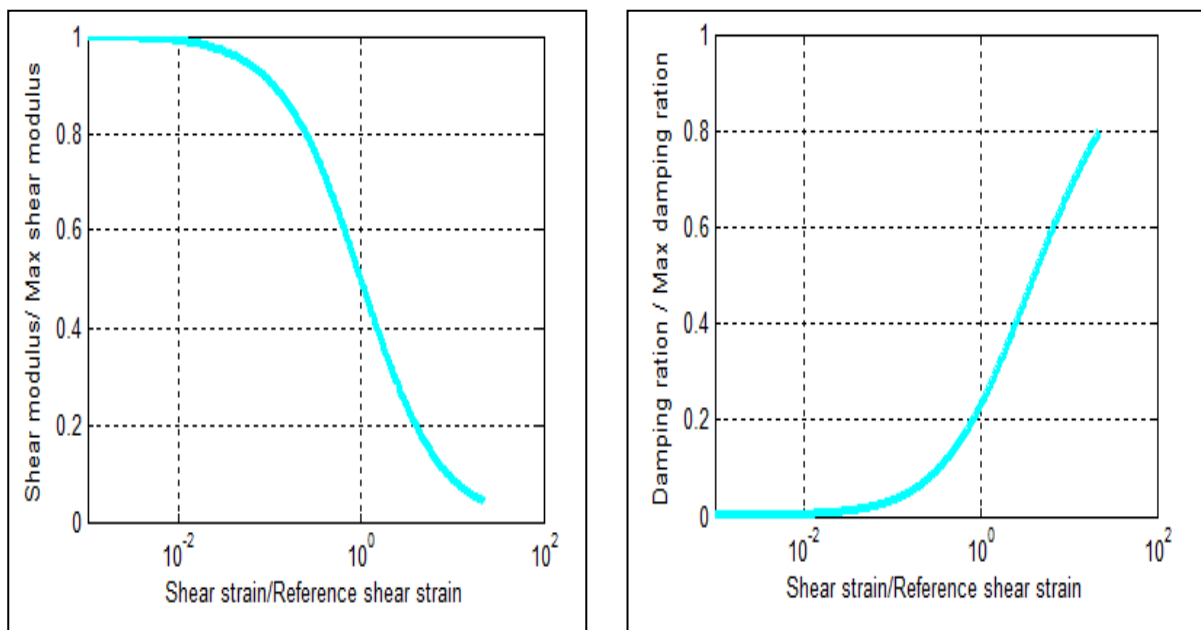


Fig. IV.14 Variation of shear modulus (G/G_{max}) and damping coefficient (ξ/ξ_{max}) as a function of shear strain (γ/γ_r) due to acceleration of the Loma Preita, 1989 (**0.4g**).

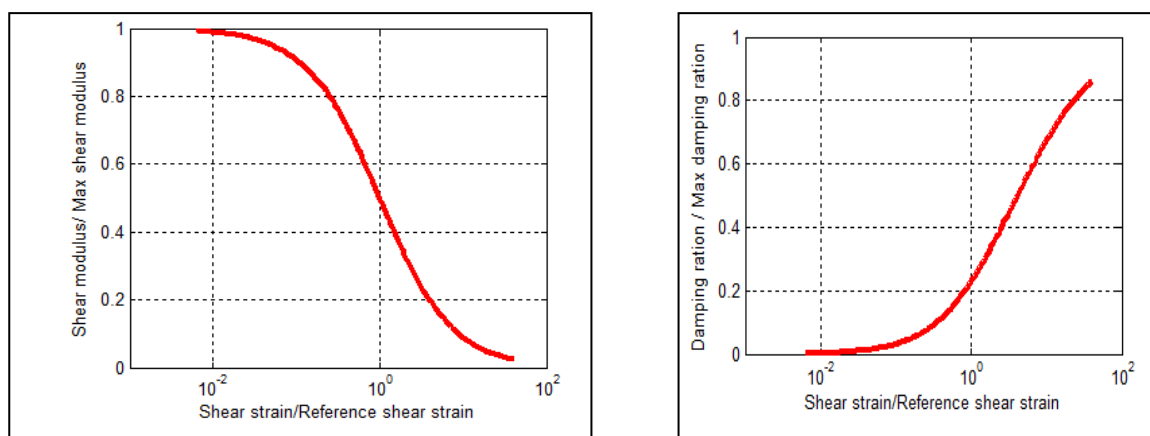


Fig. IV.15. Variation of shear modulus (G/G_{max}) and damping coefficient (ξ/ξ_{max}) as a function of shear strain (γ/γ_r) due to acceleration of the Northridge, 1994 (**0.50g**).

The variation of shear modulus (G/G_{max}) and damping coefficient (ξ/ξ_{max}) at each acceleration level of the earthquakes are shown in **Table IV.1**.

Table IV.1. Variations of the nonlinear dynamic properties of the soil vs the acceleration level of the earthquakes.

Accelerogram(s)	G/G_{max}	$\xi_g/\xi_{g\ max}$
Linear	1	0.05
Earthquake 0.1g	0.6	0.16
Earthquake 0.2g	0.26	0.43
Earthquake 0.3g	0.12	0.6
Earthquake 0.4g	0.04	0.8
Earthquake 0.5g	0.02	0.87

IV.3. PARAMETRIC ANALYSIS AND RESULTS

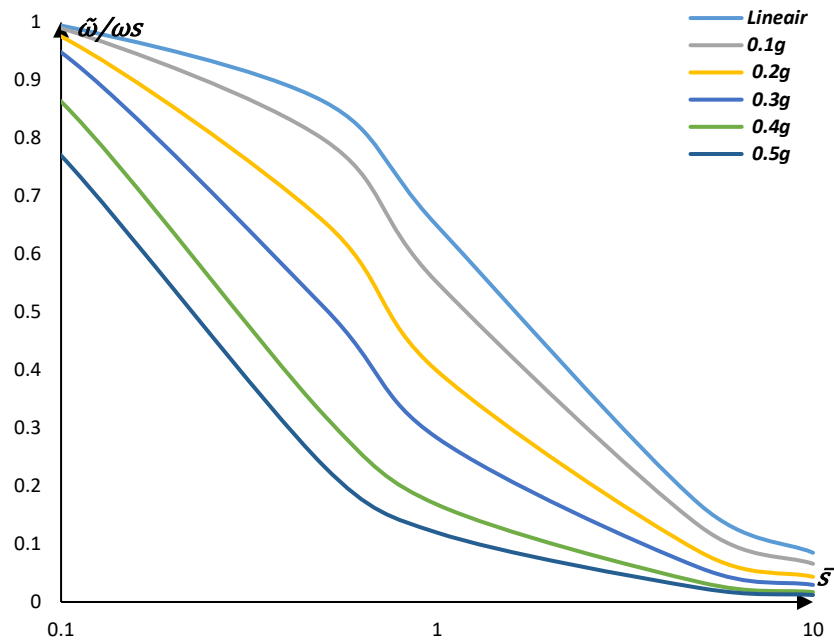
The results are presented in this study in terms of natural frequency and damping of the analog system, structural distortion, and displacement of the mass relative to the free field for

an equivalent linear soil behavior, and then they are compared to the linear case to clarify the differences between the two cases.

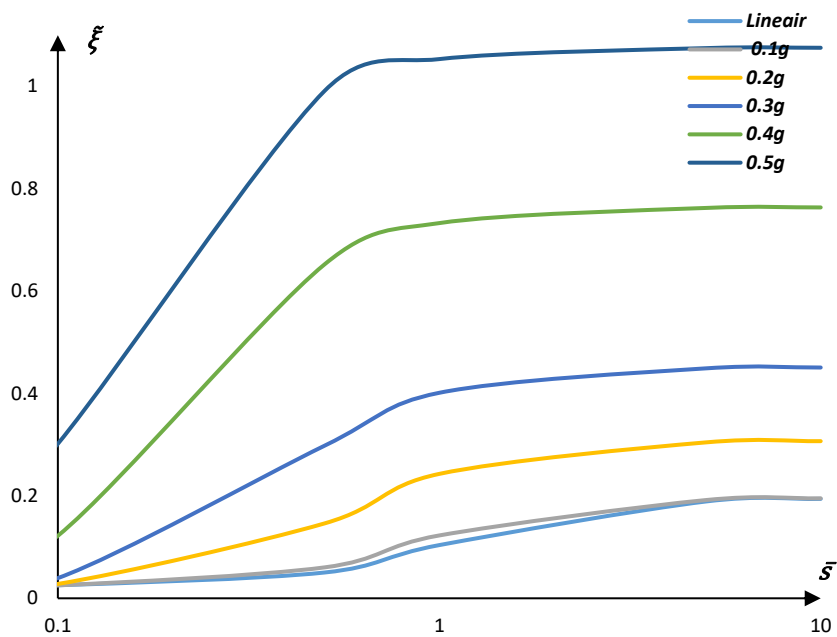
IV.3.1. Natural frequency and damping of the soil-structure system

Fig. IV.16 and **Fig. IV.17** show the properties of the coupled system obtained according to the dynamic equivalent linear soil behavior and plotted as a function of \bar{s} ($=0.1, \dots, 10$), five earthquake records ($G/G_{max}, \xi_g/\xi_{g max}$), and for the two impedance function cases: independent and dependent frequencies (static impedance function, dynamic impedance function), including the linear case. It can be seen from these figures that the effect of the nonlinear soil behavior is remarkable. Both the natural frequency and the hysteretic damping ratio $\tilde{\xi}$ of the equivalent system change from the linear case as the excitation amplitude changes. It is observed that the magnitude of the frequency ratio $\tilde{\omega}/\omega_s$ decreases and the equivalent damping $\tilde{\xi}$ increases significantly from the linear case as the excitation amplitude increases, i.e., the soil damping increases while the shear modulus decreases, so, this effect is reflected in the value of the deformations. This means that when considering the SSI with equivalent linear soil behavior, the natural frequency of the system is shifted to low frequencies, which should be considered in the design of structures to avoid the resonance effect. Furthermore, the increase in damping will cause the reduction of the vibrations of the structure giving it more safety.

From the results obtained using the frequency-dependent impedance function expressions with equivalent linear soil behavior (**Fig. IV.17(a), (b)**), the trends of the properties of the analog system are similar to those of the static case (frequency-independent impedance function expressions) with equivalent linear soil behavior (**Fig. IV.16(a), (b)**). For the same parameters and excitation levels, it's clear from **Fig. IV.17(b)** that the values of the damping ratio for the case of dynamic impedance function with $a_0 = 3$ are about four times the values of the static case. The higher the excitation amplitude, the greater the shift of the damping ratio curve to higher values in the dynamic case (the frequency-dependent impedance function expressions).

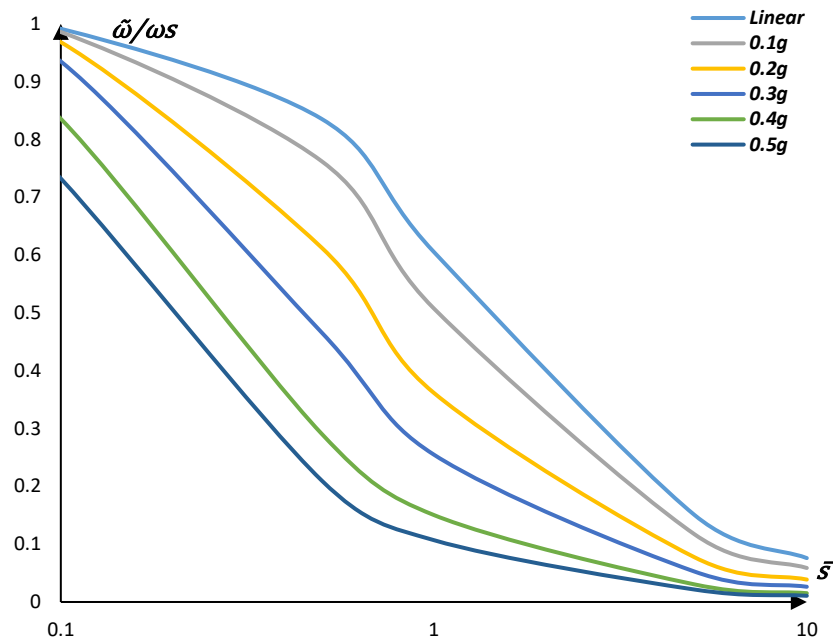


(a) Natural frequency.

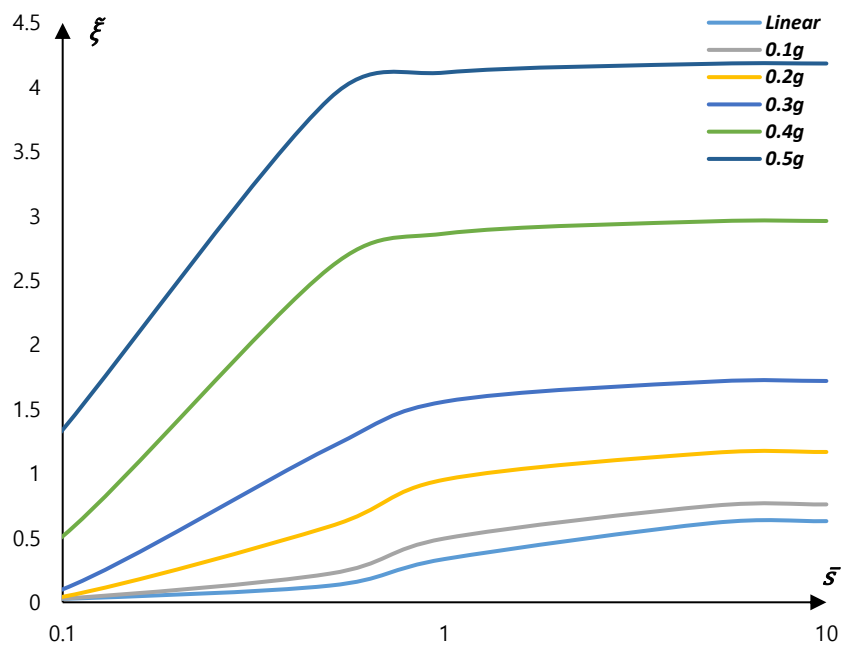


(b) Damping.

Fig. IV.16. Properties of the equivalent one degree of freedom system for the frequency-independent impedance function expressions with equivalent linear soil behavior ($\bar{m}=3$, $\bar{h}=1$, $\nu=0.33$, $\xi=0.025$, $\xi_g=0.05$).



(a) Natural frequency.



(b) Damping.

Fig. IV.17. Properties of the equivalent one degree of freedom system for the frequency-dependent impedance function expressions with equivalent linear soil behavior ($\bar{h}=1$, $\bar{m}=3$, $\nu=0.33$, $\xi=0.025$, $\xi_g=0.05$, $a_0=3$).

On the other hand, it was shown that the increase of the dimensionless frequency \bar{s} (c_s small, soft soil) in all cases (Garevski, M., & Ansal 2010) also significantly affects the two

equivalent parameters ($\tilde{\omega}/\omega_s$ and $\tilde{\xi}$), where a significant decrease in the natural frequency ratio is observed and its deviation from the value of the unit, and an increase in the equivalent damping ratio, where the non-zero value of the latter at a very low value of the soil stiffness ratio ($\bar{s}=0.1$) indicates the presence of hysteretic dissipation of the structure (assumed to be 2.5%), and for a significant soil-structure-interaction effect, the ratio $\tilde{\xi}$ essentially converges to the soil material damping ratio $\xi_g=0.05$. The few small undulations observed in the curves are the result of resonance phenomena in the soil-structure system. (Alzabeebee 2021; Kaklamanos et al. 2015; Mylonakis and Voyagaki 2006)

IV.3.2. Relative and absolute displacement of the structure

Using **Eq. (III.9)**, **Eq. (III.12)** and **Eq. (III.13)**, the equivalent linear dimensionless amplitudes of the different displacements of the structure (u/u_g , $u + u_0 + h\phi/u_g$) for the two cases of the impedance function form (static, dynamic) were plotted against the dimensional frequency ω/ω_s ($= 0 \dots \dots 1.4$) and for 05 seismic acceleration levels $\text{Acc}(g)$ ($=0.1g, 0.2g, 0.3g, 0.4g, \text{ and } 0.5g$) in **Fig. IV.18**, **Fig. IV. 19**, and **Fig. IV.20**. The same data were used as in the previous section, except in the case of the dynamic impedance functions, where two values of the dimensionless frequency a_0 ($= 1$ and 3) were studied.

From **Fig. IV.18**, **Fig. IV. 19**, and **Fig. IV.20**, the dynamic response of the structure decreases with the implementation of equivalent linear soil behavior for both cases of impedance function shape (static and dynamic). From the following results, it is clear that the equivalent linear soil behavior (nonlinear), i.e., increasing the soil damping and decreasing the shear modulus, introduces additional seismic wave absorption. This is consistent with the results of Raychowdhury (2011), who use a beam-on-nonlinear-Winkler-foundation (BNWF) technique to describe the nonlinear soil-structure interaction behavior and evaluate its effect on the seismic response of low-rise steel moment-resisting frame (SMRF) buildings. They find that the force and displacement demands are significantly reduced when the foundation nonlinearity is accounted for, and that the foundation compliance has a significant effect on the structural response.

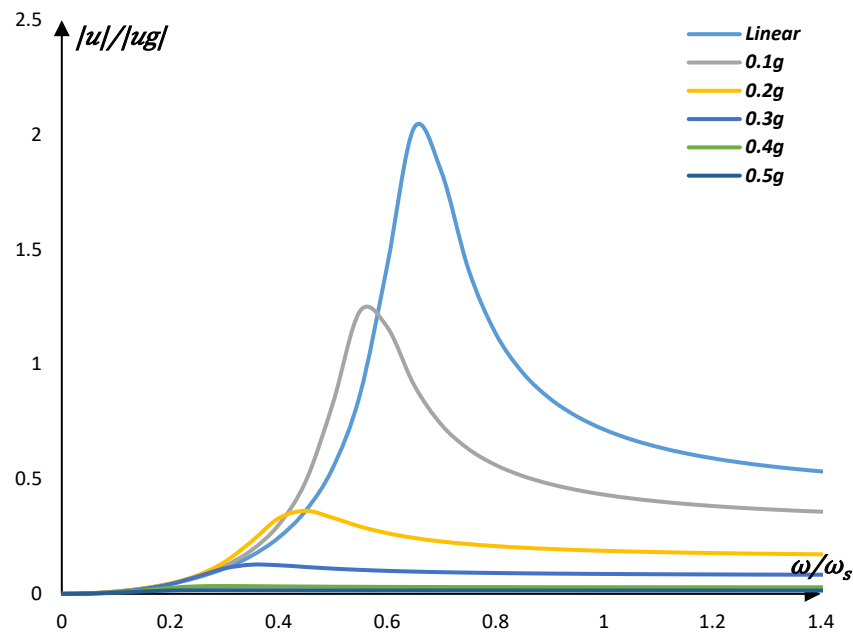
An increase in the soil nonlinearity does not only significantly attenuates the peak values of the structural distortion and the mass displacement, but also shifts the frequency to the left (low frequencies) with a widening of the frequency content, implying that the soil becomes more rigid (**Fig. IV.18** and **Fig. IV.19**). The results are also similar to those obtained

by Guellil, Harichane, and Çelebi (2019, 2020), who used the strain-dependent shear modulus and the damping ratio to take into account for the nonlinear behavior in order to perform a comparative study between the nonlinear and stochastic methods. They showed that the impedance functions and the response of the coupled system are strongly affected by the nonlinear method compared to the stochastic method, and that the displacements decrease with a remarkable shift of the frequency ratio for the displacements.

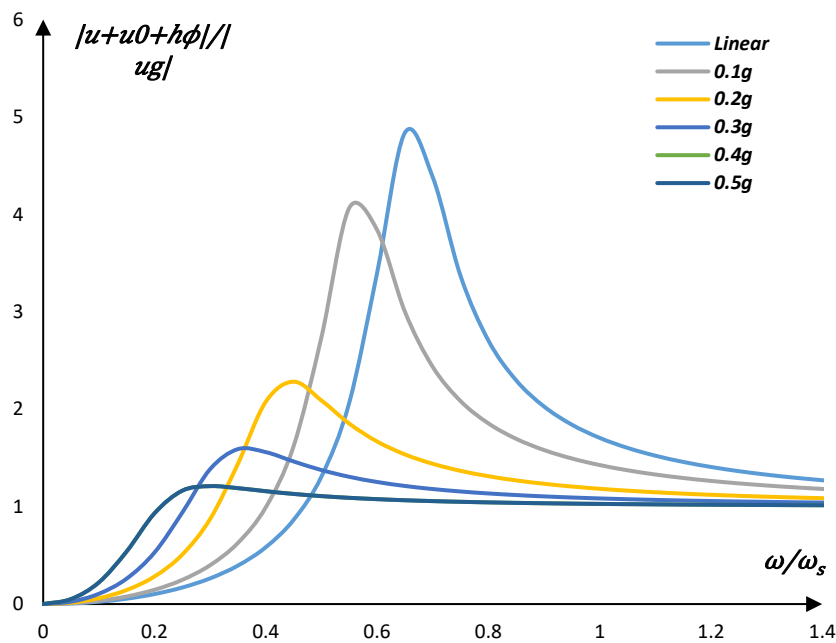
In this section, the same trend as in the linear case appears in all the curves, and the peaks progressively disappear and become flat curves as the level of seismic load increases, due to the progressive increase in the hysteretic damping of the soil material.

On the other hand, in addition to the effect of the equivalent linear soil behavior, **Fig. IV.19** and **Fig. IV.20** show the effect of the impedance function form on the structural distortion and mass displacement relative to the free field using frequency-dependent expressions (dynamic impedance function). It is clear that the effect of the impedance function form greatly affects the response of the structure. For $a_0 = 1$, it is observed that the same structure responds as in the previous case (static impedance function with the equivalent linear soil behavior) with a negligible difference. In **Fig. IV.20**, the displacement values are reduced compared to those of **Fig. IV.19**, especially the peak values, since in the case of $a_0=3$ and for an earthquake acceleration equal to $0.2g$, the peak value has been reduced by about 50% of the case of $a_0=1$. This returns to the soil behavior representing soft soil ($a_0=3$), which behaves like a damper, by reducing the displacement amplitude and widening the range of the peak value. These results are in agreement with those obtained by Pitilakis, Moderessi-farahmand-razavi, and Clouteau (2013); Sbartai (2018), who illustrated the effect of soil material nonlinearity on the estimation of dynamic impedance functions using an equivalent linear process. They found that with increasing seismic acceleration level and dimensionless frequency a_0 , the dynamic stiffness coefficients decrease and the damping coefficients increase compared to the linear case. This is also consistent with the findings of other researchers, such as (Pais, Kausel, and Eirgirreerirg 1988; Zafarkhah and Dehkordi 2017), who presented the effects of soil type variability (different shear moduli) and structure height variability on soil-structure system response. (Forcellini 2022; Forcellini, Mina, and Karampour 2022; El Hoseny et al. 2023; Zhidong et al. 2021)

For $\omega/\omega_s = 0.5$, and $a_0 = 3$ we notice that for any seismic acceleration level $u + u_0 + h\phi \cong u_g$ (see in **Fig. IV.20(b)**), which shows that the structure moves as a rigid body.

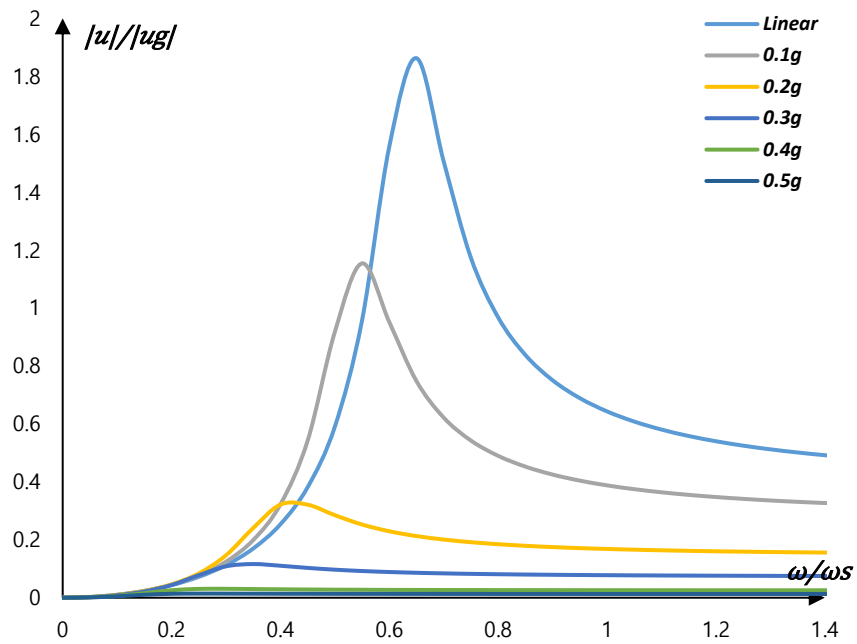


(a) Structural distortion.

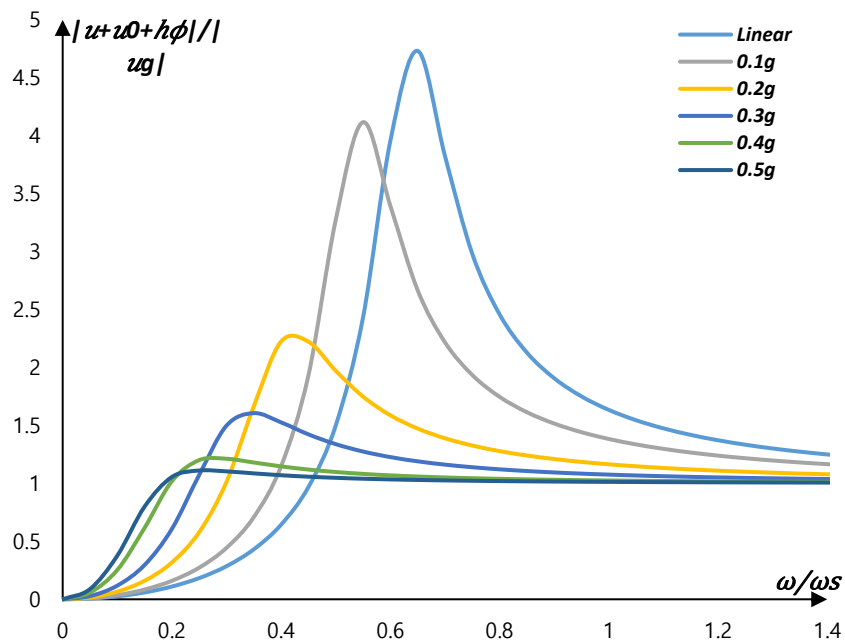


(b) Displacement of the mass relative to free field.

Fig. IV.18. Influence of soil-structure interaction as a function of excitation frequency (case for the frequency-independent impedance function expressions with equivalent linear soil behavior) ($\bar{m}=3$, $\bar{h}=1$, $\nu=0.33$, $\xi=0.025$, $\xi_g=0.05$).

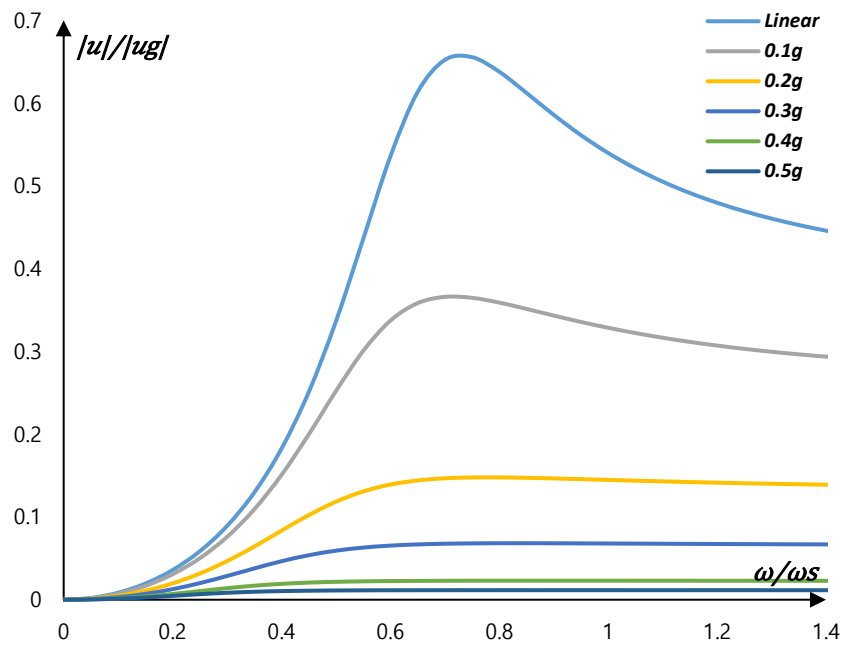


(a) Structural distortion.

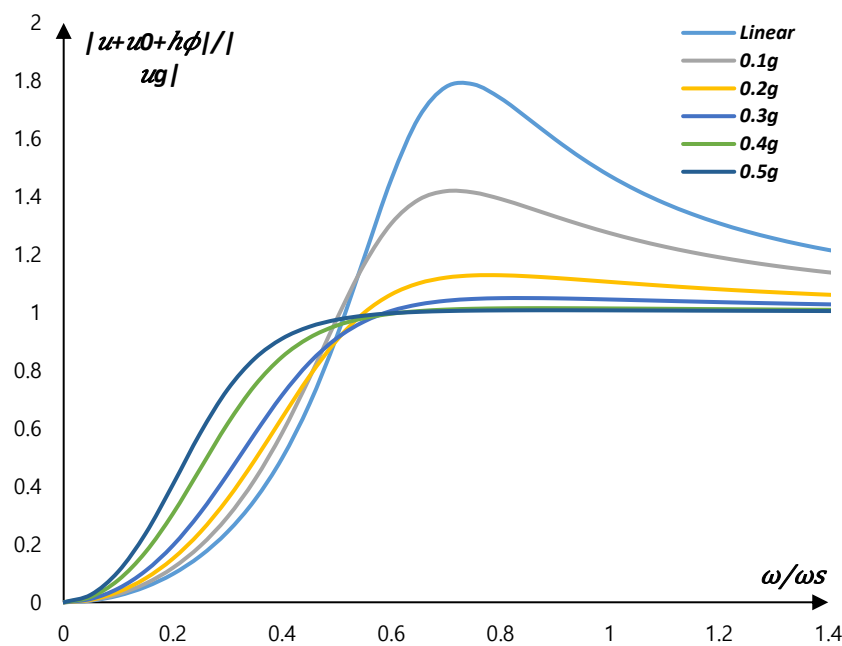


(b) Displacement of the mass relative to free field.

Fig. IV.19. Influence of soil-structure interaction as a function of excitation frequency (case for the frequency-dependent impedance function expressions with equivalent linear soil behavior) ($\bar{m}=3$, $\bar{h}=1$, $\nu=0.33$, $\xi=0.025$, $\xi_g=0.05$, $a_0=1$).



(a) Structural distortion.



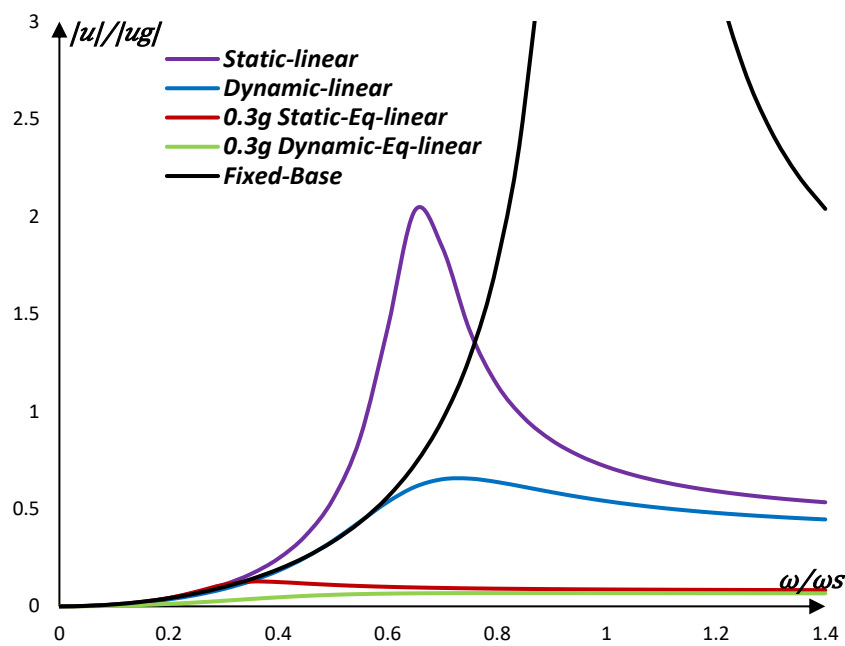
(b) Displacement of the mass relative to free field.

Fig. IV.20. Influence of soil-structure interaction as a function of excitation frequency (case for the frequency-dependent impedance function expressions with equivalent linear soil behavior) ($\bar{m}=3$, $\bar{h}=1$, $\nu=0.33$, $\xi=0.025$, $\xi_g=0.05$, $\alpha_0=3$).

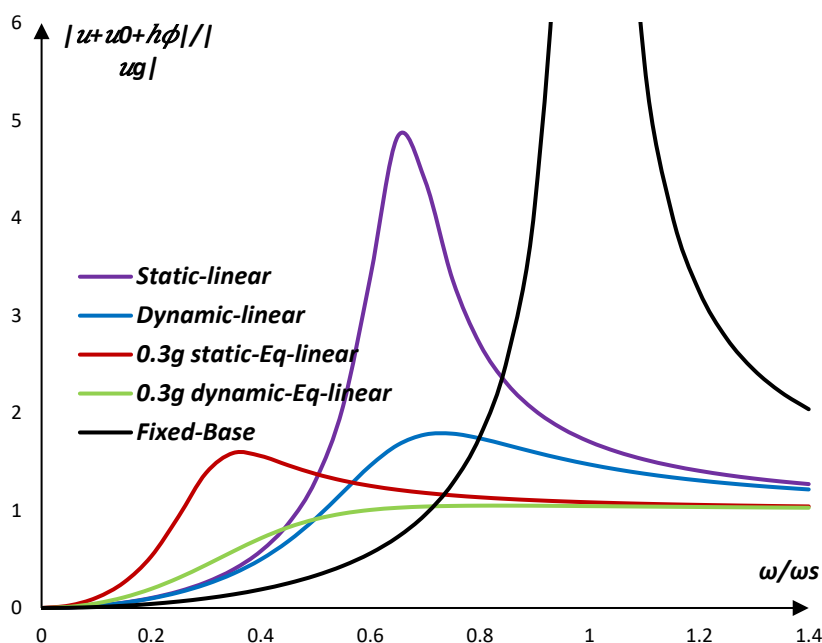
IV.3.3. Superposition of the different studied cases

The following graphs (see **Fig. IV.21**) have been constructed for the different cases with (or without) soil-structure interaction, namely:

- Fixed base.
- Flexible base:
 - Visco-elastic soil behavior with static impedance function (frequency-independent impedance function).
 - Visco-elastic soil behavior with dynamic impedance function (frequency-dependent impedance function).
 - Equivalent linear soil behavior with static impedance function (frequency-independent impedance function).
 - Equivalent linear soil behavior with dynamic impedance function (frequency-dependent impedance function).



(a) Structural distortion.



(b) Displacement of the mass relative to free field.

Fig. IV.21. Comparison of the four analysis cases with the fixed base case ($\bar{m}=3$, $\bar{h}=1$, $\nu=0.33$, $\xi=0.025$, $\xi_g=0.05$, $\alpha_0=3$).

In **Fig. IV.21**, the displacements before and after the introduction of the equivalent linear soil behavior for the two forms of the impedance function are compared to the fixed base case. Our illustrative superposition curves show that both flexibility and soil behavior play an important role in the dynamic response of the structures. The different displacement curves indicate that the same structure responds differently in all the cases studied (fixed base, flexible base: static, dynamic; visco-linear, equivalent linear...) and that the equivalent linear behavior of the soil influences the different displacements of a soil-structure system to a greater extent than the SSI effects alone. Furthermore, it is noted that its introduction in the analysis of the soil-structure interaction system significantly reduces the values of displacement of the linear case. However, the model shows the same tendency as in the case of the fixed base, but reaches lower values. Moreover, in **Table IV.2**, which summarizes the resonance peak and the difference margin between "visco-linear and fixed base", "equivalent linear and fixed base responses" and between "equivalent linear and visco-linear responses", we observe that the nonlinear behavior of the soil and the effects of the dynamic impedance functions form combined lead to a more significant decrease in displacement. It was also observed that the structural distortion is reduced up to 89.85% when the flexibility of the base is introduced (visco-linear), where it further decreases to about 96% when frequency-

dependent impedance functions are used. However, the reduction rate becomes 98% and 99%, respectively, when both soil flexibility and equivalent linear soil behavior are considered at a seismic acceleration level of 0.2g using static impedance functions.

For an earthquake amplitude of 0.2g, the absolute displacement ($u + u_0 + h\phi/u_g$) in the dynamic equivalent linear case is reduced by about 37% compared to the dynamic linear case. Similarly, ω/ω_s decreases less for softer soils. This shift is primarily due to the hysteretic material damping of the equivalent system, which increases as the excitation level increases.

In addition, the dimensionless frequency is shifted to the left (low frequencies) by 30% and 6.67%, respectively, for the flexible base with equivalent linear soil behavior using static and dynamic impedance functions relative to the visco-linear soil, implying that the soil becomes more flexible.

Table IV.2. Difference in maximum displacement and frequency margin between an SSI system and equivalent linear soil behavior.(lagaguine and Sbartai 2023)																	
SSI response	Fixed base	Difference displacement				Difference margin (%)											
		Visco-linear		Equivalent linear (0.2g)		Visco-linear vs. Fixed base		Equivalent linear vs. Fixed base		Equivalent linear vs. Visco-linear							
		Static impedance function	Dynamic impedance function	Static impedance function	Dynamic impedance function	Static impedance function	Dynamic impedance function	Static impedance function	Dynamic impedance function	Static impedance function	Dynamic impedance function						
$ u / u_g $	20	2.03	0.655	0.36	0.1477	-	-	-	-	-	-	89.85	96.72	98.2	99.26	82.66	77.45
$ u + u_0 + h\phi / u_g $	20	4.84	1.788	2.28	1.1207	-	-	-	-	-	-	75.80	91.06	88.6	94.36	52.89	37.32
ω/ω_s for $ u + u_0 + h\phi / u_g $	1	0.65	0.75	0.45	0.7	- 35	- 25	- 55	- 30	- 30	-						6.667

IV.4. NEW ANALYTICAL NONLINEAR RELATIONSHIPS

Fig. IV.22 shows the maximum values of structural distortion and mass displacement for each case studied (static, dynamic) and with equivalent linear soil behavior as a function of seismic acceleration, it can be clearly observed that the nonlinearity has a strong influence on the reduction of the peak values. The higher the level of seismic acceleration, the greater the effect of soil nonlinearity. The trend curves were also calculated by polynomial interpolation (dotted line) of the nonlinear function. The nonlinear relationships between the dimensionless displacement $|u|/|u_g|$ and the acceleration level $Acc(g)$ can be predicted with the followings relations:

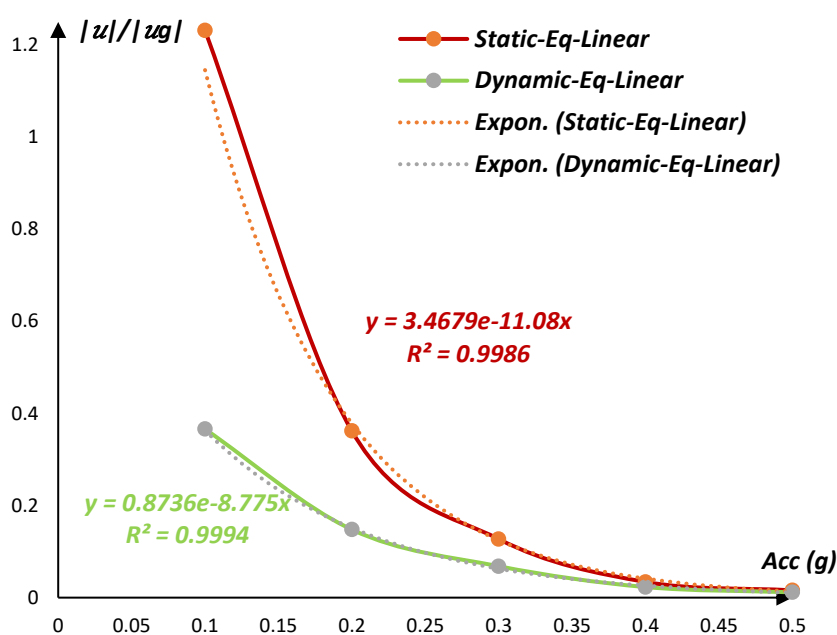
- For the static equivalent linear:

$$|u|/|u_g| = 3.4679 e^{-11.08Acc(g)} \quad (IV.7)$$

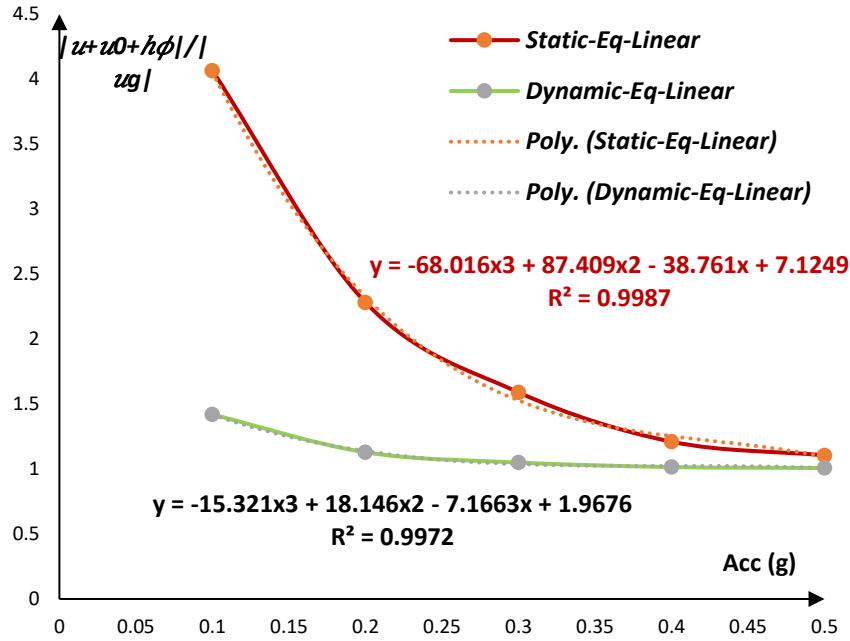
- For the dynamic equivalent linear:

$$|u|/|u_g| = 0.8736 e^{-8.775Acc(g)} \quad (IV.8)$$

The goodness of statistical fit of the equations (**Eq. (IV.7)** and **Eq. (IV.8)**) are $R^2 = 0.9986$ and $R^2 = 0.9994$, respectively. Thus, the two proposed formulas (**Eq. (IV.7)** and **Eq. (IV.8)**) correctly predict the results presented in this study.



(a) Structural distortion.



(b) Absolute displacement of the mass.

Fig. IV.22. Max Displacement-Seismic acceleration curves of the soil-structure system ($\bar{m}=3$, $\bar{h}=1$, $\nu=0.33$, $\xi=0.025$, $\xi_g=0.05$, $a_0=3$).

A nonlinear relation between $|u + u_0 + h\varphi|/|u_g|$ and the acceleration level $Acc(g)$ can be assumed. The given relations are equal to:

➤ For the static equivalent linear:

$$|u + u_0 + h\varphi|/|u_g| = -68.016Accg^3 + 87.409Accg^2 - 38.761Accg + 7.1249 \quad (\text{IV.9})$$

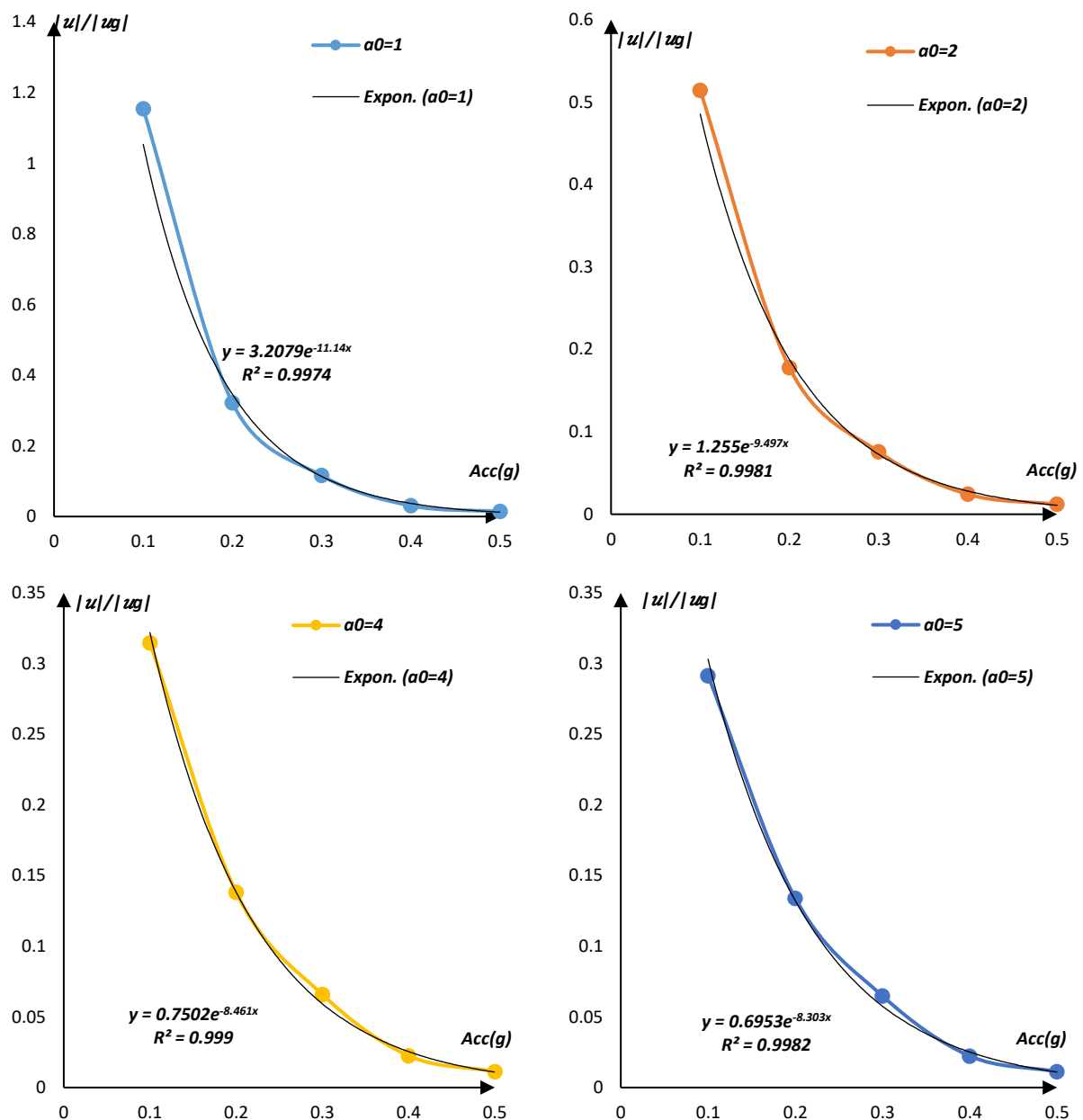
➤ For the dynamic equivalent linear:

$$|u + u_0 + h\varphi|/|u_g| = -15.321Accg^3 + 18.146Accg^2 - 7.1663Accg + 1.9676 \quad (\text{IV.10})$$

The statistical goodness of fit of both **Eq. (IV.9)** and **Eq. (IV.10)** are $R^2=0.9987$ and $R^2=0.9972$, respectively. Thus, the two proposed formulas (**Eq. (IV.9)** and **Eq. (IV.10)**) correctly predict the results presented in this study.

It should be noted that the adjusted R^2 statistic is generally the best indicator of the quality of the fit when its value is closer to one. These curves describe the nonlinear behavior of the equivalent system, which allows for the determination of the maximum value of the displacement at any desired level of seismic acceleration for $a_0 = 3$.

For different ranges of the dimensionless frequency a_0 , we want to clarify how the seismic acceleration levels modify the structural displacement u/u_g and the total displacement of the mass $u + u_0 + h\phi/u_g$. Thus, it can be seen from **Fig. IV.23** and **Fig. IV.24** that u/u_g and $u + u_0 + h\phi/u_g$ are not only a function of the seismic acceleration levels themselves, but also a function of a_0 . This has not been extensively discussed in the literature. Therefore, revised displacements u/u_g and $u + u_0 + h\phi/u_g$ are proposed here. They depend on both $\text{Acc}(g)$ and a_0 .



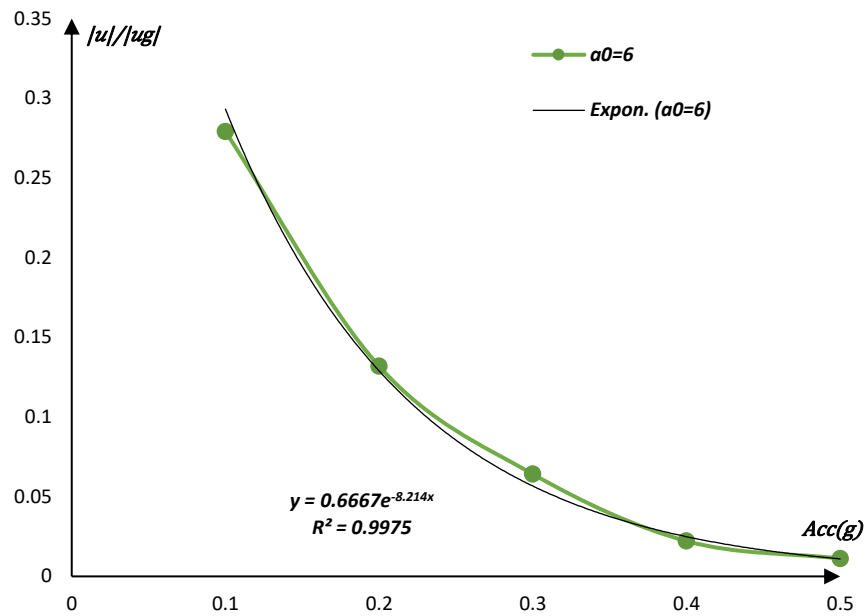
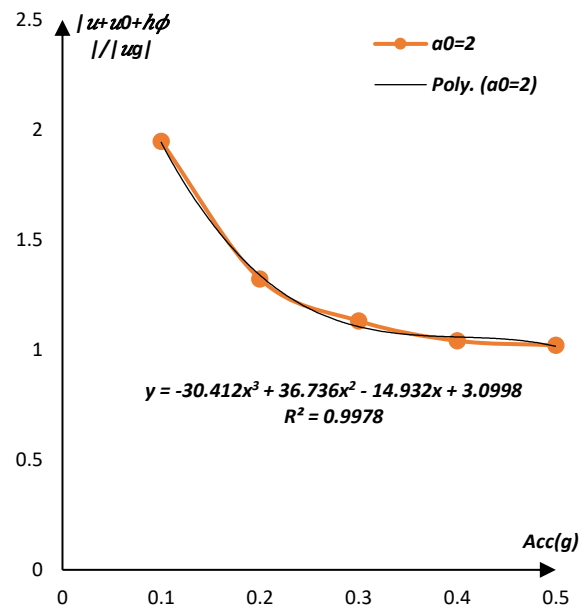
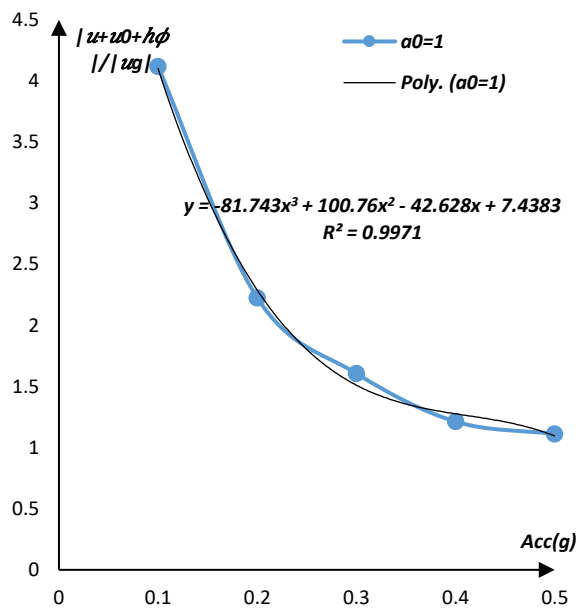


Fig. IV.23. Max Structural distortion versus seismic acceleration levels of the soil-structure system: $\bar{h}=1$, $\bar{m}=3$, $\nu=0.33$, $\xi=0.025$, $\xi_g=0.05$, α_0 ($= 1, 2, 4, 5$, and 6).



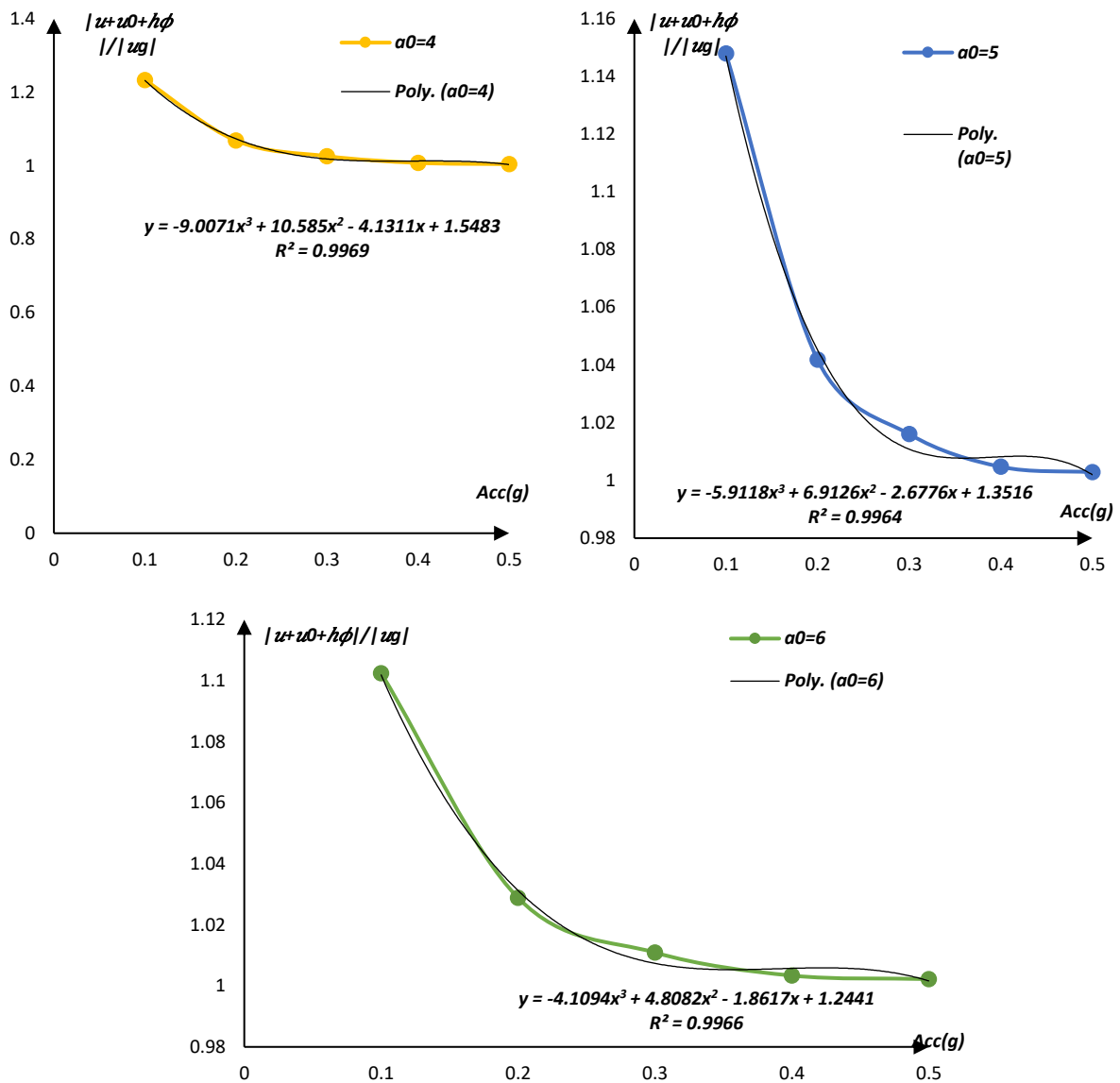


Fig. IV.24. Max absolute displacement versus seismic acceleration levels of the soil-structure system: $\bar{h}=1$, $\bar{m}=3$, $\nu=0.33$, $\xi=0.025$, $\xi_g=0.05$, a_0 ($= 1, 2, 4, 5$, and 6).

From **Fig. IV.23**, the best-fit curve for the structural distortion correction versus seismic acceleration levels was an exponential function for each frequency in the form of:

$$\frac{|u|}{|u_g|} = b_0 \cdot e^{-b_1 \cdot Acc(g)} \quad (\text{IV.11})$$

The values of the coefficients b_0 , and b_1 were recorded for $a_0 = 1, 2, 3, 4, 5, 6$. **Fig. IV.25** shows the values of b_0 and b_1 , thus simulating the dependence of $\frac{|u|}{|u_g|}$ on a_0 . From the

Fig. IV.23, it is clear that b_0 and b_1 follow a different trend and have been fitted with power and logarithmic functions, respectively, see **Table IV.3**.

From **Fig. IV.24**, the best fit curve for the absolute displacement versus seismic acceleration levels was a polynomial function for each frequency in the form of:

$$\frac{|u + u_0 + h\varphi|}{|u_g|} = b_2 \text{Acc}(g)^3 + b_3 \cdot \text{Acc}(g)^2 + b_4 \cdot \text{Acc}(g) + b_5 \quad (\text{IV.12})$$

The values of the coefficients b_2 , b_3 , b_4 , and b_5 were recorded for $a_0 = 1, 2, 3, 4, 5, 6$.

Fig. IV.26 shows the values of b_2 , b_3 , b_4 and b_5 , thus simulating the dependence of $\frac{|u+u_0+h\varphi|}{|u_g|}$ on a_0 . From the **Fig. IV.26**, it is clear that b_2 and b_3 follow a different trend and were given different polynomial functions, see **Table IV.4**.

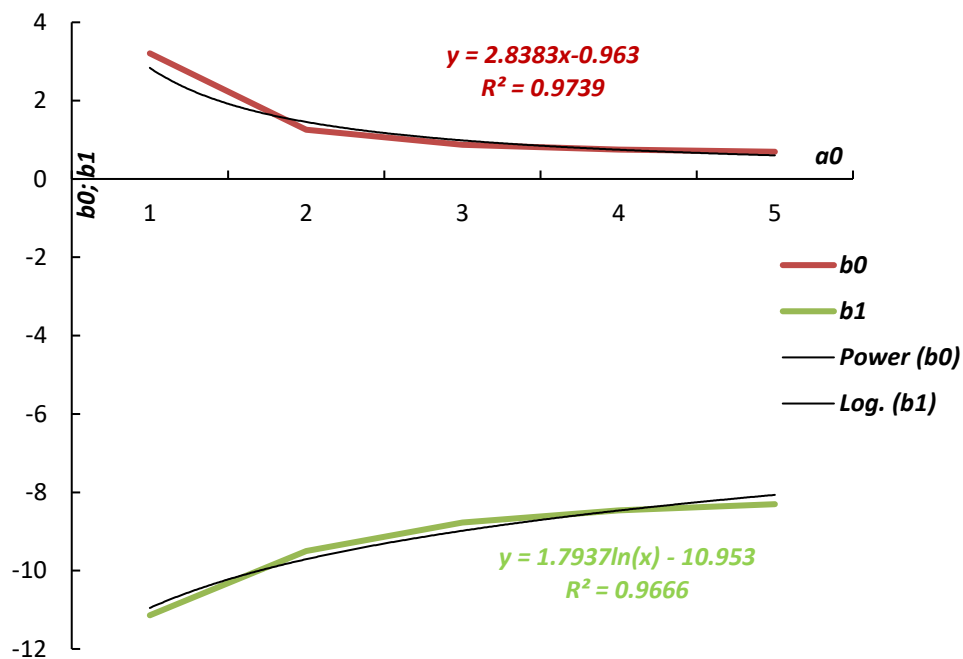


Fig. IV.25. Variation of the coefficients b_0 and b_1 with a_0 .

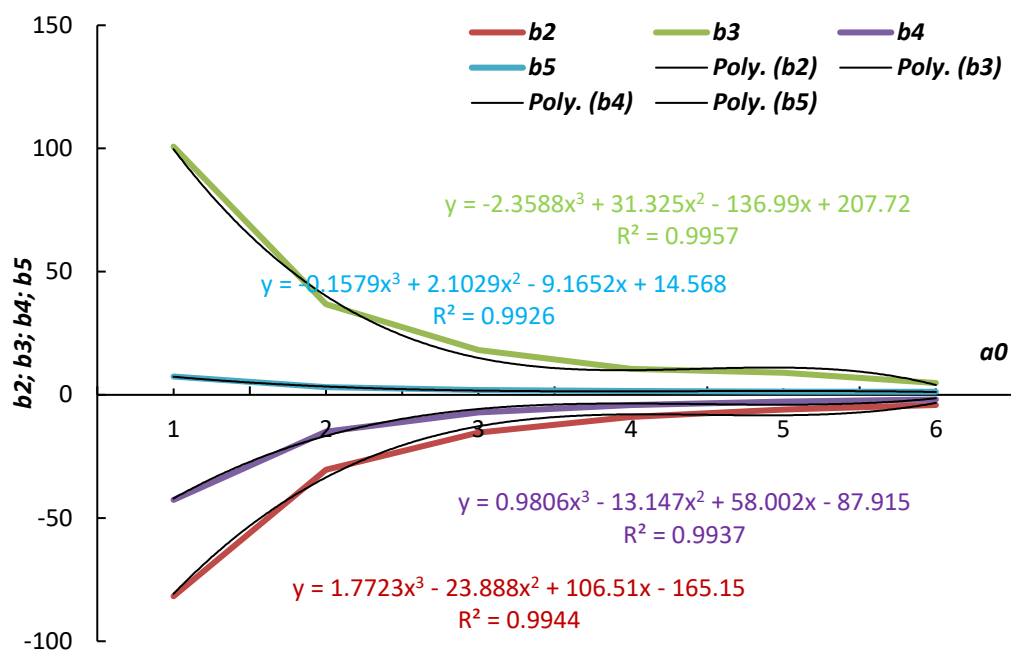


Fig. IV.26. Variation of the coefficients b_2 , b_3 , b_4 and b_5 with a_0 .

Table IV.3. The fitting functions of the b_0 and b_1 coefficients.

Coefficients	Fit Equations	R^2
b_0	$b_0 = 2,8383a_0^{-0,963}$	0,9737
b_1	$b_1 = 1,7937\ln(a_0) - 10,953$	0,9666

Table IV.4. The fitting functions of the b_2 , b_3 , b_4 and b_5 coefficients.

Coefficients	Fit Equations	R^2
b_2	$b_2 = 1,7723a_0^3 - 23,888a_0^2 + 106,51a_0 - 165,15$	0,9944
b_3	$b_3 = -2,3588a_0^3 + 31,325a_0^2 - 136,99a_0 + 207,72$	0,9957
b_4	$b_4 = 0,9806a_0^3 - 13,147a_0^2 + 58,002a_0 - 87,915$	0,9937

$$b_5 \quad b_5 = -0,1579a_0^3 + 2,1029a_0^2 - 9,1652a_0 + 14,568 \quad 0,9926$$

As a result, from the above analysis, the structural distortion and absolute displacement correction can be summarized by equations **Eq. (IV.13)** and **Eq. (IV.14)**:

$$\frac{|u|}{|u_g|} = 2,8383a_0^{-0,963} \cdot e^{(1,7937 \ln a_0 - 10,953) \cdot Acc(g)} \quad (\text{IV.13})$$

$$\begin{aligned} \frac{|u + u_0 + h\varphi|}{|u_g|} &= (1,7723a_0^3 - 23,888a_0^2 + 106,51a_0 - 165,15) \cdot Acc(g)^3 \\ &+ (-2,3588a_0^3 + 31,325a_0^2 - 136,99a_0 + 207,72) \cdot Acc(g)^2 \quad (\text{IV.14}) \\ &+ (0,9806a_0^3 - 13,147a_0^2 + 58,002a_0 - 87,915) \cdot Acc(g) \\ &+ (-0,1579a_0^3 + 2,1029a_0^2 - 9,1652a_0 + 14,568) \end{aligned}$$

These new analytical nonlinear relationships between the relative and absolute displacement of the structure, the acceleration level $Acc(g)$ and the dimensionless circular frequency of the excitation are proposed in order to consider this influence in a simple way in the calculation of the soil-structure interaction for different acceleration level $Acc(g)$ and for different seismic excitation frequencies.

IV.5. CONCLUSION

This chapter performs an analytical analysis based on the dynamic equilibrium of the soil-structure system modeled by an analog model with three degrees of freedom to obtain the seismic response of the selected structure with equivalent linear soil behavior using the CALDYNASOIL computational code of Sbartai and Filali (2012). To explore the sensitivity of the response of a soil-structure system to different soil and structure parameters, this chapter investigates the effect of adopting different impedance function types on the structural response of the soil-structure system using springs and dashpots with two frequency cases: independent and dependent frequencies.

Finally, new analytical nonlinear relationships are proposed between the displacements of the structure, the acceleration level $Acc(g)$ and the dimensionless circular frequency of the excitation, in order to consider in a simple way this influence in the calculation of the soil-structure interaction for different soil types and seismic excitation frequency.

From the analyses presented in this chapter, we can conclude that

- The Our illustrative results show that the soil behavior plays an important role in the dynamic responses of the structures.
- The dynamic response of a soil structure system depends on more parameters in the case of nonlinear soil behavior which is more complex than the linear elastic soil behavior, where the energy dissipation depends on the amplitude of the motion and its frequency, the type of impedance function form (static, dynamic), shear modulus reduction and damping increase.
- The effect of the change in soil behavior due to the imposed seismic motion is very remarkable and strongly related to the form of the impedance function at all frequencies. This effect is characterized by an overestimation of the displacement of the structure and a strong dependence on the type of impedance function and the soil properties. Compared to the viscoelastic soil, we find that the structural distortion has a displacement decrease of about 82% and 77%, respectively, for the static and dynamic impedance function and the equivalent linear soil, while the displacement of the mass decreases by about 52% and 37%, respectively.
- The higher the excitation amplitude, the greater the attenuation of the amplitude of the structural distortion and the displacement of the mass to lower values.
- As the nonlinearity of the soil becomes important, i.e., the soil damping increases and the shear modulus decreases, the amplitude of the structural deformation as well as the displacement of the mass are dominated by lower frequencies (shift to the left in the dimensionless frequency of the flexible base with equivalent linear soil behavior using the static and dynamic impedance function by 30% and 6.67%, respectively, compared

to the visco-linear soil behavior). This variation explains that the structure becomes more stiffer and the soil becomes more flexible.

- It is clear that the dynamic response of a structure under a seismic motion and taking into account the soil-structure interaction can strongly depend on the type of soil (c_s), the characterization of the impedance function (static or dynamic) and the soil behavior.
- We observe that the combined (SSI) effects and frequency-dependent impedance functions lead to an increased value of change in the results.

Using ABAQUS software, a detailed numerical analysis with the same model and its comparison with the analytical results is presented in the following chapter.

CHAPTER V: NUMERICAL ANALYSIS

V.1. INTRODUCTION

The numerical method is an approach to solving structural design problems using mathematical and computer techniques. It consists of approximating the behavior of a real structure by discretizing it into smaller elements and using mathematical equations to describe the behavior of these elements. (Amina et al. 2015; Castelli et al. 2021)

The most commonly used numerical method for structural design is the Finite Element Method (FEM). FEM divides a structure into a set of finite elements, such as triangles or quadrilaterals for 2D structures, or tetrahedrons or hexahedrons for 3D structures. Each finite element is assigned material and geometric properties such as stiffness, elasticity, and loading conditions. (Naji, Firoozi, and Firoozi 2020)

FEM is based on the principle that the behavior of a finite element can be described by simple mathematical equations. By assembling all the finite elements, a system of equations is obtained that represents the overall behavior of the structure. This system of equations is then solved numerically to obtain the strains, stresses, and other quantities of interest. (Nagakumar, Ajay, and John 2022)

The finite difference method is another commonly used numerical method for structural design. It consists of discretizing the point space and approximating the derivatives of the differential equations describing the behavior of the structure by finite differences. This approach transforms the differential equations into a system of algebraic equations that can then be solved numerically. (Wei, Cui, and Dai 2013)

Great efforts have been made at the numerical level to make the modeling and analysis of civil engineering structures more reliable, easier, and less expensive, and today's more powerful computer tools allow the use of more complicated meshes. Many numerical analyses (Andreotti and Lai 2017; Bolisetti, Whittaker, and Coleman 2018; Boudaa et al. 2021; Tahar Berrabah et al. 2012) have been carried out to study the soil-structure interaction phenomena using different calculation codes (ABAQUS, ADINA, ANSYS), which have confirmed the reliability and usefulness of these programs.

The following chapter gives a general presentation of ABAQUS, including the definition of the program and its characteristics, as well as the methods adopted to use it to

simulate the same model studied in the analytical analysis. Finally, a comparison between the analytical and numerical results is presented.

V.2. ABAQUS

Abaqus is a numerical simulation software for the analysis of mechanical structures and systems. It is widely used in the engineering field to perform behavioral and performance analysis of various structures such as automotive components, aircraft, bridges, buildings, etc. It provides a wide range of capabilities for modeling, simulating, and analyzing complex structures (**Fig. V.1**). The software uses the finite element method, a numerical technique that approximates the behavior of materials and structures by dividing them into small finite elements.

Abaqus users can create virtual models of their structures by defining material properties, loading conditions, and simulation parameters. The software also allows users to perform static, dynamic, thermal, electromagnetic, creep, fracture, and other analyses. The results of these analyses help to understand the behavior of structures and optimize their design to improve their performance and safety.

Abaqus has an easy-to-use interface that allows you to define models, view results, and generate analysis reports. It is also compatible with other computer-aided design (CAD) and computer-aided manufacturing (CAM) software, making it easy to integrate the design and analysis process.

In summary, Abaqus is a powerful and versatile software package for the numerical simulation and analysis of mechanical structures. It helps engineers and researchers to understand the behavior of structures and to make informed decisions in the design and optimization of products and systems.

The choice of the ABAQUS code in this thesis is based on two main reasons. On the one hand, many numerical modeling works adapted to soil-structure interaction problems with nonlinear behavior have been successfully performed using this code. On the other hand, the various capabilities of this code correspond well to our needs.

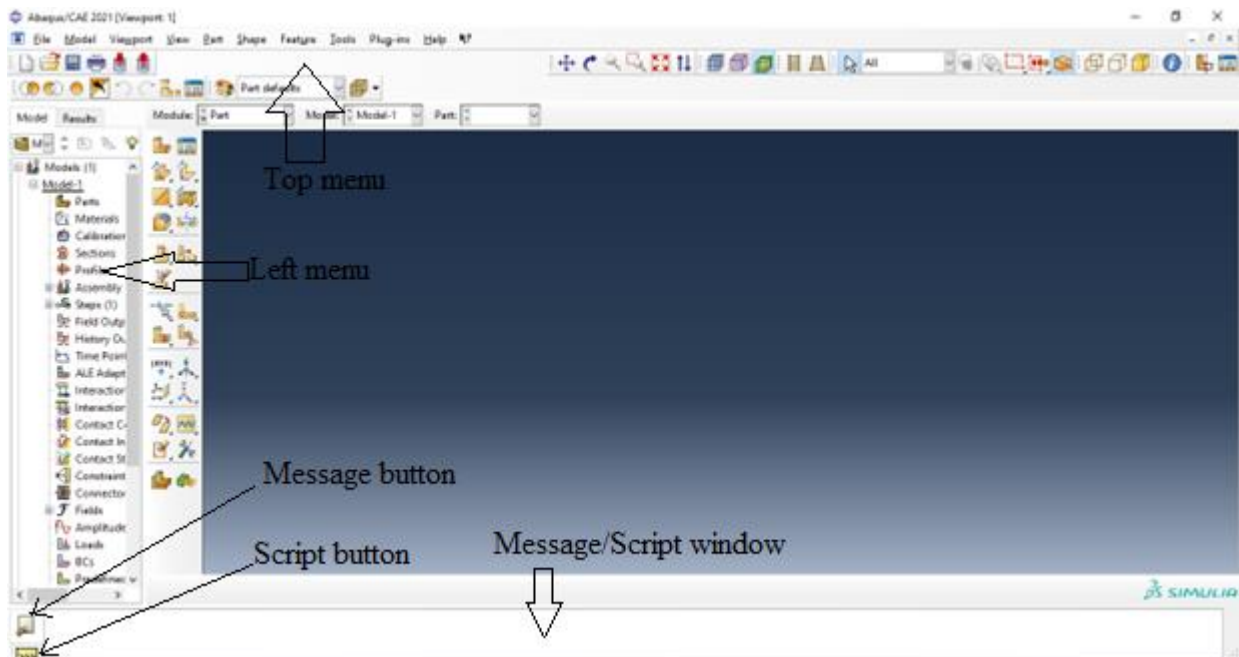


Fig. V.1. The main window of the Abaqus CAE 2021 software.

V.2.1. Element Types in ABAQUS

ABAQUS provides a huge library of element types that can be used in the analysis. The possible basic types are four: point, line, area, and volume.

- A single node is usually used to specify a point element, such as a mass element.
- The one-dimensional (1D) element is usually a line or arc connecting two or three nodes, such as a beam, truss, or member.
- A two-dimensional (2D) element is a shell element or a 2D solid element with a triangular or quadrilateral shape, such as plates in bending.
- A three-dimensional (3D) element is a solid element with a tetrahedral or brick shape. tetrahedral, hexahedral, etc.

and there are other elements such as springs, dashpot and rigid. The different elements can be summarized in the following figure:

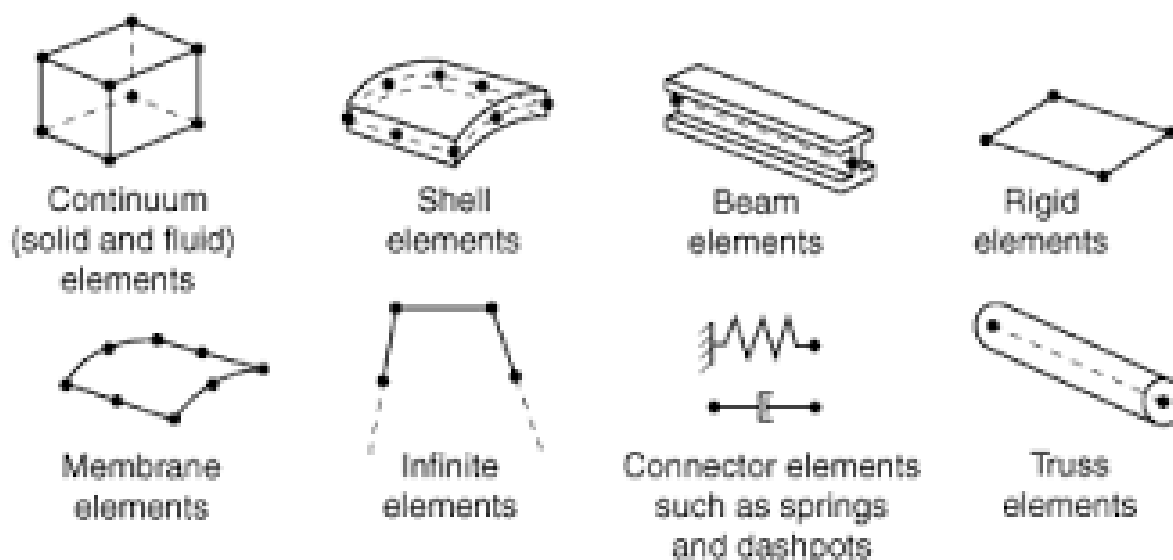


Fig. V.2. Some of the most commonly used elements (Abaqus document).

V.3. REPRESENTATION OF THE STUDIED MODEL:

In addition to the analytical results, we conducted a numerical study to investigate the effect of soil-structure interaction on the dynamic response of structures. We numerically simulated the dynamic response of a fully coupled soil-structure system by (2D) finite element modeling using ABAQUS software, see **Fig. V.3**, which shows the representation of the Abaqus model in its initial states for fixed and flexible base. By considering two soil behaviors, visco-linear, and linear-equivalent, which are described by the dynamic soil shear modulus and damping coefficient for a series of earthquake records (see **Table IV.1**).

V.3.1. Calculation assumptions, model geometry and material properties

To validate the analytical results with this numerical analysis, we have modeled the same model shown in **Fig. III.1**. The superstructure is represented in a simplified manner as a one-degree-of-freedom system resting on a circular shallow foundation resting on a circular shallow foundation resting on a soil deposit. The structure is described by its mass m , a lateral stiffness with spring coefficient K , and a damper with coefficient C placed at a height h of a rigid beam. The soil-foundation system is modeled by discrete elements, including horizontal and rocking equivalent linear springs and viscous dashpots with frequency-independent (**Eq. (III.16)** to **Eq. (III.19)**) and frequency-dependent (**Eq. (III.22)** to **Eq. (III.25)**) coefficients, where the spring and damping coefficients are given by K_h and C_h in the horizontal direction and K_r and C_r in the rotational direction.

Calculation Assumption:

- The soil behavior law used in this study is the "equivalent linear method". This behavior is determined by the CALDYNASOIL design code of Sbartai and Filali (2012).
- The behavior law used for the structure is linear elastic.

In the ABAQUS modeling, using the same values as in the analytical analysis, we have used a point element to model it as the mass of the structure connected to a rigid beam, and the soil-foundation interface was modeled using elastic springs and appropriate dashpot elements in ABAQUS and the model was subjected to a harmonic oscillator (Eq. (V.1)).

$$y(t) = A \cos(\omega t) \quad (\text{V.1})$$

Where, A is the maximum amplitude of the force, taken as unit in the present work, and ω is the excitation frequency ($= 0, 0.2, 0.4, 0.6, 0.8, 1, 1.2, 1.4$) (Fig. V.4).

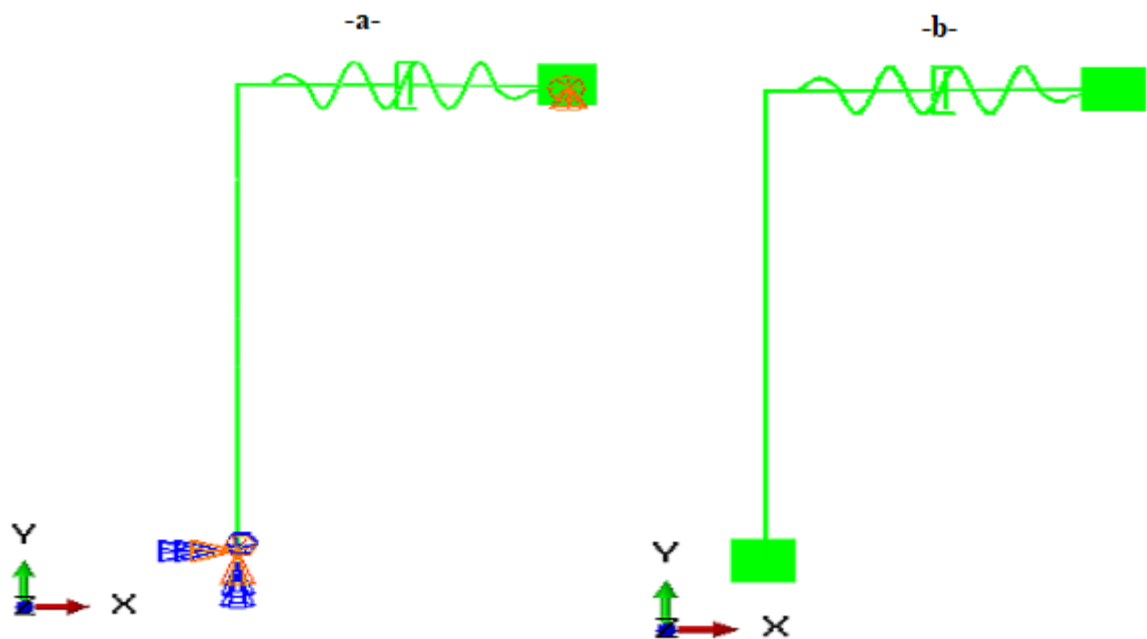


Fig. V.3. Representation of the Abaqus model in the initial states (a) fixed base (b) flexible base.

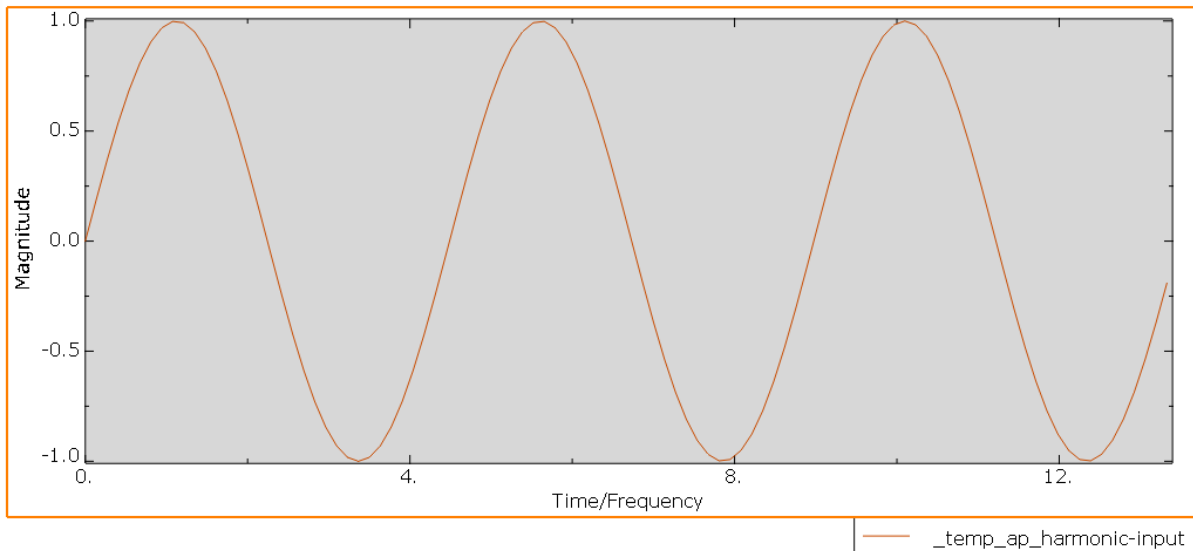


Fig. V.4 Harmonic input motion (Abaqus, 2021).

V.4. COMPARISON BETWEEN THE ANALYTICAL AND NUMERICAL RESULTS

Fig. V.5 shows the representation of the Abaqus model in its deformed states for fixed and flexible base. It is clear from this figure how the deformation is different for the fixed and flexible base conditions. It can be seen that the relative displacement is more pronounced in the case of the flexible support than in the case of the fixed support.

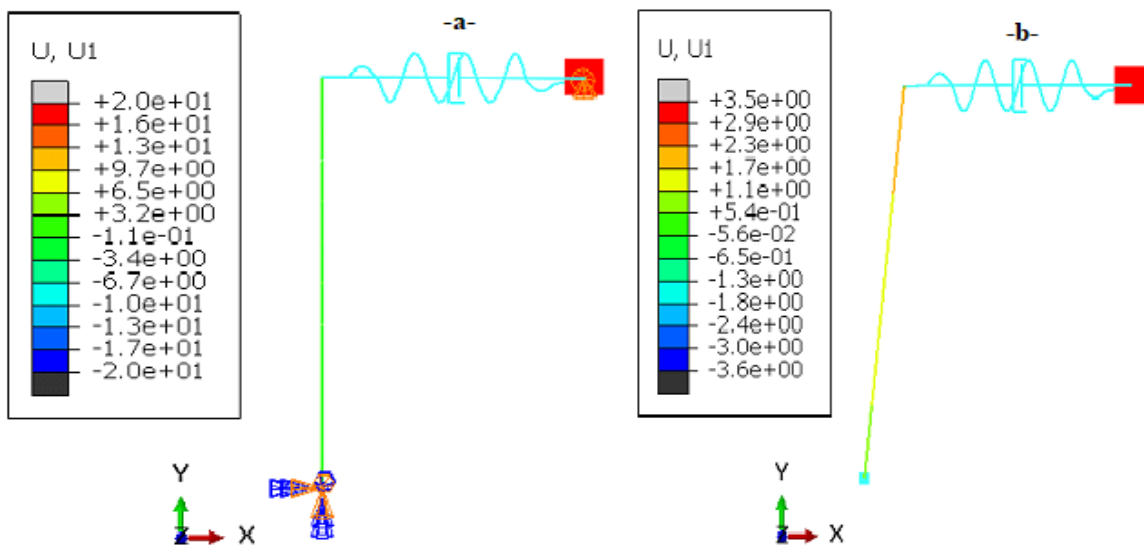


Fig. V.5. Representation of the Abaqus model in deformed state (a) fixed base (b) flexible base.

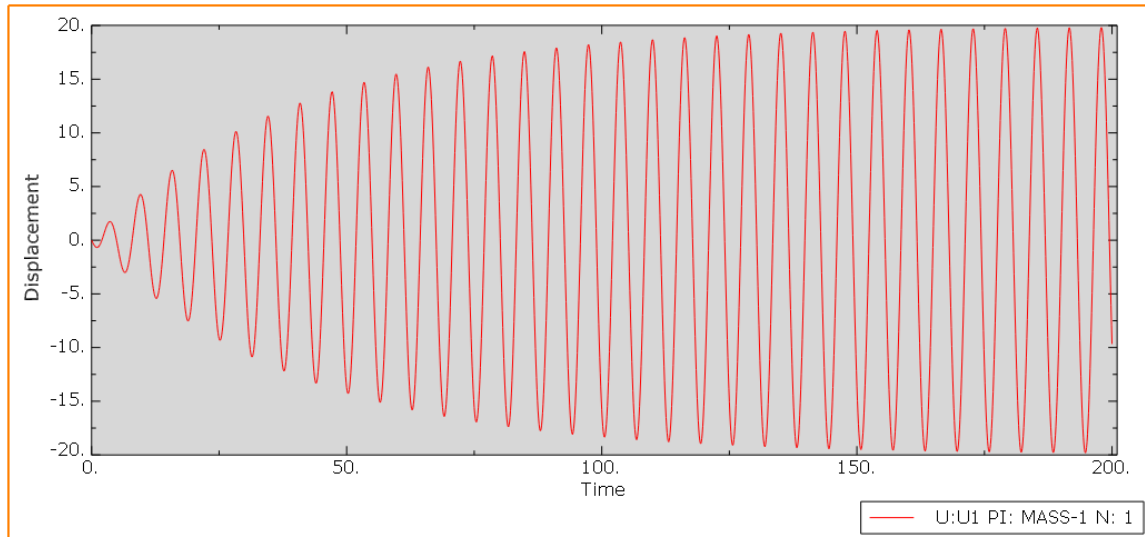


Fig. V.6. Absolute displacement of the fixed base structure (Abaqus, 2021).

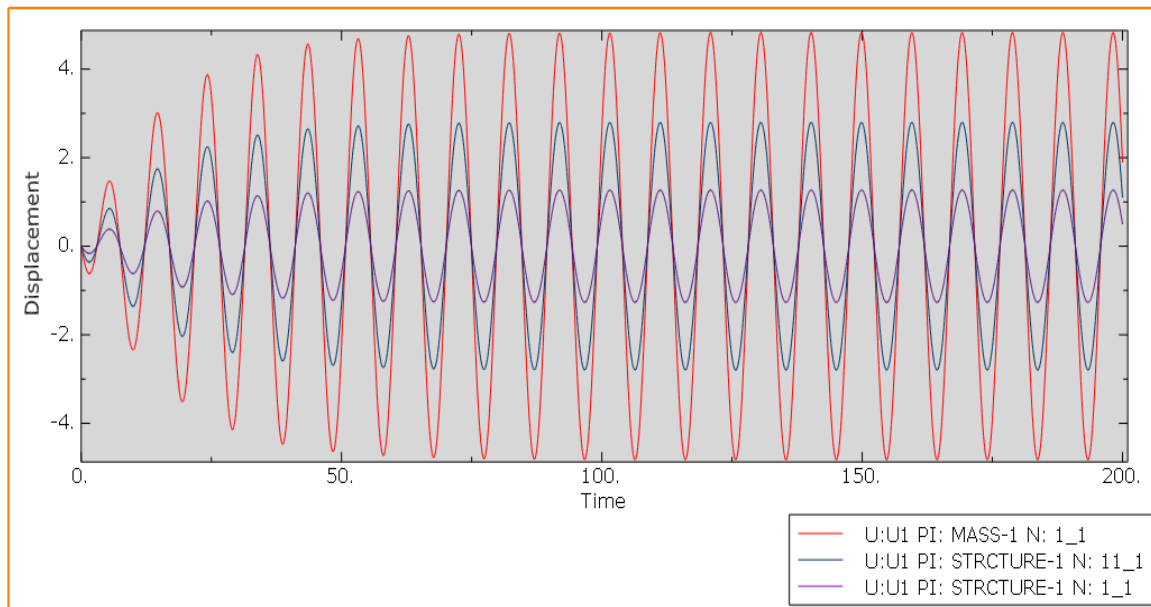


Fig. V.7. Different displacements of the flexible base structure: total or relative displacement ($u + u_0 + h\phi$; red line); displacement of the base ($u_0 + h\phi$; blue line); horizontal displacement of the base (u_0 ; purple line) (Abaqus, 2021).

This part is divided into two parts, the first part is dedicated to the analysis of the soil-structure interaction with a viscoelastic soil behavior, and the second part will be dedicated to the analysis of the soil-structure interaction with a nonlinear soil behavior using the equivalent linear method, which is determined by the CALDYNASOIL design code by Badreddine and Fillali (2012) in the present study. Before starting the study of the influences of the nonlinear soil behavior in the ABAQUS 2D model, we will first validate it with the

analysis of the soil-structure interaction with a viscoelastic behavior of the soil under harmonic loading.

V.4.1. Part I: Viscoelastic soil behavior

Using the same values as in the analytical analysis of the viscoelastic soil behavior, in the following part we have simulated the model numerically using ABAQUS software.

The following graphs (see **Fig. V.8** and **Fig. V.9**) have been constructed for the different cases with (or without) soil-structure interaction, namely:

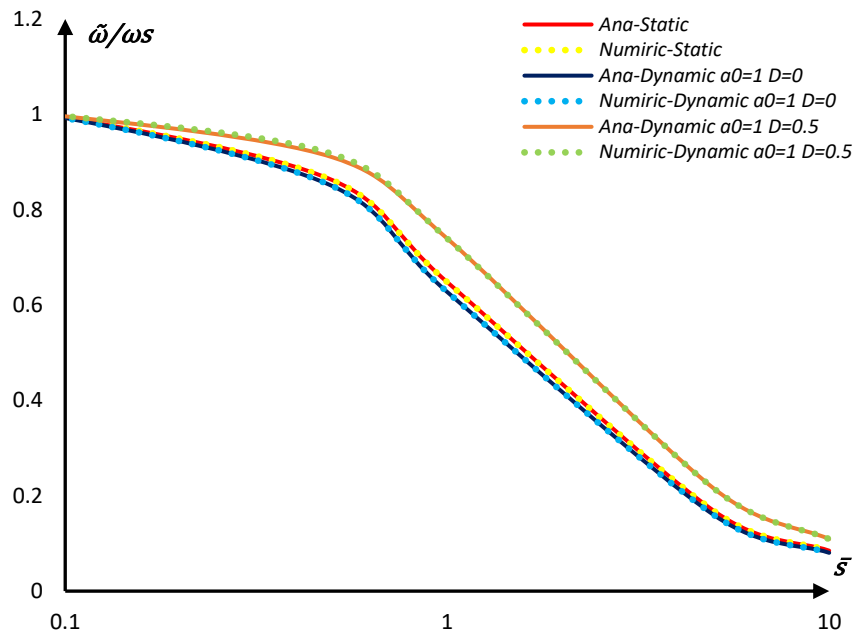
- Fixed base.
- Flexible base:
 - Visco-elastic soil behavior with static impedance function (frequency-independent impedance function).
 - Visco-elastic soil behavior with dynamic impedance function (frequency-dependent impedance function).

It should be noted that in the following graphs we denote by:

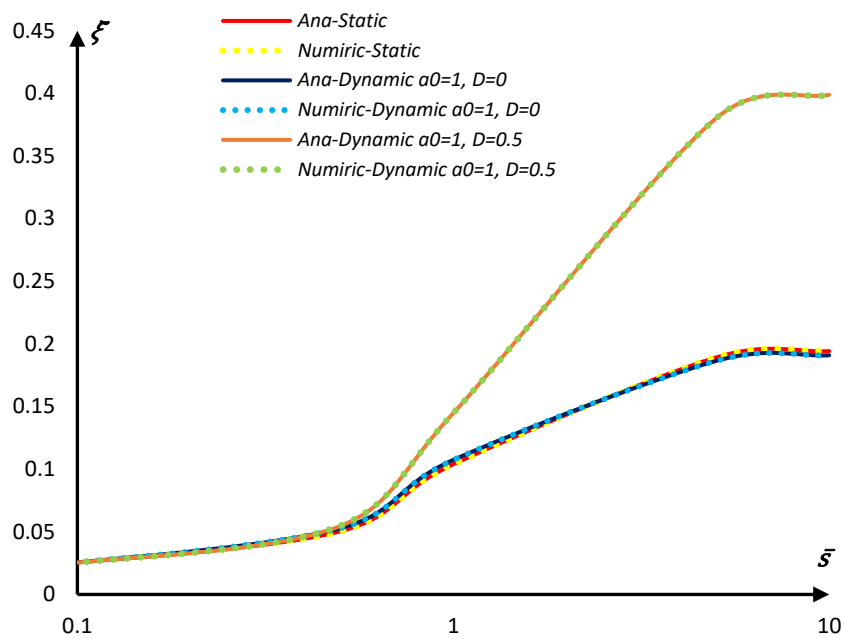
- **Ana**: Analytical results (solid line).
- **Num**: Numerical results (dotted line).
- **Static**: Results Using the Frequency Independent Impedance Function.
- **Dynamic**: Results Using the Frequency Dependent Impedance Function.

V.4.1.1. Natural frequency and damping of the soil-structure system

Fig. V.8(a), (b) shows the properties of the coupled system $\tilde{\omega}/\omega_s$ and $\tilde{\xi}$ obtained numerically for the different cases that were studied and mentioned above, and plotted as a function of \bar{s} ($=0.1, \dots, 10$).



(a) Natural frequency.



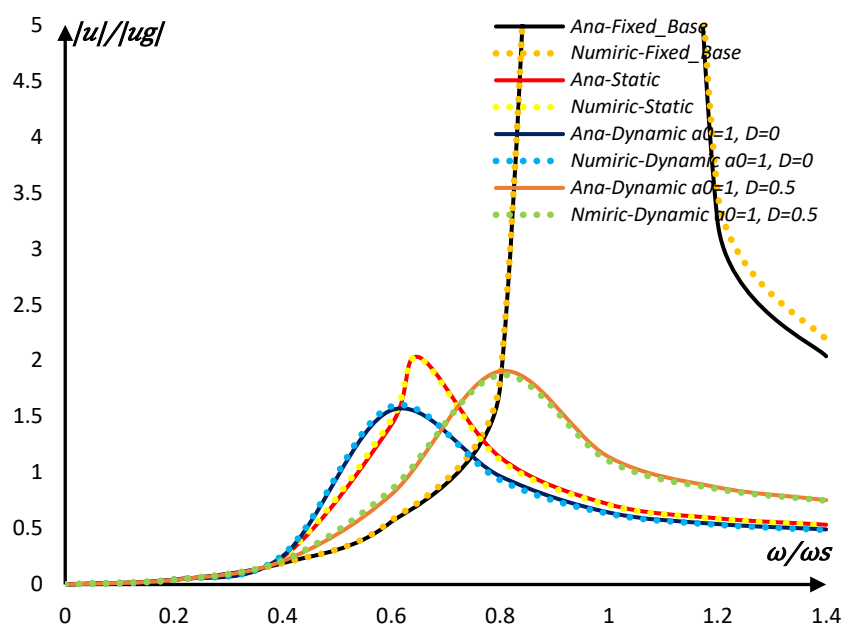
(b) Damping.

Fig. V.8. Numerical results of the properties of the equivalent one-degree-of-freedom system for the viscoelastic soil behavior ($\bar{m}=3$, $\bar{h}=1$, $\nu=0.33$, $\xi=0.025$, $\xi_g=0.05$): (a), (b).

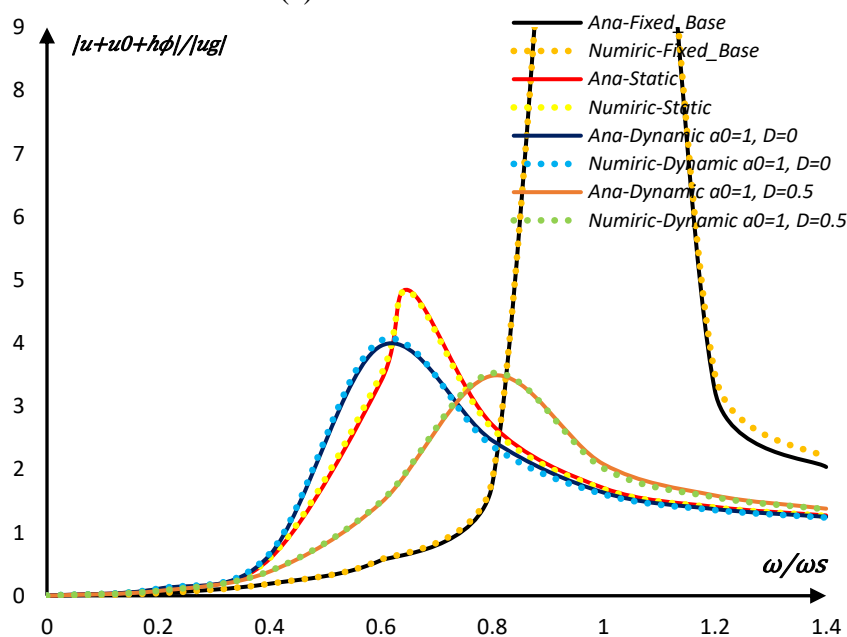
V.4.1.2. Relative and absolute displacement of the structure

The relative and absolute displacements of the structure (u/u_g , $u + u_0 + h\phi/u_g$) for the two cases of the structure base condition (fixed and flexible bases) and for the two cases of the impedance function form (static, dynamic) and for the two viscoelastic soil behavior

were numerically analyzed and plotted against the dimensionless frequency ω/ω_s ($= 0 \dots \dots 1.4$) in **Fig. V.9(a), (b)** and compared to the analytical analysis.



(a) Structural distortion.



(b) Displacement of the mass relative to free field.

Fig. V.9. Numerical results of the relative and absolute displacements of the structure for the viscoelastic soil behavior: (a), (b).

As can be seen from the results presented in **Fig. V.8(a), (b)** and **Fig. V.9(a), (b)**, a very satisfactory agreement is observed between the two types of analysis used in the present work (analytical analysis (solid line), numerical analysis (dotted line)), which is due to the good

simulation of the model. These results confirm the capability of the numerical method. After these validations, we can say that our model simulation is capable of numerically determining the response of the soil-foundation interaction problem, taking into account the nonlinear behavior of the soil.

V.4.2. Part II: Equivalent linear soil behavior

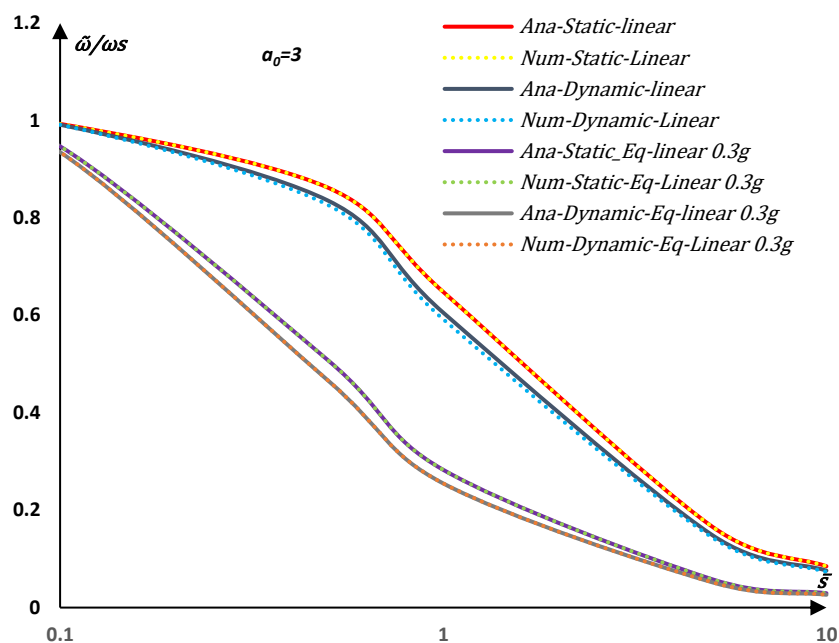
In the following section, we have simulated the model numerically using ABAQUS software, using the same values as in the analytical analysis of the equivalent linear soil behavior. The results of the numerical simulation are compared with the results of the analytical analysis.

The following graphs (see **Fig. V.10**, **Fig. V.11** and **Fig. V.12**) have been constructed for the different cases with (or without) soil-structure interaction, namely:

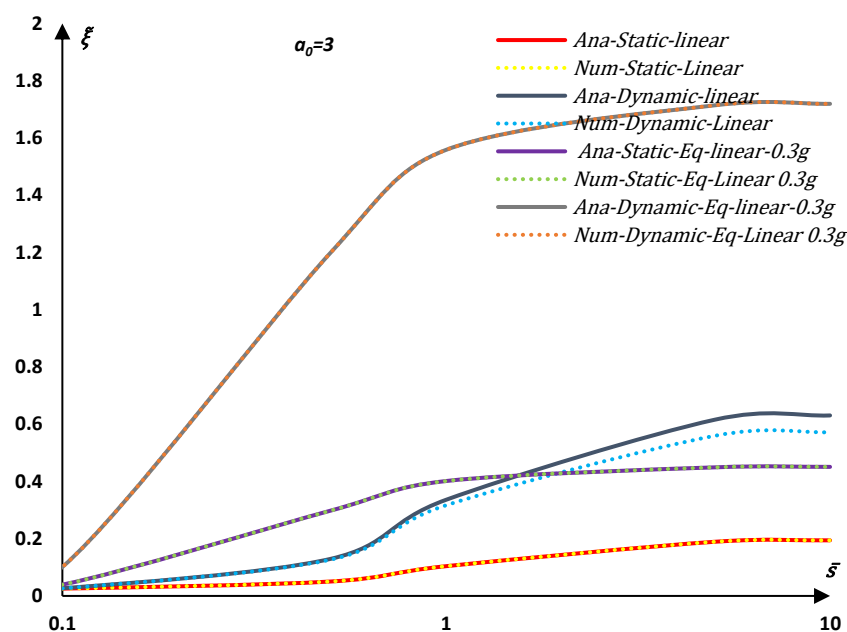
- Fixed base.
- Flexible base:
 - Visco-elastic soil behavior with static impedance function (frequency-independent impedance function).
 - Visco-elastic soil behavior with dynamic impedance function (frequency-dependent impedance function).
 - Equivalent linear soil behavior with static impedance function (frequency-independent impedance function).
 - Equivalent linear soil behavior with dynamic impedance function (frequency-dependent impedance function).

V.4.2.1. Natural frequency and damping of the soil-structure system

Fig. V.10 shows the properties of the coupled system $\tilde{\omega}/\omega_s$ and $\tilde{\xi}$ obtained numerically for the different cases studied and plotted as a function of $\bar{s}(=0.1, \dots, 10)$.



(c) Natural frequency.



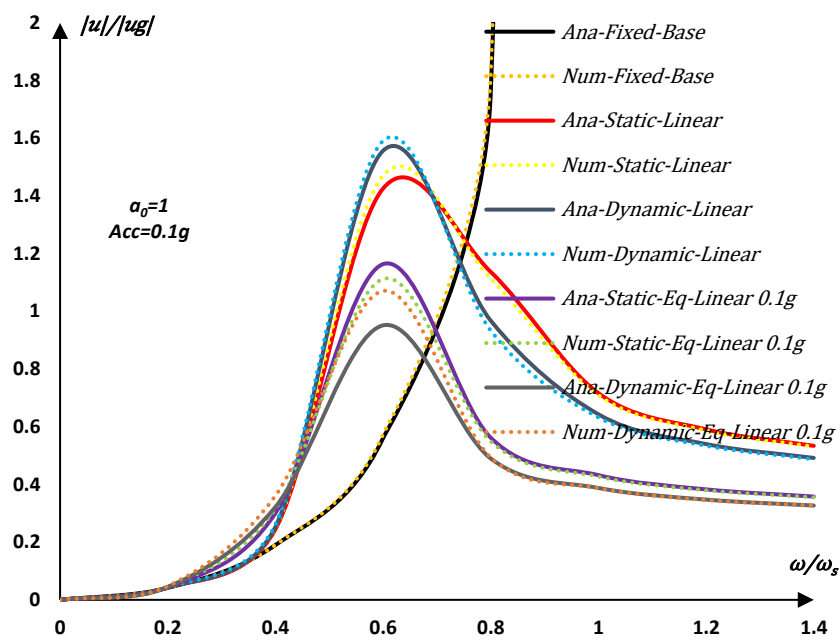
(d) Damping.

Fig. V.10. Numerical results of the properties of the equivalent one-degree-of-freedom system for the various cases studied ($\bar{m}=3$, $\bar{h}=1$, $\nu=0.33$, $\xi=0.025$, $\xi_g=0.05$): (a), (b).

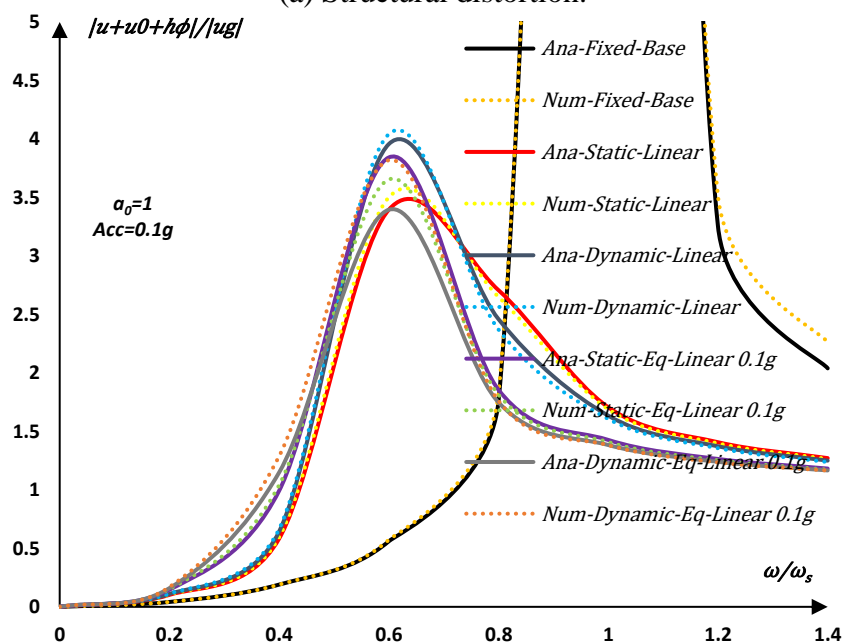
V.4.2.2. Relative and absolute displacement of the structure:

The relative and absolute displacements of the structure (u/u_g , $u + u_0 + h\phi/u_g$) for the two cases of the structure base condition (fixed and flexible bases) and for the two cases of the impedance function form (static, dynamic) and for the two soil behaviors (viscoelastic and equivalent linear soil behavior) were numerically analyzed and compared with the

analytical results and plotted against the dimensionless frequency ω/ω_s ($= 0 \dots \dots 1.4$) in **Fig. V.11** and **Fig. V.12**. The same data were used as in the previous section, except in the case of the dynamic impedance functions, where two values of the dimensionless frequency a_0 ($= 1$ and 3) were studied, and in the case of the equivalent linear soil behavior, where two values of the seismic acceleration levels $Acc(g)$ ($=0.1g$ and $0.3g$) were also studied (**Fig. V.12**).



(a) Structural distortion.



(b) Displacement of the mass relative to free field.

Fig. V.11. Numerical results of the relative and absolute displacements of the structure: (a), (b).

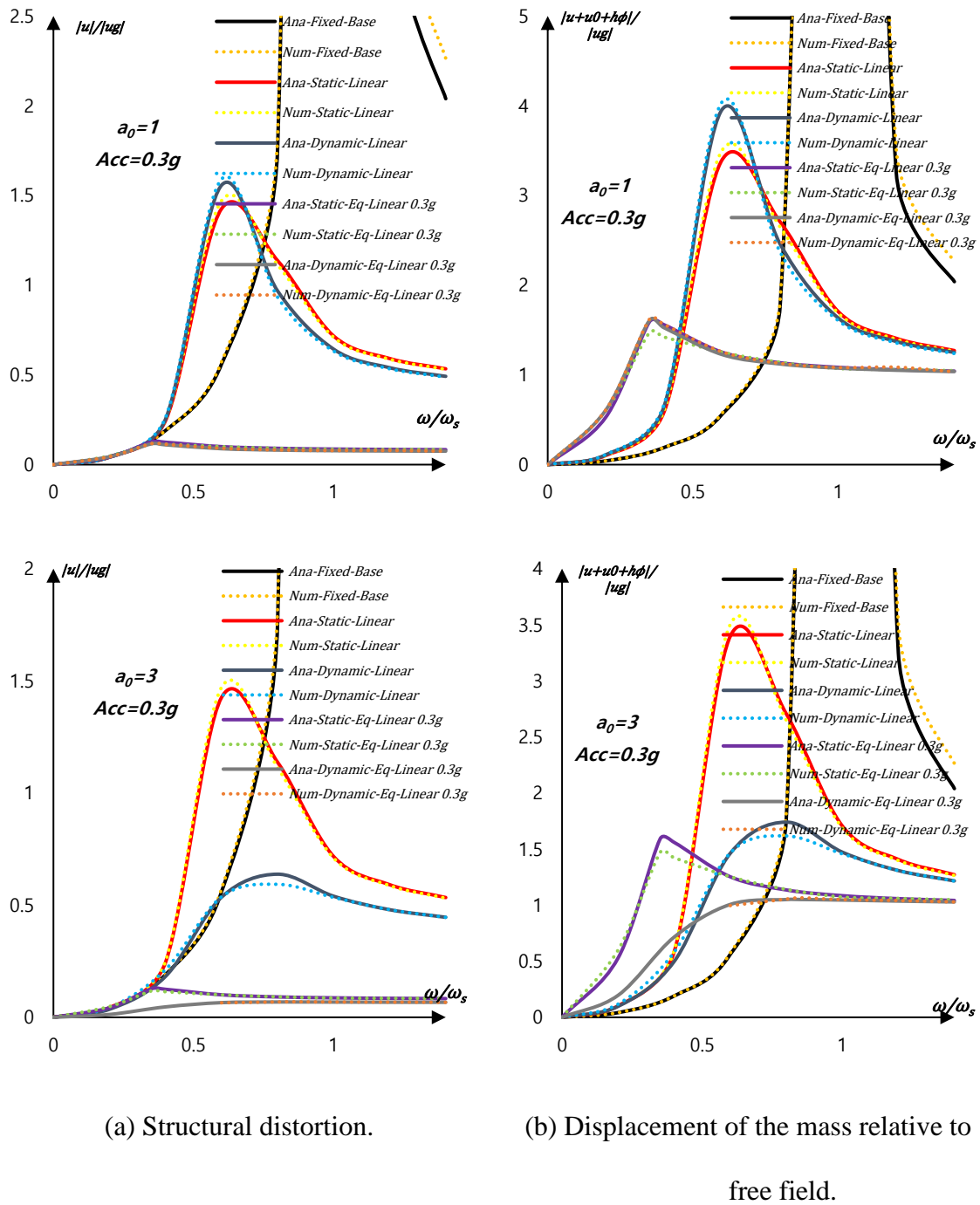


Fig. V.12. Comparative study between the analytical and numerical analysis: (a), (b).

The comparisons of the numerical data (dotted line) (see **Fig. V.10**, **Fig. V.11** and **Fig. V.12**) with the predictions obtained by an analytical formulation based on the dynamic equilibrium of the soil-structure system modeled by an analogous model with three degrees of freedom (solid line) show, in general, a very good agreement between the analytical and the numerical results, especially, in phase I (results obtained according to the visco-elastic soil

behavior), where the agreement is excellent. In the case of the second soil behavior approach (equivalent linear), a slight deviation in displacements is observed, which can be related to the numerical precision. However, the differences found are very small. This is a significant computational advantage for the designer who wants to take into account the nonlinearity of the soil, without having to apply cumbersome and lengthy procedures.

V.5. CONCLUSION

Simulation is widely used in many fields, including engineering. The purpose of simulation is to reproduce or represent the behavior or operation of a particular system, phenomenon, or situation in a realistic way. To do this, the physics of the problem and the mechanical parameters must be taken into account by the numerical model.

In this chapter, we have presented a numerical analysis of the behavior of the soil-structure system under dynamic loading for two cases of the structure base condition (fixed and flexible bases), for two cases of the impedance function form (static, dynamic), and for two soil behaviors (viscoelastic and equivalent linear soil behavior). A brief comparison with the analytical results is then presented.

The same analytical model has been simulated numerically using ABAQUS software, and the same analyses performed analytically in previous chapters have been performed numerically in this chapter. The comparisons made between these two types of analyses generally show a very good agreement, especially in Phase I (results obtained according to the viscoelastic soil behavior), where the agreement is excellent. In the case of the second soil behavior approach (equivalent linear), a slight deviation in the displacements is observed, which can be related to the numerical precision. However, the differences found are very small.

GENERAL CONCLUSION

GENERAL CONCLUSION

In this work, we have investigated the influence of nonlinear soil behavior using an equivalent linear model on the seismic response of buildings resting on shallow foundations. This behavior is determined by the CALDYNASOIL design code of Sbartai and Filali (2012). First, an analytical formulation based on the dynamic equilibrium of the soil-structure system represented by an analog model, and second, numerical analysis using 2D finite element modeling with ABAQUS software. Results of the latter analysis were compared with those of the analytical solution. The present work presents a holistic methodology for considering nonlinear soil behavior and soil-foundation-structure interaction in a modular manner.

In this study, the following main points are considered:

The dynamic response of a structure under seismic motion and taking into account the soil-structure interaction can strongly depend on the type of soil (c_s), the characteristic of the structure (massive, slender, ...), the foundation embedment ratio D , and the dimensionless excitation frequency (a_0), since its increase leads to a decrease of the displacement amplitude and an increase of the equivalent damping $\tilde{\xi}$. And it is also highly dependent on the characterization of the impedance function (static or dynamic) and the ground behavior.

Propose new analytical formulas that allow the calculation of the equivalent frequency and equivalent damping of a soil-structure system based on frequency-dependent impedance functions. These formulas have shown how the combined (SSI) effects and frequency-dependent impedance functions lead to an increased value of change in the results and demonstrate the differences that occur due to the effect of the form of the impedance function (static or dynamic).

The presence of soil significantly modifies the dynamic characteristics and the seismic response of the structure. This effect depends entirely on the damping radiation of the soil.

The massive and/or higher structures, the soft soil and the excitation frequency are the main parameters where the SSI effect is more evident. The soil behavior also plays an important role in the dynamic responses of the structures.

The dynamic response of a soil structure system depends on more parameters in the case of nonlinear soil behavior which is more complex than the linear elastic soil behavior, where the energy dissipation depends on the amplitude of the motion and its frequency, the

type of impedance function form (static, dynamic), shear modulus reduction and damping increase.

The dynamic responses of the structure are quite dependent on the excitation amplitude, since its increase leads to a decrease in the magnitude of the frequency ratio $\tilde{\omega}/\omega_s$ and an increase in the equivalent damping $\tilde{\xi}$ from the linear case, and this effect is reflected in the deformation value. The higher the excitation amplitude, the greater the attenuation of the amplitude of the structural distortion and the displacement of the mass to lower values.

The effect of the change in soil behavior due to the imposed seismic motion is very remarkable and strongly related to the form of the impedance function at all frequencies. This effect is characterized by an overestimation of the displacement of the structure and a strong dependence on the type of impedance function and the soil properties. Compared to the viscoelastic soil, we find that the structural distortion has a displacement decrease of about 82% and 77%, respectively, for the static and dynamic impedance function and the equivalent linear soil, while the displacement of the mass decreases by about 52% and 37%, respectively.

As the nonlinearity of the soil becomes important, i.e., the soil damping increases and the shear modulus decreases, the amplitude of the structural deformation as well as the displacement of the mass are dominated by lower frequencies (shift to the left in the dimensionless frequency of the flexible base with equivalent linear soil behavior using the static and dynamic impedance function by 30% and 6.67%, respectively, compared to the visco-linear soil behavior). This variation explains that the structure becomes more stiffer and the soil becomes more flexible.

New analytical nonlinear relationships are proposed for the viscoelastic soil behavior between the relative and absolute displacement of the structure, the embedment ratio of the foundation and the dimensionless circular frequency of the excitation, and for the equivalent linear soil behavior between the relative and absolute displacement of the structure, the acceleration level $Acc(g)$ and the dimensionless circular frequency of the excitation, in order to consider this influence in a simple way in the calculation of the soil-structure interaction for different soil and structure types and for different seismic excitation frequencies.

Excellent agreement between the finite element analysis and the analytical results, obtained thanks to the judicious representation of the model, which is an important computational advantage for the designer who wants to take into account the nonlinearity of the soil without using cumbersome and lengthy procedures.

In conclusion, neglecting the effect of soil-structure interaction and the effect of soil behavior and/or the approximate representation of impedance functions in the analysis of structures can, under certain circumstances, result in behavior that is very different from the real one and, therefore, can lead to misdirection in the engineer's decision-making process, thus affecting the seismic safety of buildings. Therefore, it is strongly recommended that practicing engineers and engineering companies to consider the effects of soil-structure interaction and properly address the dynamic characteristics of the soil and its behavior simultaneously in seismic analysis and building design to ensure safety and structural integrity against seismic actions.

❖ **Perspectives:**

The study of the seismic response of a structure, taking into account the nonlinear soil behavior found in this thesis, opens the door to verify the response of several structures in the field of civil engineering, especially those structures located in the most seismic zones.

To conclude this work, it is useful to draw up a list of topics that could be developed in future research:

- Use of other types of foundations (rectangular, square, shallow or deep) and other types of structures (comparison of the response between regular and irregular structures; tall structures with and without piles, ...etc.).
- Use other types of soils (loose, firm, rocky) and other types of nonlinear models to study the SSI system.
- Study the influence of the choice of soil behavior laws on the modeling.
- Use a more powerful model than the analogous three-degrees-of-freedom model.

REFERENCES

- ABAQUS CAE 2021. Standard User's Manual. Version 2021.
- Abate, Glenda, and Maria Rossella Massimino. 2017. "Parametric Analysis of the Seismic Response of Coupled Tunnel–Soil–Aboveground Building Systems by Numerical Modelling." *Bulletin of Earthquake Engineering* 15(1): 443–67.
- Abdeddaim, Mahdi et al. 2022. "Optimal Design of Magnetorheological Damper for Seismic Response Reduction of Base-Isolated Structures Considering Soil-Structure Interaction." *Structures* 38: 733–52. <https://doi.org/10.1016/j.istruc.2022.02.039>.
- Abdel Raheem, Shehata E., Mohamed M. Ahmed, and Tarek M. A. Alazrak. 2015. "Evaluation of Soil–Foundation–Structure Interaction Effects on Seismic Response Demands of Multi-Story MRF Buildings on Raft Foundations." *International Journal of Advanced Structural Engineering* 7(1): 11–30. <http://link.springer.com/10.1007/s40091-014-0078-x>.
- Ahmad, S, and A.K Rupani. 1999. "Horizontal Impedance of Square Foundation in Layered Soil." *Soil Dynamics and Earthquake Engineering* 18(1): 59–69. <https://linkinghub.elsevier.com/retrieve/pii/S0267726198000281>.
- Alzabeebee, Saif. 2021. "Influence of Soil Model Complexity on the Seismic Response of Shallow Foundations." *Geomechanics and Engineering* 24(2): 193–203.
- Amina, Tahar Berrabah, Belharizi Mohamed, Laulusa André, and Bekkouche Abdelmalek. 2015. "Fluid–Structure Interaction of Brezina Arch Dam: 3D Modal Analysis." *Engineering Structures* 84: 19–28. <https://linkinghub.elsevier.com/retrieve/pii/S0141029614006993>.
- Anastasopoulos, I., and Th Kontoroupi. 2014. "Simplified Approximate Method for Analysis of Rocking Systems Accounting for Soil Inelasticity and Foundation Uplifting." *Soil Dynamics and Earthquake Engineering* 56: 28–43. <http://dx.doi.org/10.1016/j.soildyn.2013.10.001>.
- Andreotti, G., and C. G. Lai. 2017. "A Nonlinear Constitutive Model for Beam Elements with Cyclic Degradation and Damage Assessment for Advanced Dynamic Analyses of Geotechnical Problems. Part II: Validation and Application to a Dynamic Soil–Structure Interaction Problem." *Bulletin of Earthquake Engineering* 15(7): 2803–25.
- Andrzej Truty. 2018. "On Consistent Nonlinear Analysis of Soil – Structure Interaction Problems." *Studia Geotechnica et Mechanica* 40(2): 86–95.
- ASCE, 2010: Applied Technology Council. "Tentative Provisions for the Development of Seismic Regulations for Buildings" ATC-3-06: California
- Assimaki, Dominic, and Eduardo Kausel. 2002. "An Equivalent Linear Algorithm with Frequency- and Pressure-Dependent Moduli and Damping for the Seismic Analysis of Deep Sites." *Soil Dynamics and Earthquake Engineering* 22(9–12): 959–65.
- ATC, "Improvement of Nonlinear Static Seismic Analysis Procedures (FEMA 450)," Edition. Washington, D.C.: Applied Technology Council, Federal Emergency Management Agency, 2005.
- Avilés, Javier, and Luis E. Pérez-Rocha. 2005a. "Design Concepts for Yielding Structures on Flexible Foundation." *Engineering Structures* 27(3): 443–54.
- Avilés, Javier, and Luis Eduardo Pérez-Rocha. 2005b. "Influence of Foundation Flexibility on R_{μ} and C_{μ} Factors." *Journal of Structural Engineering* 131(2): 221–30. <https://ascelibrary.org/doi/10.1061/%28ASCE%290733-9445%282005%29131%3A2%28221%29>.
- Awchat, G. D., and A. S. Monde. 2021. "Influence of Soil-Structure Interaction on the Seismic Response of the Structure on Mat Foundation." *Civil Engineering Journal (Iran)* 7(10): 1679–92.
- Badreddine, Sbartaï, and Kamel Fillali. 2012. "Estimation of the Liquefaction's Risk of a Soil Deposit under Seismic Solicitations: Petrochemical Zone of Skikda City." *Applied Mechanics and Materials* 166–169: 2315–20. <https://www.scientific.net/AMM.166-169.2315>.
- Bahuguna, Ashish, and Mohd Firoj. 2021. "Nonlinear Seismic Performance of Nuclear Structure with Soil–Structure Interaction." *Iranian Journal of Science and Technology - Transactions of Civil Engineering* (0123456789). <https://doi.org/10.1007/s40996-021-00728-2>.
- Belkhir, Hamoudi, Badreddine Sbartaï, Kamel Filali, and Salah Messioued. 2022. "Linear Equivalent Seismic Response of a Surface Foundation Excited by an SH Harmonic Wave." *European Journal of Environmental and Civil Engineering* 0(0): 1–18. <https://doi.org/10.1080/19648189.2022.2162978>.
- Beltrami, C, C.G.LAI, A. Pecker, Seismic Soil Structure Interaction in Large Diameter Shaft Foundations, Research Report No. ROSE – 2006/04, ROSE School – EUCENTRE, Pavia, Italy, 2006.

- Betti, R., A. M. Abdel-Ghaffar, and A. S. Niazy. 1993. "Kinematic Soil–Structure Interaction for Long-Span Cable-Supported Bridges." *Earthquake Engineering & Structural Dynamics* 22(5): 415–30. <https://onlinelibrary.wiley.com/doi/10.1002/eqe.4290220505>.
- Bolisetti, Chandrakanth. 2015. "Site Response, Soil-Structure Interaction and Structure-Soil-Structure Interaction for Performance Assessment of Buildings and Nuclear Structures." *ProQuest Dissertations and Theses* (Cmmi): 446. http://search.proquest.com/docview/1658211292?accountid=40695%5Cnhttp://sfxhosted.exlibrisgroup.com/polymtl?url_ver=Z39.88-2004&rft_val_fmt=info:ofi/fmt:kev:mtx:dissertation&genre=dissertations+&+theses&sid=ProQ:ProQuest+Dissertations+&+Theses+A&I&atit.
- Bolisetti, Chandrakanth, Andrew S. Whittaker, and Justin L. Coleman. 2018. "Linear and Nonlinear Soil-Structure Interaction Analysis of Buildings and Safety-Related Nuclear Structures." *Soil Dynamics and Earthquake Engineering* 107(January): 218–33. <https://doi.org/10.1016/j.soildyn.2018.01.026>.
- Boudaa, Souad, Salah Khalfallah, Mechanical Engineering, and Emilio Bilotta. 2021. "INFLUENCE OF THE SOIL-STRUCTURE INTERACTION ON FREE VIBRATIONS OF BEAM BY THE SPECTRAL ELEMENT METHOD." 16(1): 51–60.
- Boumekik, A. (1985). Fonctions impédances d'une fondation vibrante en surface ou partiellement encastree dans un sol multicouche. Free University of Bruxelles (Doctoral dissertation, Ph. D. Thesis).
- Burman, A., Parsuram Nayak, P. Agrawal, and Damodar Maity. 2012. "Coupled Gravity Dam–Foundation Analysis Using a Simplified Direct Method of Soil–Structure Interaction." *Soil Dynamics and Earthquake Engineering* 34(1): 62–68.
- Çakır, Özcan, and Nart Coşkun. 2021. "Theoretical Issues with Rayleigh Surface Waves and Geoelectrical Method Used for the Inversion of Near Surface Geophysical Structure." *Journal of Human, Earth, and Future* 2(3): 183–99.
- Castelli, Francesco, Salvatore Grasso, Valentina Lentini, and Maria Stella Vanessa Sammito. 2021. "Effects of Soil-Foundation-Interaction on the Seismic Response of a Cooling Tower by 3d-Fem Analysis." *Geosciences (Switzerland)* 11(5).
- Cavaliere, Francesco, António A. Correia, Helen Crowley, and Rui Pinho. 2020. "Dynamic Soil-Structure Interaction Models for Fragility Characterisation of Buildings with Shallow Foundations." *Soil Dynamics and Earthquake Engineering* 132(December).
- Çelebi, E., S. Firat, and I. Çankaya. 2006. "The Evaluation of Impedance Functions in the Analysis of Foundations Vibrations Using Boundary Element Method." *Applied Mathematics and Computation* 173(1): 636–67.
- Çelebi, E., F. Göktepe, and N. Karahan. 2012. "Non-Linear Finite Element Analysis for Prediction of Seismic Response of Buildings Considering Soil-Structure Interaction." *Natural Hazards and Earth System Sciences* 12(11): 3495–3505.
- Chatzigogos, C. T., A. Pecker, and J. Salençon. 2009. "Macroelement Modeling of Shallow Foundations." *Soil Dynamics and Earthquake Engineering* 29(5): 765–81.
- Cremer, Cécile, Alain Pecker, and Luc Davenne. 2001. "Cyclic Macro-Element for Soil-Structure Interaction: Material and Geometrical Non-Linearities." *International Journal for Numerical and Analytical Methods in Geomechanics* 25(13): 1257–84. <https://onlinelibrary.wiley.com/doi/10.1002/nag.175>.
- Crouse, C. B., and Jeff McGuire. 2001. "Energy Dissipation in Soil-Structure Interaction." *Earthquake Spectra* 17(2): 235–59. <http://journals.sagepub.com/doi/10.1193/1.1586174>.
- Davidovici, V. (1985). 'Génie Parasismique'. Presse de l'école nationale des ponts et chaussées.
- Durmuş, Ayşegül, and Ramazan Livaoglu. 2015. "A Simplified 3 D.O.F. Model of A FEM Model for Seismic Analysis of a Silo Containing Elastic Material Accounting for Soil–Structure Interaction." *Soil Dynamics and Earthquake Engineering* 77: 1–14. <https://linkinghub.elsevier.com/retrieve/pii/S0267726115001165>.
- EC8–2004 (English): Eurocode 8: Design of structures for earthquake resistance. Part 5: Foundation, retaining structures and geotechnical aspects
- El Hoseny, Mohammed, Jianxun Ma, Walid Dawoud, and Davide Forcellini. 2023. "The Role of Soil Structure Interaction (SSI) on Seismic Response of Tall Buildings with Variable Embedded Depths by Experimental and Numerical Approaches." *Soil Dynamics and Earthquake Engineering* 164: 107583. <https://linkinghub.elsevier.com/retrieve/pii/S0267726122004286>.

- Far, Harry, and Deacon Flint. 2017. "Significance of Using Isolated Footing Technique for Residential Construction on Expansive Soils." *Frontiers of Structural and Civil Engineering* 11(1): 123–29. <http://link.springer.com/10.1007/s11709-016-0372-8>.
- Farghaly, Ahmed Abdelraheem, and Hamdy Hessain Ahmed. 2013. "Contribution of Soil-Structure Interaction to Seismic Response of Buildings." *KSCE Journal of Civil Engineering* 17(5): 959–71.
- Fatahi, Behzad, and S. Hamid Reza Tabatabaiefar. 2014. "Fully Nonlinear versus Equivalent Linear Computation Method for Seismic Analysis of Midrise Buildings on Soft Soils." *International Journal of Geomechanics* 14(4): 04014016.
- FEMA 440 (2005), Recommended Improvements of Nonlinear Static Seismic Analysis Procedures, Applied Technology Council: California.
- Filali, Kamel, and Badreddine Sbartaï. 2017. "A Comparative Study between Simplified and Nonlinear Dynamic Methods for Estimating Liquefaction Potential." *Journal of Rock Mechanics and Geotechnical Engineering* 9(5): 955–66. <https://linkinghub.elsevier.com/retrieve/pii/S1674775516302256>.
- Forcellini, Davide. 2022. "Seismic Fragility of Tall Buildings Considering Soil Structure Interaction (SSI) Effects." *Structures* 45: 999–1011. <https://linkinghub.elsevier.com/retrieve/pii/S2352012422008463>.
- Forcellini, Davide, Daniele Mina, and Hassan Karampour. 2022. "The Role of Soil Structure Interaction in the Fragility Assessment of HP/HT Unburied Subsea Pipelines." *Journal of Marine Science and Engineering* 10(1).
- Gao, Zhidong, Mi Zhao, Xiuli Du, and Xu Zhao. 2020. "Seismic Soil–Structure Interaction Analysis of Structure with Shallow Foundation Using Response Spectrum Method." *Bulletin of Earthquake Engineering* 18(8): 3517–43. <https://link.springer.com/10.1007/s10518-020-00827-x>.
- Galy, B. Méthodes de conception et étude du comportement sismique des fondations superficielles sur sol naturel et traité, considérant l'interaction sol-structure, thèse de doctorat, École de technologie supérieure université du Québec, 2013.
- Garevski, M., & Ansal, A. 2010. "Earthquake Engineering in Europe." In *Angewandte Chemie International Edition*, 6(11), 951–952., Geotechnical, Geological, and Earthquake Engineering, eds. Mihail Garevski and Atilla Ansal. Dordrecht: Springer Netherlands. <http://link.springer.com/10.1007/978-90-481-9544-2>.
- Gazetas, George. 1992. "FORMULAS AND CHARTS FOR IMPEDANCES OF F." 117(9): 1363–81.
- Gazetas, G. et al. 2008. "Preliminary Design Recommendations for Dip-Slip Fault–Foundation Interaction." *Bulletin of Earthquake Engineering* 6(4): 677–87. <http://link.springer.com/10.1007/s10518-008-9082-5>.
- Gazetas, George. 1983. "Analysis of Machine Foundation Vibrations: State of the Art." *International Journal of Soil Dynamics and Earthquake Engineering* 2(1): 2–42.
- Gazetas, George. 1991. "Formulas and Charts for Impedances of Surface and Embedded Foundations." *Journal of Geotechnical Engineering* 117(9): 1363–81. <https://ascelibrary.org/doi/10.1061/%28ASCE%290733-9410%281991%29117%3A9%281363%29>.
- Gazetas, George, and Kenneth H. Stokoe. 1991. "Free Vibration of Embedded Foundations: Theory versus Experiment." *Journal of Geotechnical Engineering* 117(9): 1382–1401. <https://ascelibrary.org/doi/10.1061/%28ASCE%290733-9410%281991%29117%3A9%281382%29>.
- Ghandil, M., F. Behnamfar, and M. Vafaeian. 2016. "Dynamic Responses of Structure-Soil-Structure Systems with an Extension of the Equivalent Linear Soil Modeling." *Soil Dynamics and Earthquake Engineering* 80: 149–62. <http://dx.doi.org/10.1016/j.soildyn.2015.10.014>.
- Guéguen, P., J. L. Chatelain, B. Guillier, and H. Yepes. 2000. "An Indication of the Soil Topmost Layer Response in Quito (Ecuador) Using Noise H/V Spectral Ratio." *Soil Dynamics and Earthquake Engineering* 19(2): 127–33.
- Guellil, Mohamed Elhebib, Zamila Harichane, Hakima Djilali Berkane, and Amina Sadouki. 2017. "Soil and Structure Uncertainty Effects on the Soil Foundation Structure Dynamic Response." *Earthquake and Structures* 12(2): 153–63.
- Guellil, Mohamed Elhebib, Zamila Harichane, and Arkan Çelebi. 2019. "Comparison Between Non-Linear and Stochastic Methods for Dynamic SSI Problems." In Springer International Publishing, 191–94. <http://link.springer.com/10.1007/978-3-030-01656-2>.
- Guellil, Mohamed Elhebib, Zamila Harichane, and Erkan Çelebi. 2020. "Seismic Codes Based Equivalent Nonlinear and Stochastic Soil Structure Interaction Analysis." *Studia Geotechnica et Mechanica*

43(1): 1–14.

- Gupta, S., Lin, T. W., Penzien, J., and Yen, C. S., (1980). Hybrid modelling of soil structure interaction. Earthquake Engineering Research Center Report 80-9, University of California, Berkeley.
- Halabian, Amir M., and M. Hesham El Naggar. 2002. “Effect of Non-Linear Soil–Structure Interaction on Seismic Response of Tall Slender Structures.” *Soil Dynamics and Earthquake Engineering* 22(8): 639–58.
- Hardin B, Drnevich V (1972) Shear modulus and damping in soils: design equations and curves. J Soil Mech Found Div, ASCE 98(7):667e92
- Harichane, Zamila, Mohamed Elhebib Guellil, and Hamid Gadouri. 2018. “Benefits of Probabilistic Soil-Foundation-Structure Interaction Analysis.” *International Journal of Geotechnical Earthquake Engineering* 9(1): 42–64.
- Horace Lamb. 1904. “I. On the Propagation of Tremors over the Surface of an Elastic Solid.” *Philosophical Transactions of the Royal Society of London. Series A, Containing Papers of a Mathematical or Physical Character* 203(359–371): 1–42. <https://royalsocietypublishing.org/doi/10.1098/rsta.1904.0013>.
- Idriss, I. M. and Seed, H. B. (1968) ‘Seismic Response of Horizontal Soil Layers’, Journal of the Soil Mechanics and Foundations Division, 94(4), pp. 1003–1031. Available at: <http://www.resolutionmineeis.us/sites/default/files/references/idriss-seed-1968.pdf>.
- J-I, Chazelas. 2008. “The Kinematic and Inertial Soil-Pile Interactions : Centrifuge Modelling.” 1: 65–68.
- Jaya, K. P., and A. Meher Prasad. 2002. “Embedded Foundation in Layered Soil under Dynamic Excitations.” *Soil Dynamics and Earthquake Engineering* 22(6): 485–98.
- Jayalekshmi, B. R., Ansu Thomas, and R. Shivashankar. 2014. “Dynamic Soil-Structure Interaction Studies on 275m Tall Industrial Chimney with Openings.” *Earthquake and Structures* 7(2): 233–50.
- Jeremic, B., S. Kunnath, and Leah Larson. 2004. “Soil–Foundation–Structure Interaction Effects in Seismic Behavior of Bridges.” *13th World Conference on Earthquake Engineering* (294): 1–11. http://www.iitk.ac.in/nicee/wcee/article/13_294.pdf.
- Jeremić, Boris, Guanzhou Jie, Matthias Preisig, and Nima Tafazzoli. 2009. “Time Domain Simulation of Soil-Foundation-Structure Interaction in Non-Uniform Soils.” *Earthquake Engineering & Structural Dynamics* 38(5): 699–718. <https://onlinelibrary.wiley.com/doi/10.1002/eqe.896>.
- Jia, Junbo. 2018. *Soil Dynamics and Foundation Modeling*. Cham: Springer International Publishing. <http://link.springer.com/10.1007/978-3-319-40358-8>.
- Jiachun, Wang. 2005. “Influence of Different Boundary Conditions on Analysis of Ssi.” *Nuclear Energy (SMiRT 18)*: 3157–64.
- Jingbo, Liu, and Lu Yandong. 1998. “A Direct Method for Analysis of Dynamic Soil-Structure Interaction Based on Interface Idea.” *Developments in Geotechnical Engineering* 83(C): 261–76.
- Johansson, Jörgen, and Amir Kaynia. 2021. “Equivalent Linear Pseudostatic and Dynamic Modelling of Vertically Vibrating Monopile.” *Marine Structures* 75(May 2019).
- Kaklamanos, James, Laurie G. Baise, Eric M. Thompson, and Luis Dorfmann. 2015. “Comparison of 1D Linear, Equivalent-Linear, and Nonlinear Site Response Models at Six KiK-Net Validation Sites.” *Soil Dynamics and Earthquake Engineering* 69: 207–19. <http://dx.doi.org/10.1016/j.soildyn.2014.10.016>.
- Kamel Filali. 2018. “Modélisation Numérique de La Réponse Sismique d’un Sol et Évaluation Des Effets Induits.” 20 aout 1955-SKIKDA.
- Karabork, T., I. O. Deneme, and R. P. Bilgehan. 2014. “A Comparison of the Effect of SSI on Base Isolation Systems and Fixed-Base Structures for Soft Soil.” *Geomechanics and Engineering* 7(1): 87–103.
- Karapetrou, S. T., S. D. Fotopoulou, and K. D. Ptilakis. 2015. “Seismic Vulnerability Assessment of High-Rise Non-Ductile RC Buildings Considering Soil-Structure Interaction Effects.” *Soil Dynamics and Earthquake Engineering* 73: 42–57. <http://dx.doi.org/10.1016/j.soildyn.2015.02.016>.
- Karatzetzou, Anna, and Dimitris Ptilakis. 2018. “Modification of Dynamic Foundation Response Due to Soil-Structure Interaction.” *Journal of Earthquake Engineering* 22(5): 861–80.
- Kausel, Eduardo, Günter Waas, and José M. Roësset. 1975. “Dynamic Analysis of Footings on Layered Media.” *Journal of the Engineering Mechanics Division* 101(5): 679–93. <https://ascelibrary.org/doi/10.1061/JMCEA3.0002059>.
- Kausel, Eduardo, Robert V. Whitman, Joseph P. Morray, and Farid Elsabee. 1978. “The Spring Method for Embedded Foundations.” *Nuclear Engineering and Design* 48(2–3): 377–92.

- Lagaguine, Maroua, Sbartaï Badreddine, Boukeloua Smail, and Zaid Ismahene. 2018. "Analyse Plastique et Confortement Des Structures En Portiques Par La Méthode Incrémentale Pas à Pas Basée Sur l'Approche Des Rotules Plastique." In *La 1ère Conférence Internationale Sur La Vulnérabilité et La Réhabilitation Des Structures VUREST2018*,.
- lagaguine, Maroua, and Badreddine Sbartaï. 2023. "Non-Linear Soil-Structure Interaction Effect on the Seismic Response of a Building." *Arabian Journal of Geosciences* 16(6): 385. <https://link.springer.com/10.1007/s12517-023-11455-5>.
- Lagaguine, Maroua, Badreddine Sbartaï, and Badji Mokhtar-annaba. 2018. "EFFET DE L'INTERACTION SOL-STRUCTURE SUR LA REPOSE SISMIQUE DES." In *La 2ième Conférence Internationale de Constructions Métalliques et Mixtes CICOMM'2018*, , 9–10.
- Lesgidis, Nikolaos, Anastasios Sextos, and Oh Sung Kwon. 2017. "Influence of Frequency-Dependent Soil–Structure Interaction on the Fragility of R/C Bridges." *Earthquake Engineering and Structural Dynamics* 46(1): 139–58.
- Lin, Chi-Chang, Jer-Fu Wang, and Cheng-Hsing Tsai. 2008. "Dynamic Parameter Identification for Irregular Buildings Considering Soil-Structure Interaction Effects." *Earthquake Spectra* 24(3): 641–66. <http://journals.sagepub.com/doi/10.1193/1.2946439>.
- Liu, Shutong, Peizhen Li, Wenyang Zhang, and Zheng Lu. 2020. "Experimental Study and Numerical Simulation on Dynamic Soil-Structure Interaction under Earthquake Excitations." *Soil Dynamics and Earthquake Engineering* 138(November 2019): 106333. <https://doi.org/10.1016/j.soildyn.2020.106333>.
- Luo, Chuan et al. 2016. "Nonlinear 3D Finite Element Analysis of Soil–Pile–Structure Interaction System Subjected to Horizontal Earthquake Excitation." *Soil Dynamics and Earthquake Engineering* 84: 145–56.
- Lysmer J. 1965. Vertical Motion of Rigid Footings. PhD thesis, University of Michigan Report to WES Contract Report No. 3–115 under Contract No. DA-22-079-eng-340.
- M.Lagaguine and B.Sbartaï. 2021. "Analyse de L'effet de L'interaction Sol-Structure Sur La Réponse Sismique d'Un Bâtiment : Comparaison Entre Le Modèle Linéaire et Le Modèle Linéaire Equivalent M.Lagaguine 1 and B.Sbartaï 2, 3 1." In *2nd INTERNATIONAL SYMPOSIUM ON CONSTRUCTION MANAGEMENT AND CIVIL ENGINEERING "ISCMCE 2021"*, , 139.
- Maharjan, Sabin, and Kamal Bahadur. 2021. "Study of Soil-Structure Interaction Effects on Seismic Analysis." 8914: 294–301.
- Maheshwari, B. K., and Rajib Sarkar. 2011. "Seismic Behavior of Soil-Pile-Structure Interaction in Liquefiable Soils: Parametric Study." *International Journal of Geomechanics* 11(4): 335–47. <http://ascelibrary.org/doi/10.1061/%28ASCE%29GM.1943-5622.0000087>.
- Mahsuli, Mojtaba, and M. Ali Ghannad. 2009. "The Effect of Foundation Embedment on Inelastic Response of Structures." *Earthquake Engineering & Structural Dynamics* 38(4): 423–37. <https://onlinelibrary.wiley.com/doi/10.1002/eqe.858>.
- Martakis, Panagiotis et al. 2021. "Nonlinear Periodic Foundations for Seismic Protection: Practical Design, Realistic Evaluation and Stability Considerations." *Soil Dynamics and Earthquake Engineering* 150: 106934. <https://doi.org/10.1016/j.soildyn.2021.106934>.
- Masaëli, H., and M. Ahmadi. 2021. "Fragility Analysis of Nonlinear Soil-Structure Systems Including Foundation Uplifting and Soil Yielding." *Numerical Methods in Civil Engineering* 6(2): 77–92.
- Massimino, M R, G. Abate, S. Corsico, and R. Louarn. 2019. "Comparison Between Two Approaches for Non-Linear FEM Modelling of the Seismic Behaviour of a Coupled Soil–Structure System." *Geotechnical and Geological Engineering* 37(3): 1957–75. <https://doi.org/10.1007/s10706-018-0737-y>.
- Masing G (1926) Eigenspannungen und verfestigung beim messing. In: Proceedings of the 2nd International Congress of Applied Mechanics, pp 332–335
- Moghaddasi, M. et al. 2011. "Effects of Soil–Foundation–Structure Interaction on Seismic Structural Response via Robust Monte Carlo Simulation." *Engineering Structures* 33(4): 1338–47. <http://dx.doi.org/10.1016/j.engstruct.2011.01.011>.
- Mohammadioun, Bagher, and Alain Pecker. 1984. "Low-Frequency Transfer of Seismic Energy by Superficial Soil Deposits and Soft Rocks." *Earthquake Engineering & Structural Dynamics* 12(4): 537–64. <https://onlinelibrary.wiley.com/doi/10.1002/eqe.4290120409>.
- Murono, Yoshitaka, and Akihiko Nishimura. 2000. "Evaluation of Seismic Force of Pile Foundation

- Induced by Inertial and Kinematic Interaction.” *Twelfth World Conference of Earthquake Engineering*: 1–8.
- Mylonakis, G., and G. Gazetas. 1998. “Settlement and Additional Internal Forces of Grouped Piles in Layered Soil.” *Géotechnique* 48(1): 55–72. <https://www.icevirtuallibrary.com/doi/10.1680/geot.1998.48.1.55>.
- Mylonakis, George, and George Gazetas. 2000. “Seismic Soil-Structure Interaction: Beneficial or Detrimental?” *Journal of Earthquake Engineering* 4(3): 277–301.
- MYLONAKIS, GEORGE, ASPASIA NIKOLAOU, and GEORGE GAZETAS. 1997. “SOIL-PILE-BRIDGE SEISMIC INTERACTION: KINEMATIC AND INERTIAL EFFECTS. PART I: SOFT SOIL.” *Earthquake Engineering & Structural Dynamics* 26(3): 337–59. [https://onlinelibrary.wiley.com/doi/10.1002/\(SICI\)1096-9845\(199703\)26:3%3C337::AID-EQE646%3E3.0.CO;2-D](https://onlinelibrary.wiley.com/doi/10.1002/(SICI)1096-9845(199703)26:3%3C337::AID-EQE646%3E3.0.CO;2-D).
- Mylonakis, George, and Elia Voyagaki. 2006. “Yielding Oscillator Subjected to Simple Pulse Waveforms: Numerical Analysis & Closed-Form Solutions.” *Earthquake Engineering & Structural Dynamics* 35(15): 1949–74. <https://onlinelibrary.wiley.com/doi/10.1002/eqe.615>.
- Nagakumar, M. S., N. Ajay, and Sharu Elishuba John. 2022. 162 Lecture Notes in Civil Engineering *An Analytical Approach to Analysis of Concrete Overlay (White Topping) Over Flexible Pavement (Hot Mix Asphalt) Using ANSYS Software*.
- Naji, Maryam, Ali Akbar Firoozi, and Ali Asghar Firoozi. 2020. “A Review: Study of Integral Abutment Bridge with Consideration of Soil-Structure Interaction.” *Latin American Journal of Solids and Structures* 17(2): 1–27.
- NEHRP (2012). Soil-structure interaction for building structures. USA.
- NTC (2008) D.M. 14/01/08, “New technical standards for buildings”, Oficial Journal of the Italian Republic, 14th January 2008 (In Italian)
- Pais, Artur, Eduardo Kausel, and Civil Eirgirreerirgl. 1988. “Approximate Formulas for Dynamic Stiffnesses of Rigid Foundations.” *Soil Dynamics and Earthquake Engineering* 7: 213–27.
- Park, Jang Ho, Jinkyoo F. Choo, and Jeong Rae Cho. 2013. “Dynamic Soil-Structure Interaction Analysis for Complex Soil Profiles Using Unaligned Mesh Generation and Nonlinear Modeling Approach.” *KSCE Journal of Civil Engineering* 17(4): 753–62.
- Pecker, Alain. 2007. “Soil Structure Interaction.” In *Advanced Earthquake Engineering Analysis*, Vienna: Springer Vienna, 33–42. http://link.springer.com/10.1007/978-3-211-74214-3_3.
- Pecker, Alain, Paolucci, Roberto, Chatzigogos, Charisis, Correia, António A., Figini, Raffaele. 2014. “The Role of Non-Linear Dynamic Soil-Foundation Interaction on the Seismic Response of Structures.” *Bulletin of Earthquake Engineering* 12(3): 1157–76.
- Petridis, Christos, and Dimitris Ptilakis. 2020. “Fragility Curve Modifiers for Reinforced Concrete Dual Buildings, Including Nonlinear Site Effects and Soil–Structure Interaction.” *Earthquake Spectra* 36(4): 1930–51.
- Petridis, Christos, and Dimitris Ptilakis. 2021. “Large-Scale Seismic Risk Assessment Integrating Nonlinear Soil Behavior and Soil–Structure Interaction Effects.” *Bulletin of Earthquake Engineering* 19(15): 6423–41. <https://doi.org/10.1007/s10518-021-01237-3>.
- Petridis, Christos, Dimitris Ptilakis, Christos Petridis, and Dimitris Ptilakis. 2018. “Soil-Structure Interaction Effect on Earthquake Vulnerability Assessment of Moment Resisting Frames: The Role of the Soil.” *Proceedings of the 16th European Conference on Earthquake Engineering*: 1–11.
- Ptilakis, Dimitris et al. 2008. “Numerical Simulation of Dynamic Soil–Structure Interaction in Shaking Table Testing.” *Soil Dynamics and Earthquake Engineering* 28(6): 453–67.
- Ptilakis, Dimitris, and Didier Clouteau. 2010. “Equivalent Linear Substructure Approximation of Soil-Foundation-Structure Interaction: Model Presentation and Validation.” *Bulletin of Earthquake Engineering* 8(2): 257–82.
- Ptilakis, Dimitris, Fernando Lopez-Caballero, Arezou Modaressi-Farahmand-Razavi, and Didier Clouteau. 2005. “Study of the Soil-Structure Interaction Using an Equivalent Linear and an Elastoplastic Soil Model: Comparative Results.” *Proceedings of the 16th International Conference on Soil Mechanics and Geotechnical Engineering*: 8579–8579.
- Ptilakis, Dimitris, Arezou Moderessi-farahmand-razavi, and Didier Clouteau. 2013. “Equivalent-Linear Dynamic Impedance Functions of Surface Foundations.” (JULY): 1130–39.
- Pena Ruiz, D. and Guzman Gutiérrez, S. (2014), “Finite element methodology for the evaluation of soil

- damping in LNG tanks supported on homogeneous elastic half space”, *Bull. Earthq. Engineer, Springer*.
- Rajeev, P., and S. Tesfamariam. 2012. “Seismic Fragilities of Non-Ductile Reinforced Concrete Frames with Consideration of Soil Structure Interaction.” *Soil Dynamics and Earthquake Engineering* 40: 78–86. <http://dx.doi.org/10.1016/j.soildyn.2012.04.008>.
- Ramberg W, Osgood WR (1943) Description of stress - strain curves by three parameters. National Advisory Committee for Aeronautics, Washington, D.C, p. Technical Note No. 902. Available at: <https://ntrs.nasa.gov/archive/nasa/casi.ntrs.nasa.gov/19930081614.pdf>
- Raychowdhury, Prishati. 2011. “Seismic Response of Low-Rise Steel Moment-Resisting Frame (SMRF) Buildings Incorporating Nonlinear Soil-Structure Interaction (SSI).” *Engineering Structures* 33(3): 958–67. <http://dx.doi.org/10.1016/j.engstruct.2010.12.017>.
- Reissner, Erich. 1936. “Stationäre, Axialsymmetrische, Durch Eine Schüttelnde Masse Erregte Schwingungen Eines Homogenen Elastischen Halbraumes.” *Ingenieur-Archiv* 7(6): 381–96. <http://link.springer.com/10.1007/BF02090427>.
- Renzi, Stefano, Claudia Madaia, and Giovanni Vannucchi. 2013. “A Simplified Empirical Method for Assessing Seismic Soil-Structure Interaction Effects on Ordinary Shear-Type Buildings.” *Soil Dynamics and Earthquake Engineering* 55: 100–107. <http://dx.doi.org/10.1016/j.soildyn.2013.09.012>.
- Robert, D. J., K. Soga, and A. Britto. 2015. “Soil Constitutive Models to Simulate Pipeline-Soil Interaction Behaviour.” In *Proceedings of the International Conference on Geotechnical Engineering (ICGE 2015), 10-11 August 2015, , 347–50*.
- Ronak, Motiani, Sandip Vasanwala, and Tejaskumar Thaker. 2021. “Effect of Site Amplification on Seismic Fragility of RC Building with Different Infill Configurations Using Synthetic Ground Motions.” *Innovative Infrastructure Solutions* In press.(3): 1–19. <https://doi.org/10.1007/s41062-021-00532-x>.
- Rovithis, Emmanouil et al. 2017. “A LiDAR-Aided Urban-Scale Assessment of Soil-Structure Interaction Effects: The Case of Kalochori Residential Area (N. Greece).” *Bulletin of Earthquake Engineering* 15(11): 4821–50.
- Saitoh, Masato. 2007. “Simple Model of Frequency-Dependent Impedance Functions in Soil-Structure Interaction Using Frequency-Independent Elements.” *Journal of Engineering Mechanics* 133(10): 1101–14.
- Sameti, Amir Rezaei, and Mohammad Ali Ghannad. 2016. “Equivalent Linear Model for Existing Soil-Structure Systems.” *International Journal of Structural Stability and Dynamics* 16(2).
- Sayyadpour, Hadi, Farhad Behnamfar, and M. Hesham El Naggar. 2016. “The Near-Field Method: A Modified Equivalent Linear Method for Dynamic Soil–Structure Interaction Analysis. Part II: Verification and Example Application.” *Bulletin of Earthquake Engineering* 14(8): 2385–2404.
- Sbartai, Badreddine. 2016. “Dynamic Interaction of Two Adjacent Foundations Embedded in a Viscoelastic Soil.” *International Journal of Structural Stability and Dynamics* 16(03): 1450110. <https://www.worldscientific.com/doi/abs/10.1142/S0219455414501107>.
- Sbartai, Badreddine. 2018. “Dynamic Impedance Functions of a Square Foundation Estimated with an Equivalent Linear Approach.” In *Sustainable Civil Infrastructures, , 460–70*.
- Sbartai, Badreddine, and Ahmed Boumekik. 2008. “Ground Vibration from Rigid Foundation by BEM-TLM.” *ISET Journal of Earthquake Technology* 45(3–4): 65.
- Sbartai, Badreddine, and Kamel Fillali. 2012. “Caldynsoil : Software of Seismic Response and Liquefaction Potential of a Soil Caldynsoil : Software of Seismic Response and Liquefaction Potential of a Soil Deposit.” (September).
- Seghir, Abdelkrim, and Juan Pablo Torres-Martínez. 2011. “On Equilibrium Existence with Endogenous Restricted Financial Participation.” *Journal of Mathematical Economics* 47(1): 37–42.
- Sekhri, Khadidja. 2021. “Analyse Dynamique Non Linéaire d’un Pieu Isolé et Groupe de Pieux Sollicités Par Des Charges Sismiques.” Université Batna -2- Mostefa Ben Boulaïd Faculté de Technologie.
- Shakib, H., and A. Fuladgar. 2004. “Dynamic Soil–Structure Interaction Effects on the Seismic Response of Asymmetric Buildings.” *Soil Dynamics and Earthquake Engineering* 24(5): 379–88.
- de Silva, Filomena, Francesca Ceroni, Stefania Sica, and Francesco Silvestri. 2018. “Non-Linear Analysis of the Carmine Bell Tower under Seismic Actions Accounting for Soil–Foundation–Structure Interaction.” *Bulletin of Earthquake Engineering* 16(7): 2775–2808. <https://doi.org/10.1007/s10518-017-0298-0>.

- Sobhi, Pejman, and Harry Far. 2021. *Bulletin of Earthquake Engineering Impact of Structural Pounding on Structural Behaviour of Adjacent Buildings Considering Dynamic Soil-Structure Interaction*. Springer Netherlands. <https://doi.org/10.1007/s10518-021-01195-w>.
- Spyrakos, C C, Ch A Maniatakis, and I A Koutromanos. 2009. "Soil-Structure Interaction Effects on Base-Isolated Buildings Founded on Soil Stratum." *Engineering Structures* 31(3): 729–37.
- Sreya Dhar, Ali Güney Özcebe, Kaustubh Dasgupta ,Arindam Dey, Roberto Paolucci Lorenza Petrini. 2016. "NONLINEAR DYNAMIC SOIL-STRUCTURE INTERACTION EFFECTS ON THE SEISMIC RESPONSE OF A PILE-SUPPORTED INTEGRAL BRIDGE STRUCTURE." In *Sixth International Conference on Recent Advances in Geotechnical Earthquake Engineering and Soil Dynamics*, , 1–12.
- Stewart, Jonathan P. et al. 2003. "Revisions to Soil-Structure Interaction Procedures in NEHRP Design Provisions." *Earthquake Spectra* 19(3): 677–96.
- Stewart, Jonathan P., Raymond B. Seed, and Gregory L. Fenves. 1999. "Seismic Soil-Structure Interaction in Buildings. II: Empirical Findings." *Journal of Geotechnical and Geoenvironmental Engineering* 125(1): 38–48. <https://ascelibrary.org/doi/10.1061/%28ASCE%2910900241%281999%29125%3A1%2838%29>.
- Sung, T. Y. (1953). *Vibration in semi infinite solid due to periodic surface loading*. PhD thesis, Harvard.
- Tahar Berrabah, Amina. 2012. "DYNAMIC SOIL-FLUID-STRUCTURE INTERACTION APPLIED FOR CONCRETE DAM Presented by Amina Tahar Berrabah This Thesis Was Submitted in Partial Fulfillment of the Requirements for the Doctorate Degree in Civil Engineering Examination Committee Hanachi Nasreddine." university of aboubekr belkaid tlemcen.
- Tahar Berrabah, Amina, Mohamed Belharizi, André Laulusa, and Abdelmalek Bekkouche. 2012. "Three-Dimensional Modal Analysis of Brezina Concrete Arch Dam, Algeria." *Earth Science Research* 1(2). <http://www.ccsenet.org/journal/index.php/esr/article/view/14466>.
- Thejaswini, R. M., L. Govindaraju, and V. Devaraj. 2021. "Experimental and Numerical Studies on Setback Buildings Considering the Ssi Effect under Seismic Response." *Civil Engineering Journal (Iran)* 7(3): 431–48.
- Tileylioglu, Salih, Jonathan P. Stewart, and Robert L. Nigbor. 2011. "Dynamic Stiffness and Damping of a Shallow Foundation from Forced Vibration of a Field Test Structure." *Journal of Geotechnical and Geoenvironmental Engineering* 137(4): 344–53. <https://ascelibrary.org/doi/10.1061/%28ASCE%29GT.1943-5606.0000430>.
- Uildings, B, By Jonathan P Stewart, Raymond B Seed, and Gregory L Fenves. 1999. "S Eismic S Oil -S Tructure I Nteraction Ii : E Mpirical F Indings In." *Manager* (January): 38–48.
- Veletsos, Anestis S., and V. V. Damodaran Nair. 1974. "Torsional Vibration of Viscoelastic Foundations." *ASCE J Geotech Eng Div* 100(GT3): 225–46.
- Veletsos, Anestis S., and Jethro W. Meek. 1974. "Dynamic Behaviour of Building-foundation Systems." *Earthquake Engineering & Structural Dynamics* 3(2): 121–38.
- Veletsos, Anestis S., and Yau T. Wei. 1971. "Lateral and Rocking Vibration of Footings." *Journal of the Soil Mechanics and Foundations Division* 97(9): 1227–48. <https://ascelibrary.org/doi/10.1061/JSFEAQ.0001661>.
- Wei, Biao, Ruibo Cui, and Gonglian Dai. 2013. "Seismic Performance of a Rolling-Damper Isolation System." *Journal of Vibroengineering* 15(3): 1504–12.
- Wen, Z.P., Y.X. Hu, and K.T. Chau. 2002. "Site Effect on Vulnerability of High-Rise Shear Wall Buildings under near and Far Field Earthquakes." *Soil Dynamics and Earthquake Engineering* 22(9–12): 1175–82. <https://linkinghub.elsevier.com/retrieve/pii/S0267726102001458>.
- Wolf, John P. 1985. *Dynamic Soil-Structure Interaction*. ed. Prentice-Hall. international series in civil engineering and engineering mechanics.
- Wolf, John P. 1989. "Soil-Structure-Interaction Analysis in Time Domain." *Nuclear Engineering and Design* 111(3): 381–93.
- Wolf, J.P. (1994), *Foundation vibration analysis using simple physical models*, Prentice-Hall, Upper Saddle River, NJ
- Wolf, John P., and Matthias Preisig. 2003. "Dynamic Stiffness of Foundation Embedded in Layered Halfspace Based on Wave Propagation in Cones." *Earthquake Engineering and Structural Dynamics* 32(7): 1075–98.
- Wong, H. L., and J. E. Luco. 1985. "Tables of Impedance Functions for Square Foundations on Layered Media." *International Journal of Soil Dynamics and Earthquake Engineering* 4(2): 64–81.

- Wood, David Muir. 2014. "Soil-Structure Interaction Modeling Using Equivalent Linear Soil Behavior In The Substructure Method GRADE DE DOCTEUR Spécialité : Génie Parasismique Laboratoire d ' Accueil : Mécanique Des Sols , Structures et Matériaux Alain Pecker Jean-François Semblat." (January 2006).
- Worku, A. 2014. "Soil-Structureinteraction Provisions: A Potential Tool to Consider for Economical Seismic Design of Buildings?" *Journal of the South African Institution of Civil Engineering* 56(1): 54–62.
- Zafarkhah, Elyar, and Morteza Raissi Dehkordi. 2017. "Evaluation and Numerical Simulation of Soil Type Effects on Seismic Soil-Structure Interaction Response of RC Structures." *Journal of Vibroengineering* 19(7): 5208–30.
- Zhang, Jian, and Yuchuan Tang. 2009. "Dimensional Analysis of Structures with Translating and Rocking Foundations under Near-Fault Ground Motions." *Soil Dynamics and Earthquake Engineering* 29(10): 1330–46. <https://linkinghub.elsevier.com/retrieve/pii/S0267726109000840>.
- Zhang, C. and Wolf, J.P. (1998), *Dynamic soil-structure interaction*, Elsevier science, Netherlands.
- Zhidong, Gao et al. 2021. "Effi Cient Seismic Analysis for Nonlinear Soil-Structure Interaction with a Thick Soil Layer Abstract:" *Vol. 20, No. 3 EARTHQUAKE ENGINEERING AND ENGINEERING VIBRATION* 20(3): 553–65.